Zoran S. Vratnica

ANALYSIS OF BACTERIA DAMAGES CAUSED BY TREATMENT WITH OXYGEN RADICALS

Doctoral Dissertation

ANALIZA POŠKODB BAKTERIJ PO IZPOSTAVI KISIKOVIM RADIKALOM

Doktorska disertacija

Supervisor: A/Prof Dr Miran Mozetič

Co-Supervisor: A/Prof Dr Uroš Cvelbar

May 2009

MEDNARODNA PODIPLOMSKA ŠOLA JOŽEFA STEFANA
JOŽEF STEFAN INTERNATIONAL POSTGRADUATE SCHOOL
Ljubljana, Slovenia

Index

Abstract

The possible mechanisms for destruction of two types of bacteria with oxygen radicals were studied. Samples consisting of standard ATCC strains of Gram – positive bacteria *Staphylococcus aureus* and Gram – negative bacteria *Escherichia coli* were obtained. Bacteria were cultivated according to the standard procedures and fixed on substrates of Al foil, highly oriented graphite or highly polished silicon wafers. In last two cases, the roughness of the substrates was below a nm. The substrates with bacteria were then exposed to oxygen radicals in two different environments: 1 – inductively coupled RF plasma with the neutral atom density of $1x10^{22}$ m^{-3} and the ion density of $1.4x10^{16}$ m^{-3}, and 2 – the afterglow of the oxygen plasma with the neutral atom density of $3.5x10^{21}$ m^{-3}.

Samples were kept in plasma or its afterglow for different periods between 1 and 500 s. Immediately after the treatment, they were characterized by two complementary methods: scanning electron microscopy (SEM) and atomic force microscopy (AFM). Both techniques showed a thin film of capsule covering the bacteria as well as the space between particular bacteria in small, two – dimensional aggregates. The typical number of bacteria within an aggregate was less than 10. The SEM images obtained at low kinetic energy of primarily electrons showed that the thickness of capsule was about 100nm for *S. aureus* and about 150nm for *E. coli*.

The first effect of treatment with oxygen radicals is destruction of capsule. Both SEM and AFM images revealed that a part of capsule was disrupted in a few seconds forming numerous small droplets scattered all around bacteria. Although this effect is observed even for untreated bacteria, the number of droplets after a brief treatment increases dramatically, so it is possible to conclude that formation of numerous capsule droplets is a particular feature of treatment with oxygen radicals. The formation of the droplets was explained by a rapid increase of the surface energy of capsule due to functionalization with polar oxygen rich functional groups. The droplets, as well as the remaining capsule between particular bacteria, were completely removed with prolonged treatment.

As soon as the majority of capsule was removed, degradation of the cell wall started. AFM images showed clearly distinguishable segments on the cell walls of both types of bacteria. In any case, prolonged treatment caused increased roughness of the cell wall, tear off pieces from them until, at a certain dose, the cell wall was disrupted suddenly and these segments were scattered all around bacteria. This sudden change of the cell wall has, to the best of our knowledge, never been reported so far, and it is contradictory to classical pictures of bacterial degradation caused by plasma radicals.

After prolonged treatment the segments are almost perfectly oxidized and vanish from the surface of our samples. Once the cell wall is badly damaged, the interaction of radicals with cytoplasm starts. A slight difference in appearance between cytoplasm of *E. coli* and *S. aureus* was observed. The cytoplasm of *E. coli* was mainly spilled around bacteria, while the cytoplasm of *S. aureus* remained its spherical shape for a long time. Unlike the classical picture of the cytoplasm as a jelly-like material, our results clearly showed that the cytoplasm of *S. aureus* was pretty rigid since it preserved its shape even after removal of the cell wall. Our results are therefore just another confirmation of a new picture of bacterial cytoplasm. Namely, in 2001, a new theory of the cytoplasm structure was proposed by Jones et al, stating that the cytoplasm of *Bacillus subtilis* has a rigid structure called cytoskeleton. Our results show that the cytoplasm of *S. aureus* really has a well – organized structure and is not just a semi-liquid substance as claimed in classical literature.

A long treatment of bacteria with oxygen radicals causes an extensive degradation of their constituents and finally only traces of bacteria remain in the form of ash.

Knowing the flux of oxygen radicals onto the surface of bacteria, at which certain steps in the degradation occur, enables calculation of the appropriate doses of radicals. For destruction of the capsule on *S. aureus* the required dose is $1.6x10^{25}m^{-2}$ and $6.6x10^{25}m^{-2}$ for the case of plasma and afterglow treatments, respectively. These numbers are somehow lower for the case of capsule on *E. coli*, where the values of $0.8x10^{25}m^{-2}$ and $1.4x10^{25}m^{-2}$ are found. The dose required to destroy the bacterial cell wall is $7.1x10^{25}m^{-2}$ and $1.9x10^{26}m^{-2}$ for *S. aureus* placed in plasma and afterglow, respectively. The corresponding numbers for *E. coli* are $1.6x10^{25}m^{-2}$ and $1x10^{26}m^{-2}$ for plasma and afterglow, respectively. The dose

required for total destruction of bacteria (only ash remains) is somehow arbitrary as it is difficult to define the term "total destruction" of bacteria. Still, in the first approximation the values are $1.9x10^{26}m^{-2}$ and more than $2.7x10^{26}m^{-2}$ for *S. aureus* in plasma and afterglow, respectively. These numbers for the case of *E. coli* are $9.4x10^{25}m^{-2}$ and more than $2.7x10^{26}m^{-2}$ for plasma and afterglow, respectively.

According to our experimental results, a new model of three – dimensional organization of peptidogycan in *E. coli* cell wall is proposed. At this model, peptidoglycan is organized in flat, oval or round shaped pieces composed in such a manner, where pieces overlapping each other and looks like fish scales or tiles on a roof.

Povzetek

Raziskovali smo možne mehanizme poškodb, ki jih povzročajo kisikovi radikali na dveh vrstah bakterij. Izbrali smo po eno standardno ATCC vrsto Gram pozitivnih bakterij (*Staphylococcus aureus*) in Gram negativnih bakterij (*Escherichia coli).* Bakterije smo vzgojili po standardiziranem postopku, ki ga je predpisal proizvajalec, in fiksirali na treh različni vrstah podlag: Al foliji, visoko orientiranem grafitu in visoko poliranih silicijevih rezinah. V slednjih primerih je bila hrapavost podlag manjša od 1 nm. Podlage z bakterijami smo izpostavili kisikovim radikalom v dveh različnih okoljih: 1 – induktivno sklopljeni RF plazmi z gostoto nevtralnih atomov $1x10^{22}$ m^{-3} in gostoto ionov $1.4x10^{16}$ m^{-3} in 2 – porazelektritvenemu delu kisikove plazme, v katerem je bila gostota kisikovih atomov $3.5x10^{21}$ m^{-3}.

Čas obdelave vzorcev v plazmi in porazelektritvenemu delu smo spreminjali med 1 in 500 s. Takoj po obdelavi s kisikovimi radikali smo vzorce preiskovali z dvema dopolnjujočima se metodama: vrstično elektronsko mikroskopijo (SEM) in mikroskopijo na atomsko silo (AFM). Z obema metodama smo ugotovili, da je tako na površini bakterij kot tudi v prostoru med bakterijami znotraj posameznih dvodimenzionalnih skupkov, prisotna kapsula. Število bakterij v posameznem skupku je bilo značilno manjše od 10. Slike, ki smo jih dobili z metodo SEM, pri čemer smo uporabili nizkoenergijske primarne elektrone, so pokazale, da je debelina kapsule okoli 100 nm za bakterije S. aureus in 150 nm za E. coli.

Prvi opazni pojav pri interakciji kisikovih radikalov z našimi vzorci je poškodovanje kapsule. Tako SEM kot AFM slike so pokazale, da se je kapsula močno poškodovala že po nekaj sekundah obdelave. Del kapsule je razpadel na majhne kapljice, ki so ostale razpršene okoli bakterij. Kljub temu, da smo opazili nekaj takšnih kapljic tudi v okolici bakterij, ki niso bile izpostavljene delovanju radikalov, lahko sklepamo, da je opaženi pojav razpršitve kapsule specifična lastnost obdelave s kisikovimi radikali, saj je število kapljic po kratkotrajni obdelavi bistveno večje kot pred obdelavo. Pojav smo razložili kot posledico dramatičnega povečanja površinske energije kapsule po kratkotrajni obdelavi s kisikovimi radikali, saj le ti povzročijo funkcionalizacijo površine z zelo polarnimi s kisikom bogatimi funkcionalnimi skupinami. Kapljice kakor tudi del kapsule, ki je ostala na površini bakterij, kisikovi radikali povsem odstranijo pri podaljšani obdelavi vzorcev.

Takoj po tem, ko so radikali odstranili večji del kapsule, smo opazili strukturirano površino celične stene. AFM rezultati so jasno pokazali, da je celična stena sestavljena iz posameznih segmentov. Ugotovili smo tudi, da kisikovi radikali povzročajo večanje hrapavosti celične stene in trganje posameznih segmentov, dokler v nekem trenutku ni stena tako poškodovana, da razpade na množico posameznih segmentov, ki so raztreseni po okolici bakterij. O tovrstnem razpadu celične stene relevantna literatura ne poroča, saj je v nasprotju s klasičnimi opisi interakcije plazme ali kateregakoli drugega reagenta z bakterijsko celično steno.

Podaljšana obdelava z radikali povzroči postopno oksidacijo segmentov iz celične stene, dokler popolnoma ne izginejo s površine podlag. Po tem, ko je celična stena močno poškodovana, lahko radikali reagirajo tudi s citoplazmo. Pri tem smo opazili razliko v strukturi citoplazme *E. coli* in *S. aureus*. V primeru *E. coli* se citoplazma razlije v okolico bakterije takoj po tem, ko celična stena razpade. Ta pojav je skladen s klasično teorijo zgradbe bakterijske citoplazme, ki je predstavljena kot želatinasta napol tekoča snov. V primeru *S. aureus* pa se citoplazma ne izlije v okolico, ampak obdrži svojo prvotno kroglasto obliko tudi po tem, ko je celična stena že popolnoma uničena. Navedeni rezultat potrjuje novo teorijo o zgradbi bakterijske citoplazme, ki jo je leta 2001 predlagal Jones s sodelavci. Po njegovi teoriji ima citoplazma *Bacillus subtilis* nekakno ogrodje, ki ga imenujemo citoskeleton. Naši rezultati jasno kažejo, da ima citoplazma v bakterijah *S. aureus* tovrstno ogrodje, ki je tako togo, da obdrži obliko tudi v odsotnosti celične stene.

Zelo dolga obdelava obeh vrst bakterij s kisikovimi radikali privede do domala popolne oksidacije organskega materiala, iz katerega so sestavljene bakterije, tako da na podlagah ostane samo še pepel.
Poznavaje gostote toka kisikovih radikalov na površino bakterij omogoča izračun potrebne doze radikalov za dosego posameznih stopenj degradacije bakterij. Za odstranitev kapsule na bakteriji *S. aureus* je potrebna doza radikalov $1.6x10^{25}m^{-2}$ v primeru izpostave v plazmi in $6.6x10^{25}$ m^{-2} v primeru porazelektritvenega dela. Za Gram negativno bakterijo *E. coli* so ustrezne vrednosti nekoliko nižje in sicer

$0.8x10^{25}m^{-2}$ za obdelavo v plazmi in $1.4x10^{25}m^{-2}$ za porazelektritveni del. Doza radikalov, ki je potrebna za uničenje celične stene bakterij *S. aureus*, je $7.1x10^{25}m^{-2}$ v plazmi in $1.9x10^{26}m^{-2}$ v porazelektritvenem delu. Ustrezne vrednosti za *E. coli* so $1.6x10^{25}m^{-2}$ in $1x10^{26}m^{-2}$. Dozo radikalov, ki je potrebna za popolno oksidacijo bakterij, tako da na površini podlage ostane le še pepel, je težko oceniti, saj ni mogoče natančno in nedvoumno definirati, kdaj je ves organski material povsem oksidiran. Kljub temu lahko navedemo vsaj približne ocene, ki so naslednje: za *S. aureus* $1.9x10^{26}m^{-2}$ v plazmi in več kot $2.7x10^{26}m^{-2}$ v porazelektritvenem delu ter za *E. coli* $9.4x10^{25}m^{-2}$ v plazmi in več kot $2.7x10^{26}m^{-2}$ v porazelektritvenem delu.

Na osnovi naših rezultatov smo predlagali nov model tridimenzionalne organiziranosti peptidoglikana v celični steni bakterije *E. coli*. V našem modelu se nahaja pepdidoglikan v obliki dobro definiranih gradnikov, ki so tanke ploščice ovalne ali okrogle oblike. Gradniki so v celični steni naloženi tako, da prekrivajo spodnje gradnike, podobno kot ribje luske ali strešniki na strehi.

Abbreviations

S. aureus	=	*Staphylococcus aureus*
E. coli	=	*Escherichia coli*
Approx.	=	Approximately
Fig.	=	Figure
Figs.	=	Figures
$D_{aP\ cSa}$	=	Required dose of atoms in plasma for removal of capsule of *S. aureus*
$D_{aA\ cSa}$	=	Required dose of atoms in afterglow for removal of capsule of *S. aureus*
$D_{iP\ cSa}$	=	Recieved dose of ions in plasma of capsule of *S. aureus*
$D_{aP\ cwSa}$	=	Required dose of atoms in plasma for removal of cell wall of *S. aureus*
$D_{aA\ cwSa}$	=	Required dose of atoms in afterglow for removal of cell wall of *S. aureus*
$D_{aP\ cySa}$	=	Required dose of atoms in plasma for removal of cytoplasm of *S. aureus*
$D_{aA\ cySa}$	=	Required dose of atoms in afterglow for removal of cytoplasm of *S. aureus*
$D_{aP\ killSa}$	=	Required dose of atoms in plasma to kill *S. aureus*
$D_{aA\ killSa}$	=	Required dose of atoms in afterglow to kill *S. aureus*
$D_{aP\ cEc}$	=	Required dose of atoms in plasma for removal of capsule of *E.coli*
$D_{aA\ cEc}$	=	Required dose of atoms in afterglow for removal of capsule of *E.coli*
$D_{aP\ cwEc}$	=	Required dose of atoms in plasma for removal of cell wall of *E.coli*
$D_{aA\ cwEc}$	=	Required dose of atoms in afterglow for removal of cell wall of *E.coli*
$D_{aP\ cyEc}$	=	Required dose of atoms in plasma for removal of cytoplasm of *E.coli*
$D_{aA\ cyEc}$	=	Required dose of atoms in afterglow for removal of cytoplasm of *E.coli*
$D_{aP\ killEc}$	=	Required dose of atoms in plasma to kill *E.coli*
$D_{aA\ killEc}$	=	Required dose of atoms in afterglow to kill *E.coli*

1 Introduction

Bacteria are very tiny organisms, which belong to lower protists. They are very specific, in any kind of their being. These organisms are extremely diverse in shape, from miniature spheres, cylinders and spiral threads, to flagellated rods, and filamentous chains. Bacteria are the smallest, self-capable live organisms. They can be found almost everywhere on the Earth and they live in some of the most unusual, to other organisms inhospitable places. Most of them are not harmful in any way, and while we often first think of the bacteria that cause disease, there are numerous of bacterial species that are essential in our ecosystem.

However, some of them could be harmful and dangerous to human health or some processes in any field of human activities. Sometimes, this is a reason we want to destruct them. In many cases it is not necessary to destroy or remove all bacteria that are present at some place. In other cases, we obviously must de-vitalise or remove any kind of bacteria, to get sterile environment. Consequently, for these purposes we use different techniques.

Numerous agents can do harmful influences or damages and death of bacteria. For all of them, common name is antimicrobial agents. The response of bacteria to adverse agents depends on the type of organism, type of the agent itself, intensity and duration of acting for some specific agent. Acting points can be different structures of bacterial cell. Some antimicrobial agent can act at only one site or at multiple sites. Harmful influences and damages can be temporary, reversible, but damages can be deathly, too. Chemical or physical agents can obtain the damaging effects, but some of them can be used together, such as increasing temperature and chemicals, UV radiation and chemicals, or high temperature and ionizing radiation etc.

Several years ago it was found that low temperature gas plasma can act as antimicrobial agent, too. Gas plasma (or simply plasma, different from blood plasma) can be considered the fourth state of matter, following by order of increasing energy, the solid state, the liquid state, and the gaseous state. Strictly speaking, it is a gas containing rather large concentration of positive ions and free electrons (as for instance encountered in stars as thermal plasma). Such a state of gas can be obtained artificially, by placing a chamber containing gas in appropriate electric field.

Plasma technologies are based on electrical discharges of gases, consisted of ions, electrons, and uncharged particles such as atoms, molecules, excited radicals and light quanta. Different gases can be used, such as a mixture of a noble gas with another gas, hydrogen, air, the appropriate mixture of nitrogen and oxygen, oxygen etc. Especially suitable for biomedical applications are low – pressure plasmas in a non-equilibrium state of gas. In recent years, plasma technologies are being intensively used for improved biomedical application such as activation of surfaces of different implant devices, removal of degradation products after sterilization, sterilization itself etc.

Despite well-known facts about bacteria themselves and influence of plasma on them, there are many unknown things about these interactions. Namely, to the best of our knowledge, there are little valuable data about mechanisms of plasma acting against bacteria. The scientists working on plasma sterilization worldwide only agree that the effects could be physical, chemical and in many cases and most probably, combined influences.

In the last few years, the quality of microscopic techniques has been improved dramatically. Nowadays we can use the powerful tools such as high – resolution scanning electron microscopes (SEM) and atomic force microscopes (AFM) to investigate some details about destruction of bacteria. These two devices are available at the Department for surface engineering, Jozef Stefan Institute, and National Institute of Chemistry, Ljubljana, Slovenia, where we performed systematic investigations in order to elucidate some of these interactions and events.

1.1 Bacteria

A bacterium performs all vital processes in a single cell. This cell is virtually simple in structure, with no recognizable organelles as shown in Figure 1, but very complex in life processes and extremely capable to fit to wide variety of different influences from its environment. The structures that make possible these features and, at the same time, that can be target of different antimicrobial agents, are described below. Although new theories are being proposed occasionally, we use classical descriptions that are worldwide recognized unless stated otherwise.

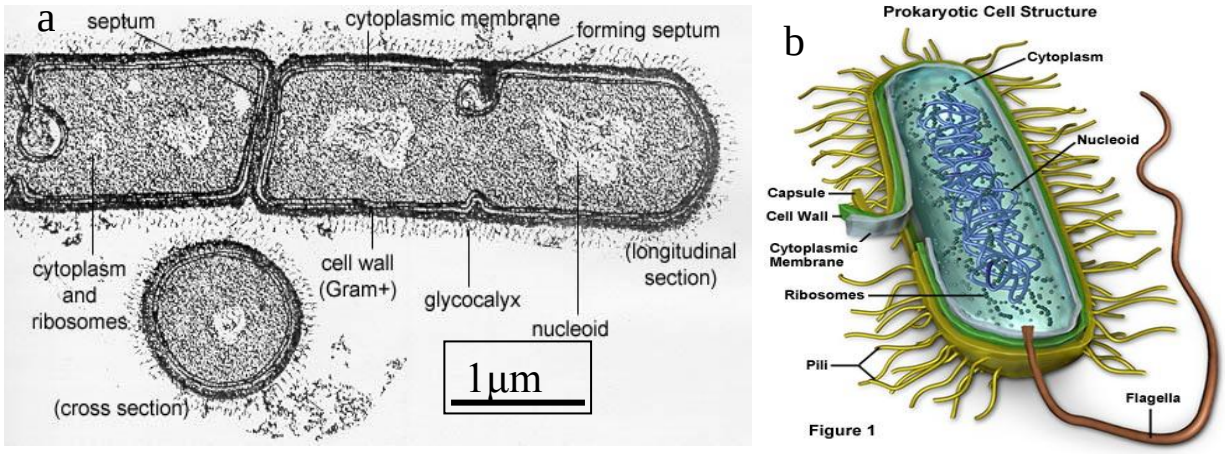

Figure 1: *Structure of bacterial cell*. **a**. TEM microphotograph **b**. Schematic diagram.

1.1.1 The cytoplasm

The cytoplasm is enclosed within the cell and does not exhibit much structure when viewed by transmission electron microscopy (Fig 1a.). It is a gel-like structure. In the cytoplasm, there are a lot of enzymes, various amino acids, sugars, fatty acids, peptides, proteins, polysaccharides, and their precursors, lipid droplets, metachromatic granule of polymerized phosphate, various ions in different concentrations etc. All of them are solved in water, which takes about 80% of complete volume of bacterial cytoplasm. [1,2,3,4,5] Structures called ribosome give the cytoplasm of bacteria a granular appearance in transmission electron micrographs. Genetic material of bacteria is enclosed in cytoplasm and does not have a well – distinguished nucleus, like other live cells.

Several years ago a longstanding "truth" about one of the major life forms on the planet (prokaryota) has been overturned. Jones et al. in 2001 discovered that bacterial actin homologs (FtsZ now) in *Bacillus subtilis* are organized into extended helical structures that play key roles in cell shape regulation. [6] Since then, the dictum that bacteria have no long-range internal structure has been slowly replaced by the realization that the interior of the bacterial cell contains a large number of organized cytoskeletal elements. [7]

1.1.1.1 The ribosomes

Ribosome consists of two subunits smaller 30 S and bigger 50 S, assembled together form 70 S functional unit, 20 – 25 nm across. Their average number in bacterial cell is about 15 000. Ribosomes looks like original nanomachines, whose function is decoding the genetic message in messenger RNA, transferred from DNK, into the production of peptide sequences (proteins). [8,9]

1.1.1.2 Genetic material

Prokaryotic chromatin is highly condensed and forms a pseudo-compartment that frequently occupies a distinct region (mostly central) within the cell, which is characterized by the absence of ribosomes. Though a membrane does not surround it, it is visibly distinct (by transmission electron microscopy) from the rest of the cell interior. This chromatin dense area is functionally equivalent to the eukaryotic nucleus and is, therefore, termed nucleoid. [10,11,12,13,14]

Bacteria generally possess one circular chromosome, even though species with multiple circular or linear chromosomes have been described. [15,16]
The chromosome is organized into plectonemically wound loops of DNA that radially emanate from a central core. This modular design of the chromosome, has been found in all bacteria studied so far is highly dynamic. [17] Cytoskeletal elements help formation of this structure and they are included in the process of replication of bacterial chromosome.[18] Many bacterial species have extrahromosomal genetic material, too. This material is organized in form called plasmids.

1.1.1.3 Cytoskeleton

We define bacterial cytoskeletal structures as filamentous structures that are based primarily on polymers of a single class of protein, that show long-range order within the cell, and that are capable of self-assembling in vitro into extended polymeric filaments. The bacterial cytoskeleton consists of several groups of intracellular structures that meet this definition. Today we know for FtsZ, FtsA, MreB, Crescentin, ParM, ParR, SopA SopB, BtubA/B, MinCDE system…Using new visualization techniques, further progress in this field is expected be achieved. Since few years ago it is known that bacterial cytoskeletal homologs exist for all of the main groups of eukaryotic cytoskeletal proteins, i.e., the actin, tubulin, and intermediate filament (IF) groups. However, important differences between the eukaryotic and prokaryotic cytoskeletal systems have also emerged. These include the discovery that there is at least one major group of bacterial cytoskeletal elements, the MinD/ParA group, that has no known eukaryotic counterpart and the finding that analogous functions are frequently carried out by different cytoskeletal classes in eukaryotes and prokaryotes, often using different mechanisms. Cytoskeletal elements play essential roles in cell division, protection, shape determination, and polarity determination in various prokaryotes. [19, 20,21,22].

1.1.2 Cell membrane

This is relatively fluid phospholipid bi-layer several nm thick, consisting of long chain fatty acids as hydrophobic tails directed inside, and phosphoric acid as hydrophilic part on membrane surface. Glycolipids, hopanoids and very rarely cholesterol are arranged inside. There are numerous proteins moving within or upon this layer that are primarily responsible for transport of ions, nutrients and waste across the membrane. This construction is much like the cytoplasmic membrane of other (e.g. prokaryotic) cells [23] as shown schematically in Figure 2.

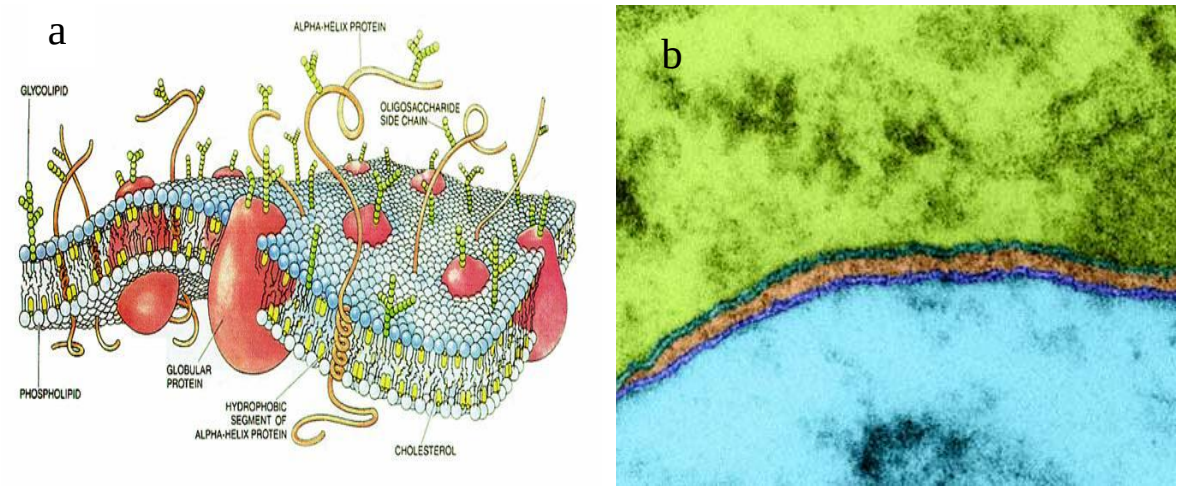

Figure 2: *Bacterial cell membrane*. **a**. schematic diagram, **b**. microphotograph of the lipid bi-layer after staining. [24,25]

Cell membrane has a seemingly contradictory double function. It is strict dividing line between internal compartments of the cell and cell's environment, but at the same time, it has to manage the exchange of substances, energy and information between the cell and the environment. This is a place of action a lot of enzymes, attached especially to interior side (but, some of them outside, too). Many of them are included in production and assembling of numerous components of the other bacterial envelopes.

1.1.3 Bacterial cell wall

Almost all bacteria have this unique structure (opposite to all other living cells). The *Bacteria* (eubacteria), with the exception of the *Chlamydia*, have a semi rigid cell wall containing peptidoglycan. The *Archaea* (archaebacteria), that are often found growing in extreme environments, also have a semi rigid cell wall, but it is composed of chemicals distinct from peptidoglycan, such as protein or pseudomurein. [26] The genus Mycoplasma is the only bacteria that naturally lack a cell wall.

Bacterial cell wall overcoat the cell membrane and is very complex, as shown in Figure 3. Many of bacterial features depend on it. This structure has a protective role, serves as a transport system, enables metabolism, growth and multiplication as well as contact with bacterial environment, and play important role pathogenicity. Cell wall is responsible for maintaining bacterial shape and proves insensibility to osmotic shocks, (e.g. *Bacillus subtilis* can resists pressure up to 50 bar [26]), so this structure give bacteria extreme capability to fit to any influence of their environment.

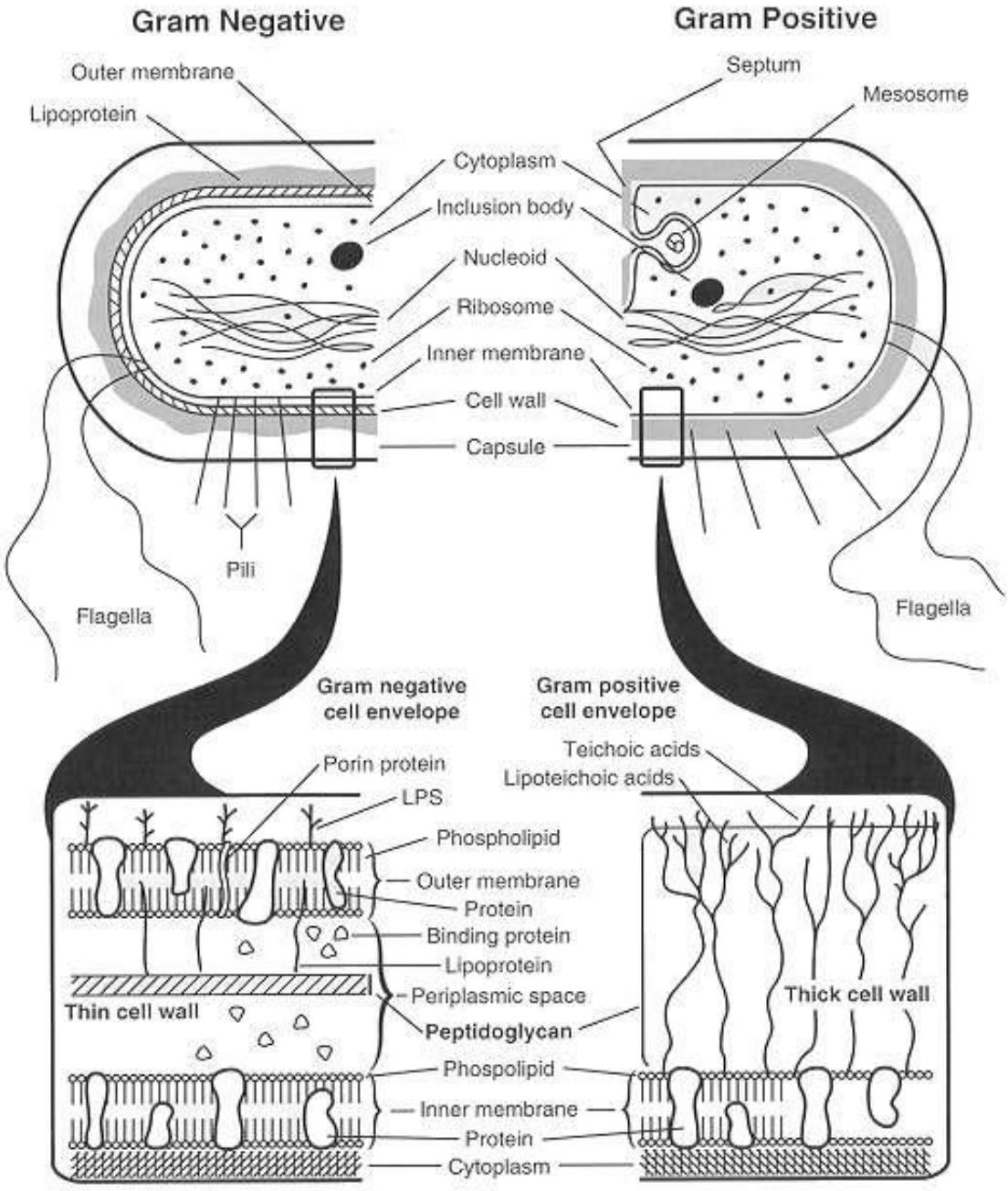

Figure 3: *Schematic structure of Gram positive and Gram negative bacterial cells.* [27]

There are two main different types of bacteria, Gram-positive and Gram-negative, according to capability to adopt different colours by Gram colouring process . Capability to adopt different colours depends on the cell wall structure, which is shown on TEM images in Figure 4. This structure is responsible for many of bacterial features and it is schematically shown in Figure 5. [2]

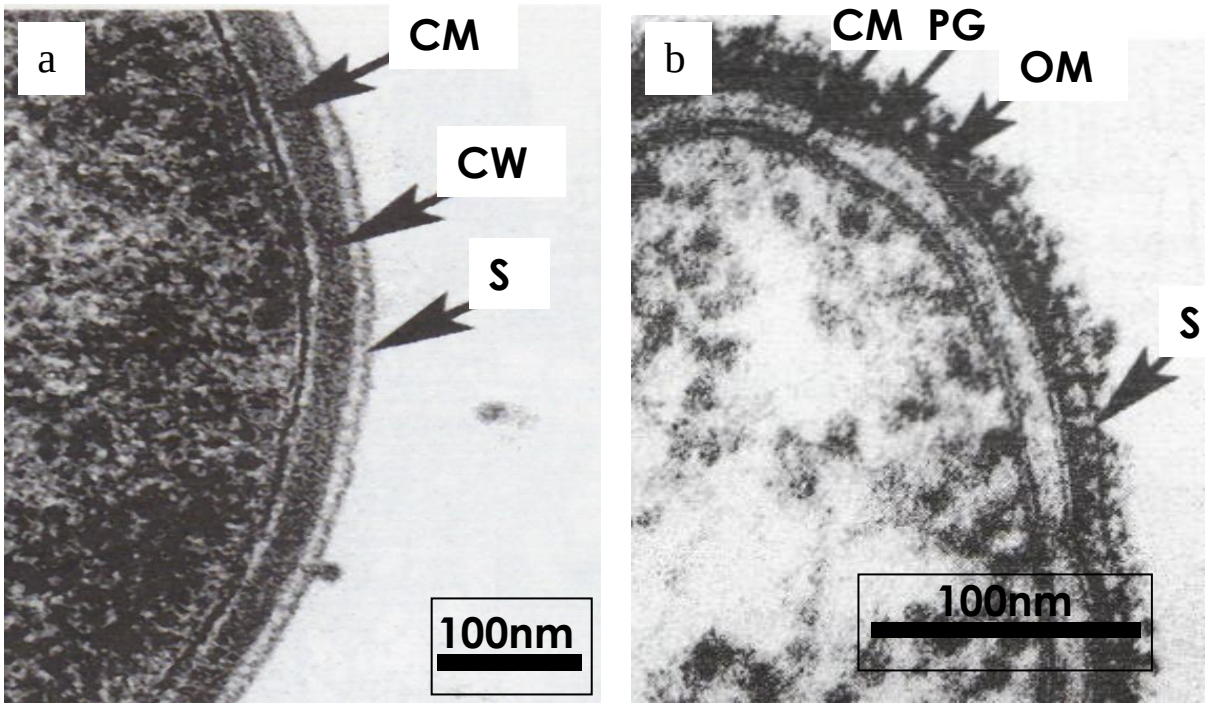

Figure 4: **a.** *TEM microphotograph of Gram-positive cell envelope.* CM cytoplasmic membrane, CW cell wall, S surface layer. **b.** *TEM microphotograph of Gram-negative cell envelope.* CM cytoplasmic membrane, PG peptidoglycan, OM outer membrane, S surface layer. [28]

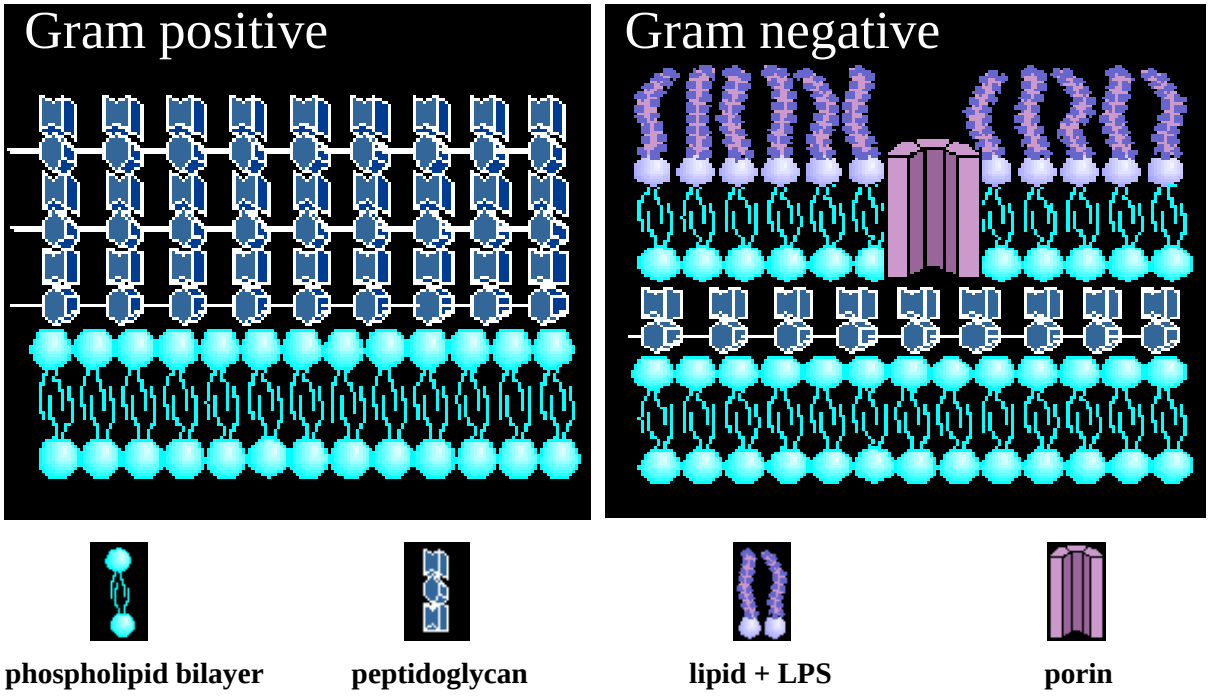

Figure 5: *Different types of the bacterial cell wall* (schematic diagram). [29]

Properties of two main types of the cell wall are shown in Table 1 and major classes of chemical components in bacterial cell wall are shown in Table 2.

Table 1: *Properties of two main types of the cell wall*.*

Property	Gram-positive	Gram-negative
Thickness of wall	20-80 nm	10-20nm
Number of layers in wall	1 (up to 40)	1-2
Peptidoglycan content	>50%	5-20%
Teichoic acid in wall	+	-
Lipid and lipoprotein content	0-3%	25-50%
Protein content	10%	30-40%
Lipopolysaccharide (LPS)	0	35-45%
Sensitive to penicillin	Yes	Less sensitive
Digested by lysozyme	Yes	Weakly

some values are approximate and may vary, depending on various factors

Table 2: *Major classes of chemical components in bacterial cell wall.*

Chemical Component	Examples
Gram-positive cell walls	
Peptidoglycan	All species
Polvsaccharides	*Streptococcus* group A, B, C substances
Teichoic acid	
Ribitol	*S. aureus, B. subtilis, Lacobacillus spp*
Glycerol	*S. epidermidis, Lactobacillus spp*
Teichuronic acids (aminogalactouronc or aminomannanouronic acid polymers)	*B. licheniformis, M. Iysodeikticus*
Peptidoglycolipids (muramylpeptide-polysacharide -mycolates)	*Corynebacterium spp, Mycobacterium spp, Nocardia spp*
Glycolipids (“waxes”) (polysaccharide-mycolates)	
Gram-negative envelopes	
LPS	All species
Lipoprotein	*E. coli* and many enteric bacteria, *Pseudomonas aeruginosa*
Porins (Major outer membrane proteins)	*E. coli, Salmonella typhi murium*
Phospholipids and proteins	All species
Peptidoglycan	Almost all species

Despite the fact that there are two main different types of cell walls, some components are the same for both of them.

1.1.3.1 Peptidoglycan

Peptidoglycan (murein) is a complex polymer, whose structure is schematically shown in Figure 6.

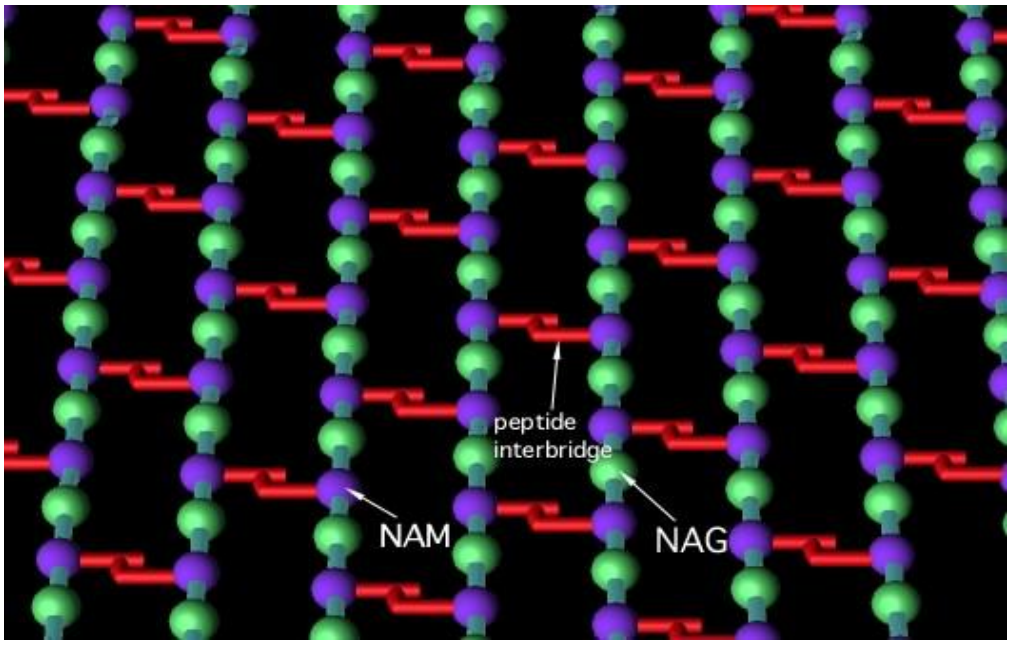

Figure 6: *Schematic structure of peptidoglycan polymer.* [30]

It consists of three parts:

a. the main structure, of repetitively sited peptidoglycan monomer**,** which consists of two amino sugars, connected via β (1,4) glycosidic bond, one of them is N-acetylglycosamine (GlkNAc, NAG), and the other one, N-acetyl muramic acid (MurNAc, NAM), actually glucosamine etherified at O-3 with lactic acid glycan consisting, both together forming glycan chain (Figure 7.)

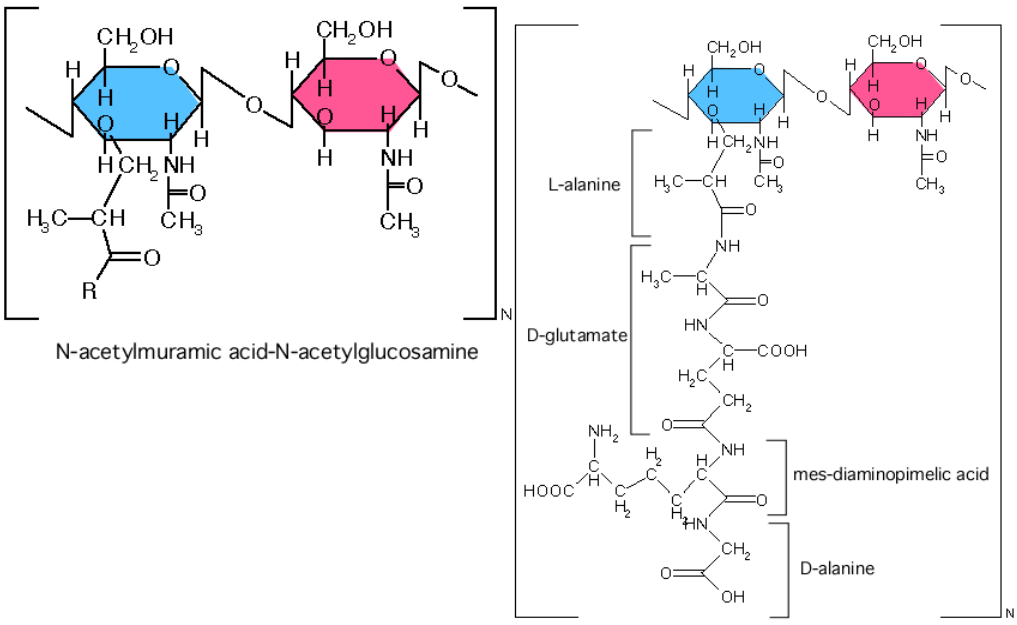

Figure 7: *Chemical structure of peptidoglycan monomer and side tetrapeptide chain.*[31]

b. identical (for each species), collaterally sited tetrapeptide amino acids chains, attached to N-acetyl muramic acid and,

c. cross links of pentaglycine (five molecules of glycine aminoacid) peptide chains between them.

Usually, L-alanine is on **1st,** position, attached to MurNAc as shown in Figure 9, D-glutamine (or replacement for it) is on **2nd,** position. Position **3rd,** it is the most variable. L- lysine or some other L- amino acid can be placed. A lot of Gram-negative bacterial species have meso diaminopimelic acid (DAP) |aminoacid| on this position. Some Gram-positive bacteria have DAP on that position, too. DAP is the element (amino acid) which could be find in bacterial cell wall only. [2] Usually, D- alanine is sited on **4th,** position of side chain as shown in Figures 6. 7. and 8. [26]

Chemical structure and bonds between components of peptidoglycan are shown in Figure 10. (numbers show targets for different enzymes). Cross-linking between peptides of adjacent glycan strands, according to composition and binding, can be possible in two ways. In group A, the cross-linking within the peptidoglycan takes place between position 3 of one and 4 of the other peptide, in those of group B, between positions 2 and 4 of the peptide subunits.

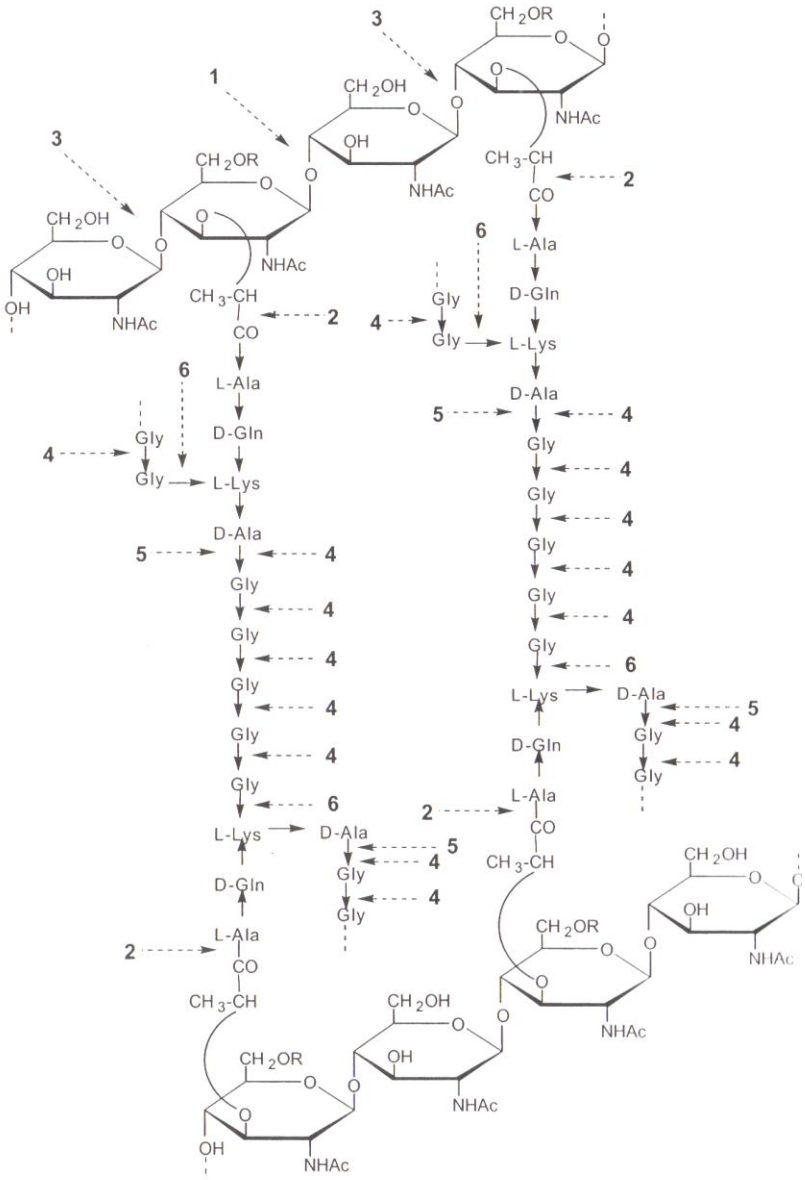

Figure 8: *Chemical structure of the peptidoglycan of Staphylococcus aureus.* Cleavage sites shown: 1 endo-N-acetylmuraminidase, 2 N-acetylmuramil-L-alanine amidase, 3 lysostaphin, 4 and 6 amidase, 5 endopeptidase.

It is found that structure of peptidoglycan is not ideal and microheterogeneicities exist to a great extent. Some of them are relate to different parts of the peptidoglycan. Amino acids in tetrapeptide chain may be different for various bacterial species. More than 100 different peptidoglycan types have been identified, based to a great extent on differences in the peptide moiety. [26] For each species, differences can depend on environmental (cultivation) conditions. For example, some of glycine molecules in the pentaglycine bridge can be replaced with serine, alanine, etc. In some cases, the number of pentaglycine bridges is reduced, resulting in fewer cross-links, so such peptidoglycan possesses a more dispersed structure, as shown in Figure 9. In some Gram – positive bacteria degree of cross – linking is distinctly higher due to multiple layers arrangement. [32]

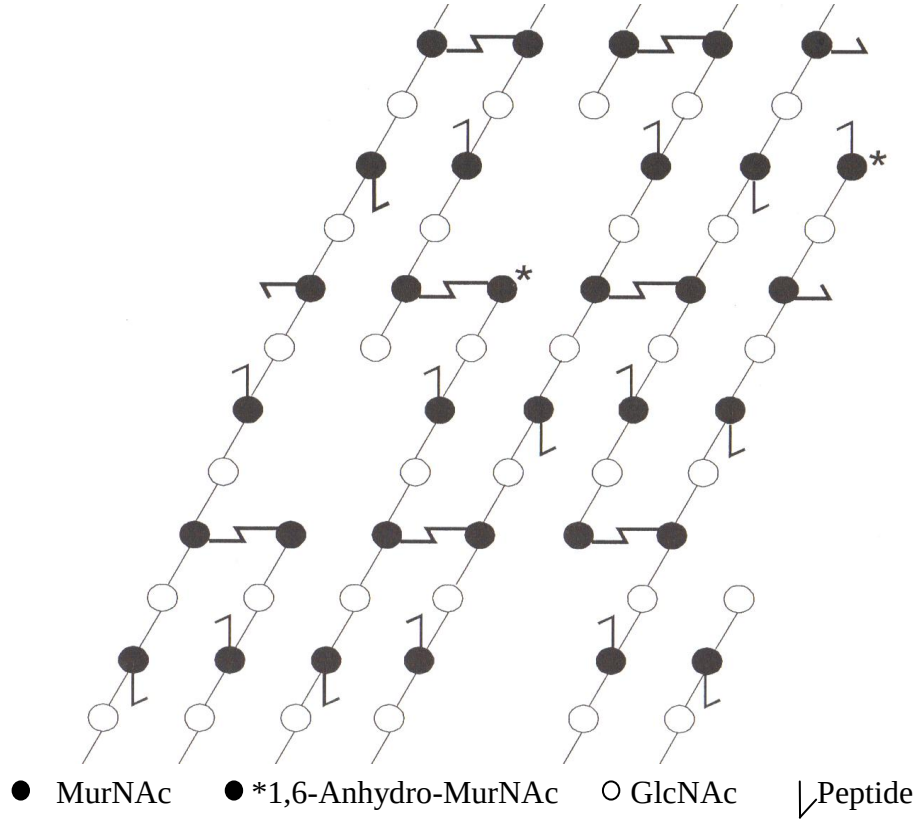

Figure 9: *Schematic spatial structure of the peptidoglycan.* Ends of peptidoglycan chain and cross-links shown

Many of Gram-negative bacteria have direct peptide bounds between DAP of the one side chain, and terminal alanine of the other side chain (lack of pentaglycine). Iregularities can be found at new peptidoglycan insertion sites, too, where hydrolytic enzymes degrading old peptidoglycan and creating acceptors sites. [26] Length of peptidoglycan chains may vary, from one disaccharide unit, to more than hundred. For example, in case of *Staphylococcus aureus*, an average of 15 disaccharide units was found. In case of *Escherichia coli* average chain length of only 9 disaccharide units for about 70% of glycan chains is supposed, and of about 45 units for remaining 30%. [26] It is found that the terminal muramic acid exists in its 1,6-anhydro form (Figure 9).

1.1.3.1.1 Spatial structure of peptidoglycan

Because peptidoglycan chains have cross-links, it was supposed for decades that entire layer functions as a single huge molecule. Initial idea of the spatial structure of peptidoglycan was that of para-crystalline network enclosing the entire bacterium with presumably longitudinal polysaccharide strands arranged in ring shape around the cell and it's cross-linking by peptide bridges. The cross-linked peptidoglycan molecules form a network, which covers the cell like a grid, as shown in Figures 6 and 9.

Gram-positive bacteria have up to 40 layers of above-mentioned peptidoglycan, which can consists more than 50% of bacterial cell wall. Gram-negative bacteria have one or two peptidoglycan layers only, which form 5–20 % of their cell wall.

Koch [33] supposed that saccharide chains and peptide bridges form hexagonal structures – tesserea (shown in Figure 10) which are fused together to form patches of a covalent structure. These patches are linked together by peptide bonds to cover the cell.

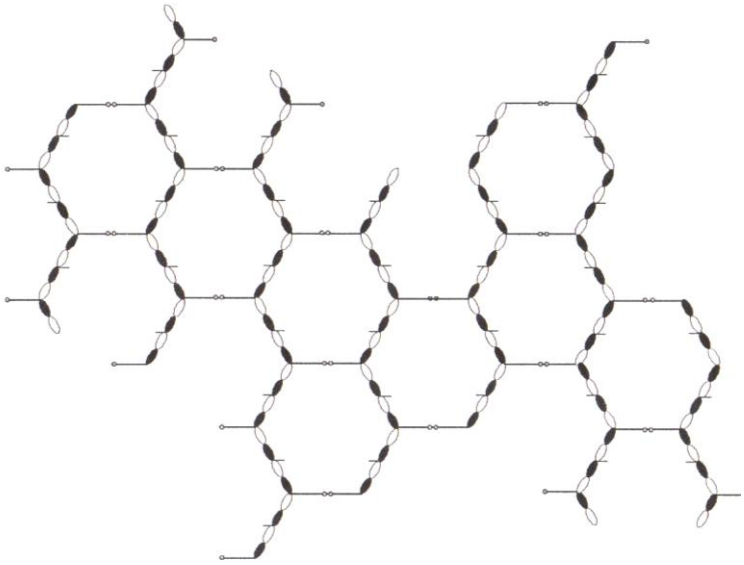

Figure 10: *Hypothetical structure of a patch consisting of eight tesserea*. [34]

Labischinski et al. [35] proposed a model where the polysaccharide chains of adjacent peptidoglycan layers in Gram – positive bacterial cell wall are parallel to the cell surface, but do not point in the same direction. The resulting diverse spatial orientations of the single peptodoglycan layers additionally stabilise the cell wall.

Dimitriev et al. have proposed a fundamentally new model of peptidoglycan of the cell wall, in which glycan strands are arranged not parallel, but vertically to the cell wall plane, and every strand is connected with four others by the peptide bridges placed within the cell wall plane. In Gram – negative bacteria the thickness of the layer corresponds to the height of one turn of polysaccharide helix (four disaccharide units; 3,92 nm), which is necessary to complete cross-linking. In the Gram-positive bacteria the glycan strands comprise 100-200 disaccharide units and are cross-linked throughout the entire length. In this way, a thick matrix with helix-shaped channels is formed that harbor either teichoic acids or lipoteichoic acids piercing outwards through the wall. [36]

1.1.3.2 Specific components of Gram-positive bacterial cell wall

Beside peptidoglycan, there are some structural components, specific for Gram-positive bacterial cell wall. Gnenerally, complex polysaccharides called teichoic acids, acid polysaccharides and proteins can be incorporated in cell wall of Gram positive bacteria. Their composition differs in various types of bacteria.

1.1.3.2.1 Teichoic acids family

A lot of Gram positive bacterial species have specific complex polysaccharides, teichoic acids and teichuronic acids (produced if the bacteria grow under phosphate-deficient conditions), which can be up to 50% of complete cell wall. These components are specific structures in the Gram-positive cell wall, which represent the long, thin molecules that weave through the peptidoglycan. These molecules are the phosphodiesters polymers of glycerol or ribitol joined by phosphate groups. Poly-(Polyolphosphate)-Teichoic Acids and Poly-(Glycosilpolyolphosphate)-Teichoic acids can be found. Monocaccharide molecules (manose, glucose, galactose etc.) are connected in repeating building units. Aditionally, glucose and amino acids such as D-alanine can be attached as substituents on free –OH groups. The chemical formula of the teichoic acids is shown in Figure 11. Teichoic acid can be directly covalently linked to muramic acid via simple phosphodiester bridge or, in some cases, with binding unit (glycerol phosphate represents common component) inserted between them, so it can stitches various layers of the peptidoglycan mesh together.

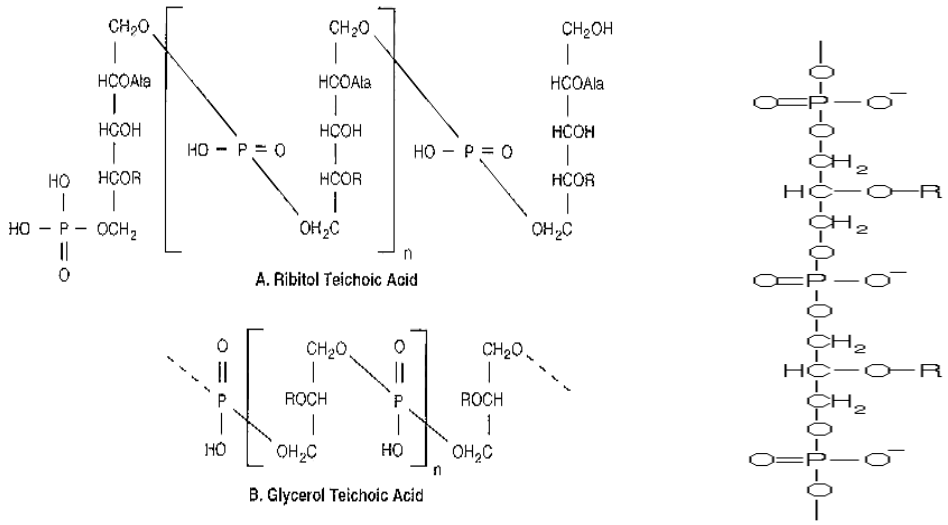

Figure 11: *Chemical structure of teichoic acids.* [37]

There are two types of teichoic acids in the cell wall: teichoic acids of the wall, covalently connected to peptydoglycane, and teichoic acid of the cell membrane which have lipid component (lipoteichoic acid), additionally anchored to membrane's glycolipides by hydrophobic forces. [38] All of these molecules are negatively charged and can bind metal ions, mainly Mg^{2+}, Ca^{2+} and K^{+}. Teichoic acid stabilizes the cell wall and makes it stronger. It plays an important role in growth and division of the cell, [26]. Also, these molecules prove hydrophillicity of cell surface and have protective functions.

1.1.3.2.2 Acid polysaccharides

Acid polysaccharides are the group of polysaccharides in Gram – positive bacterial cell wall that include sugar phosphate polymers, anionic polysaccharides and lipoglycanes. Sugar poly phosphate polymers may consist of repeating units of 1 – 8 monosaccharides linked via phosphodiestar bridges. Monosaccharides can be glucose, galactose, manose rhamnose etc. Anionic polysaccharides contain acid groups as side chains such as glycerol phosphate, organic acids (pyruvic and succinic) or sulfate that provide the polysaccharides with strong negative charge. Lipoglycans differ from polymers described above due to the fact that they are bound to membrane via hydrophobic parts. They consist of linear or branched homo- or heteropolysaccharides and may have glycerol phosphate as side chains.

1.1.3.2.3 Proteins

These components incorporated in Gram – positive cell wall represent complex high molecular compounds, which are completely or mainly composed of amino acids. According to their polarity and electric charge, essential amino acids can be divided into non-polar hydrophobic, polar uncharged and charged amino acids. These features of the amino acids are of great importance for spatial structure and placement of the proteins inside bacterial cell wall. Amino acids are connected by peptide bonds between carboxylic group of the first one and amino group of the next amino acid, so they form linear chains. Branching is not possible. It represents primary structure of the protein.

The expression of secondary structure stands for the conformation of the basal scaffold of the peptide chain. The three-dimensional arrangement of the polypeptide chains is called tertiary structure. Low-energy linkages as well as mainly hydrophobic linkages and hydrogen bridges, but also ionic and van der Waals bonds, play an important role in the stabilization of this structure. Essential is stabilization and fixation by S-S bridges between two cysteine residues. Because of the fairly low energy of its stabilizing linkages, the tertiary structure is a rather labile arrangement. Various agents can disrupt this structure. However, in accordance with the fact that the tertiary structure is determined by the primary structure and mostly represents a structure with lowest energy, a complete re-naturation is possible under suitable conditions.

The association of several peptide chains to a defined complex represents quaternary structure. Primary, secondary, tertiary and quaternary structures are very important for placement and function of membrane proteins. They have structural and functional duties.

According to their functions, two types of proteins in Gram – positive cell wall can be distinguished. The first group represents those located between periplasmic membrane and peptidoglycan layer, in a space similar to the periplasmic space of Gram – negative bacterium [39], which have biosynthetic functions. In

the other group are proteins placed further outside which interact with the bacterial environment. Three categories of surface proteins can be differentiated: 1) those that anchor at the C – terminal end of the molecule, using to span cytoplasmic membrane, 2) those that bind by their charge or by hydrophobic interactions and 3) those that are fixed via their N – terminal region (lipoproteins). [26]. The proteins of the first group usually consist of three regions, a C – terminal anchor region, a wall associated region and a surface – exposed region and they are responsible for various biological effects. Many of them have a so–called sorting signal (sequence). The second group mainly consists of enzymes such as isomerases, dehydrogenases, kinases, mutases, enolases etc. Proteins from the third group may play a role as adhesins in the infection process.

There are various types of proteins in various Gram – positive bacteria. For example, in genus S*treptococcus* can be found M – proteins, T – proteins, OF apoproteinase, and also enzymes neuraminidase, β-N-acetylxehosaminicase, β-D-fructosidase and dextranase. In genus *Staphylococcus* protein A, clumping factor (coagulase) and collagen – binding protein are described. Both of these genera have fibronectin – binding proteins. Both of them possess various other types of proteins, which can bind different host proteins. [40]

Almost all of these proteins are synthesised at polysomes, an arrangement of several ribosome, bound at the inner layer of cytoplasmic membrane and subsequently exported to the various places of the bacterial cell wall. In the cell wall, proteins are mostly covalently bounded.

1.1.3.3 Specific components of Gram-negative bacterial cell wall

The cell wall of Gram-negative bacteria is much thinner, but much more complex and, consisting only up to 20% peptidoglycan. Gram-negative bacteria also have two unique regions, which surround the plasma membrane: the periplasmic space and the outer membrane.

1.1.3.3.1 Periplasmic space

The periplasmic space is the region between cytoplasmic and outer membrane (pointed between arrows in Figure 12.). It contains a concentrated gel – like matrix, periplasma, consisted of aqueous solution of mono and oligosacharides, amino acids, peptides, peptidoglycan precursors, other small molecules and enzymes that can destroy potentially dangerous foreign matter present in this space. Calculated volume of this space is 8 – 16% of total cell volume. Embedded in it, covalently linked to outer part of the cell wall, a rigid peptidoglycan layer is placed.

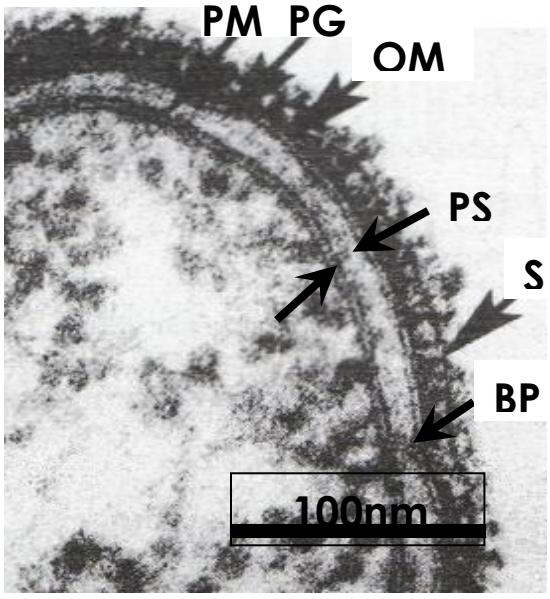

Figure 12: *TEM microphotograph of Gram – negative bacterial cell wall.* OM Outer membrane, PG peptidoglycan, CM cytoplasmic membrane, S surface layer, PS periplasmic space pointed between arrows, BP Bayer's patches. [28]

It seems that cytoplasmic and outer membranes are connected with adhesion zones through periplasmic space, so – called Bayer’s patches.

1.1.3.3.2 Outer membrane

Adjacent to the exterior peptidoglycan layer, complex bi-layer structure similar to that in the cell membrane is located. In various bacteria, different types of lipids (glycerolphospholipids, glycolipids, hopanoids…) as well as proteins can be incorporated inside, and all together form the structure what is known as outer membrane. This structure is much more asymmetrical than cell membrane. [41]

Inner leaflet of outer membrane consists of phospholipids and proteins. Outer one consists of polysaccharides connected with lipids – lipopolysaccharides (LPS), specific polysaccharides, proteins and very small (if any) amount of phospholipids. This structure is attached to the peptidoglycan by Braun's lipoproteins (see Figs. 21). On average, outer membrane consists of 35-45% of lipopolysaccharide (LPS), 30-40% of proteins and 25% of lipids.

1.1.3.3.2.1 Lipopolysaccharides (LPS)

Like many components of the cell wall, LPS, whose chemical structure is shown in Figure 13, contain anionic amphiphilic substances. They consist of a hydrophobic and a hydrophilic part.

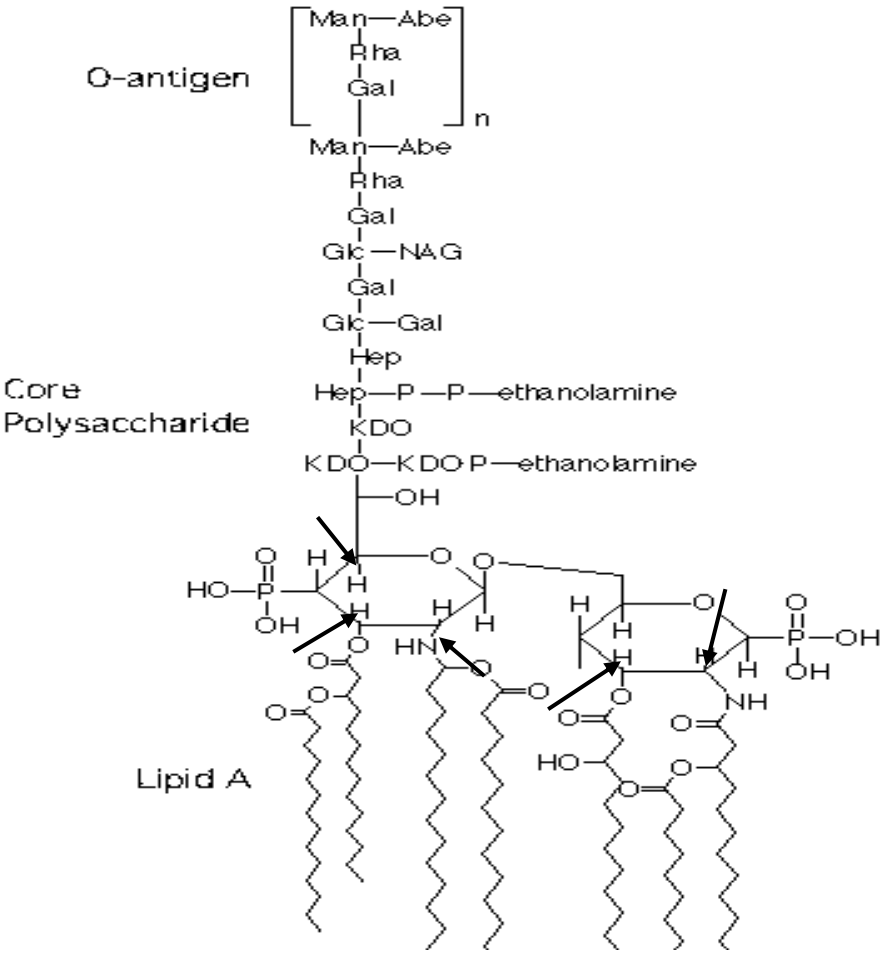

Figure 13: *A chemical structure of LPS*. Binding sites for fatty acids and Kdo pointed with arrows. [42]

Hydrophobic part of LPS, Lipid A, represents in most but not all cases endotoxic centre of LPS, as well as hydrophobic anchor for its incorporation into the outer membrane. This part of LPS does not occur in the free form but can be deliberated by mild hydrolysis. It has a relatively stabile structure, consisting of a phosphorylated N-acetylglucosamine (NAG) dimmer. Six or seven long chain fatty acids, pointed in some direction, can be attached on 2, 3, 2′ and 3′ sites, while position 6′ is a binding site for the first Kdo of the core region. (shown by arrows in Figure 13.) The hydrophilic part represents often a long chain of polysaccharides consisting of two different regions, which are called the core region and the O-specific polysaccharide (shown in Figure 13.). The latter elongates into surrounding medium away from the bacterial surface.

Core region is a highly conserved polysaccharide part of LPS, which consists of two different parts, i.e. the inner core (heptose-Kdo-region) and the outer core (hexose region), shown in Fig. 14.

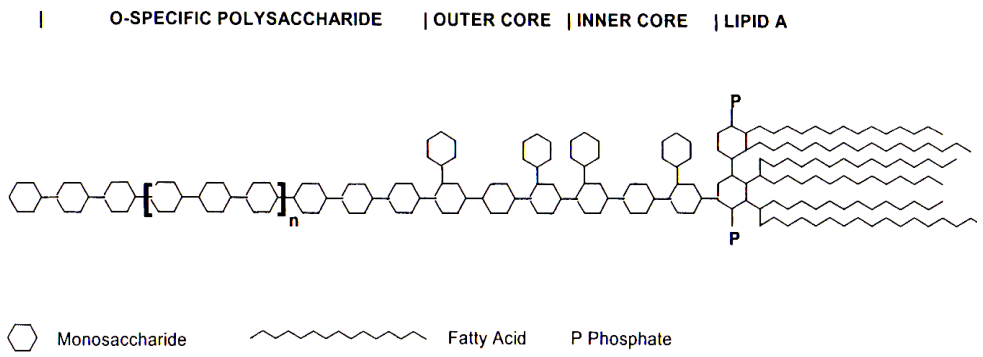

Figure 14: *Schematic structure of LPS.* [26]

The high degree of phosphorylation together with the carboxyl groups of the Kdo molecule create an important preponderance of high negative charges in this region being important for the function of LPS as a components of the outer membrane. Several core types are found in LPS of different Gram–negative bacteria. [43] In R–forms (rough forms) of bacteria, core region is most prominent in outer space.

In so – called S – form (smooth form), which represents wild type (usual) of the most of Gram – negative bacteria, most prominent to outer space, is an extremely variable O-polysaccharide antigen. O-antigen is present in S – type of bacteria only. It can be up to 90% of the whole LPS amount. It consists of polysaccharides with 20 – 40 repeating units containing two to eight monosacharides. These sugars present in O-antigen may vary greatly, even within single species. The structures of several hundred O-specific polysaccharides from various bacteria have been elucidated. [44] Polysaccharides that extend out from the bi-layer also contribute to the toxicity of the LPS. [26]

In outer membrane, part of LPS is hydrophobically bound, the rest via Mg^{2+} and Ca^{2+} bridges. LPS molecules held together by hydrophobic bonds and Me^{2+} bridges in the membrane plane, by the high number of Me^{2+} bridges between the anionic groups of the inner core region, as well as by hydrogen bridges between the polysaccharide chains of the LPS. [26]

1.1.3.3.2.2 Enterobacterial common antigen (ECA)

Similar to LPS, ECA represents polysaccharide with ampihphilic character. It is found in all enterobacteria (Gram – negative bacteria living in bowl – enteron in old Greek). It is linked to LPS in the outer membrane partly via hydrophobic, partly via covalent bonds in its haptenic form. In its immunogenic form ECA is covalently linked to the core of LPS carrying no O-specific chains. All ECA forms consists of repeating units of the structure **→3)-α-Fuc*p*4NA(1→4)-β-ManN*p*AcA-(1→4)-α-Glc*p*NAc-(1→**.

1.1.3.3.2.3 Proteins of outer membrane (OMP)

These proteins can consist up to 50% of the total mass of outer membrane of Gram - negative bacteria. Mostly, they are in α-helix and β-sheet structures (which represent secondary structure). In the case of α-helix, peptide chain appears in the form of screw shaped, coiled structure. The β-sheet structure is created in such a manner that H bridges are between parallel running peptide chains. Membrane proteins of Gram – negative bacteria express specific tertiary structure. Generally, for energetic reasons, peptide chains in the proteins are arranged in such a way that the hydrophobic regions point inwards. However, membrane proteins, especially the integral, trans-membrane ones, are exceptional since they are located in a hydrophobic environment, so they are hydrophobically bound. Proteins can be found in the Gram – negative cell wall in various chemical compositions such as glycoproteins, lipoproteins and phosphoproteins, too.

According to their function, membrane proteins appear in several forms. Channel-forming proteins, (porin proteins, specific channels forming proteins OmpC, OmpF, PhoE) play an important role in the nutrients supply of bacterial cell and the disposal of metabolic waste products. High affinity receptor proteins serve as high affinity transporters for the uptake of substances like Fe^{3+} ions or vitamin B_{12}. Structure proteins (Braun's lipoprotein, OmpA protein) anchor outer membrane to peptydoglycan and stabilize it, especially in conjunction with LPS, because LPS are necessary for the correct orientation of the proteins. There are some other types of proteins with various functions in different regions of membrane.

Similar as proteins of Gram – positive bacteria, those of Gram – negative bacteria are synthesised at polysomes at the inner layer of cytoplasmic membrane and subsequently exported.

1.1.3.4 Cell wall models

Beside the fact that producing of the cell wall is genetically determined, its composition and structure is not invariable. It can vary, depending on cell age, composition of surrounding medium, pH, redoxpotential, and some other parameters.

On the basis of various experimental techniques, a number of models of Gram – positive and Gram – negative cell walls have been developed in the past. In the light of the present knowledge, it is reasonably to say that any of them represent only an average of several possible structures. So we can conclude that, at this moment, there is no general, precise, and exact model of the bacterial cell wall. All the models developed until now postulate existence of one, electron dense, structure called peptidoglycan, which vary in thickness, depending on the type of the bacteria. Its composition and spatial orientation is described above. Various models deal with composition and structure of peptidoglycan, as well as some other components of the cell wall.

Here, we will present some of newly developed models of Gram – positive and Gram – negative cell walls.

1.1.3.4.1 Cell wall models of Gram – positive bacteria

The Gram – positive cell wall is thick and relatively simply structured. In electron microphotographs of cell envelopes of this type of bacteria, two or three electron – dense regions can be seen (see Fig. 4a). The innermost is cytoplasmic membrane, more outside is located cell wall and finally, if present at all, a surface layer is observed.

Recently, models assuming a mosaic – like cell wall structure, have been proposed. [45] According to these models, the Gram – positive cell wall consists of only one thick layer, which is not homogenous (Fig. 15).

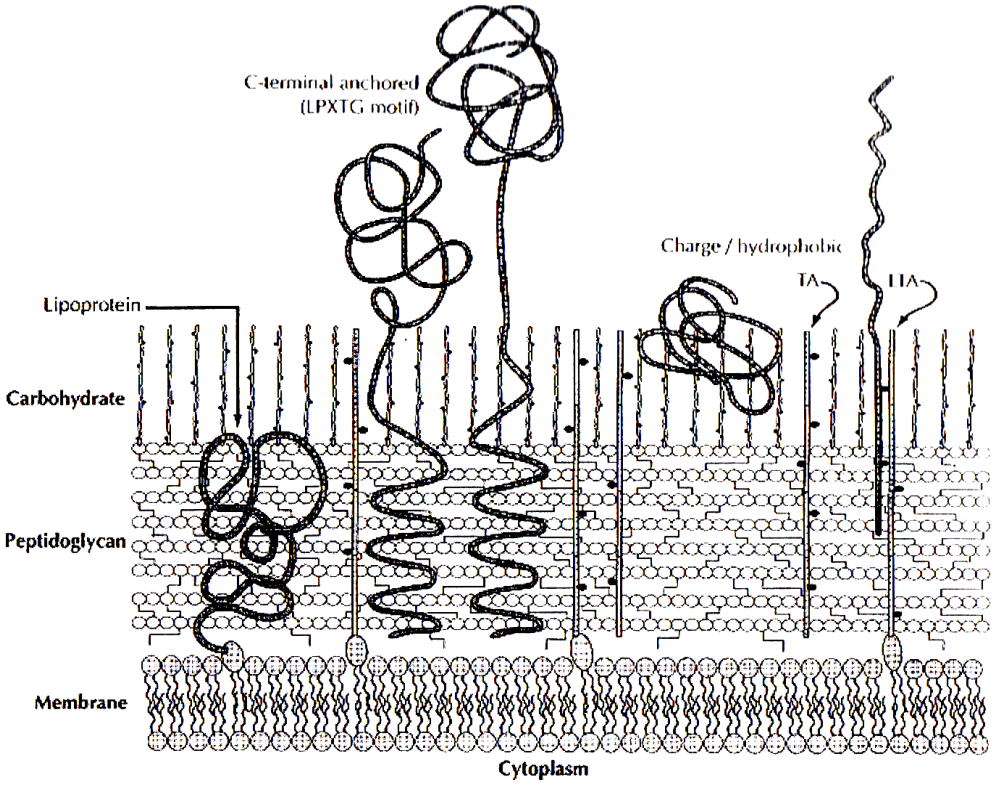

Figure 15: *Model of the Gram – positive cell wall according to Fischetti et al.*

All components more or less penetrate each other, however, proteins and polysaccharides are more predominantly present in the outer part and the peptidoglycan predominantly located in the inner region of

the cell wall. The long glycan strands of teichoic, teichuronic or membrane bound lipoteichoic acids, are assumed to more or less span the whole layer. Some proteins are covalently bound to the peptidoglycan but simultaneously detectable on the surface. Other proteins (e.g. proteins M and A) are fixed in the peptidoglycan layer, may form fibrils that protrude outwards from the cell surface. They are non-covalently attached to the cell wall, for instance to lipoteichoic acids.

As mentioned above, Dimitriev et al. published completely new concept of the cell wall in which glycan strands are arranged not parallel, but vertically to the cell wall plane, and every strand is connected with four others by the peptide bridges placed within the cell wall plane. (Fig.16)

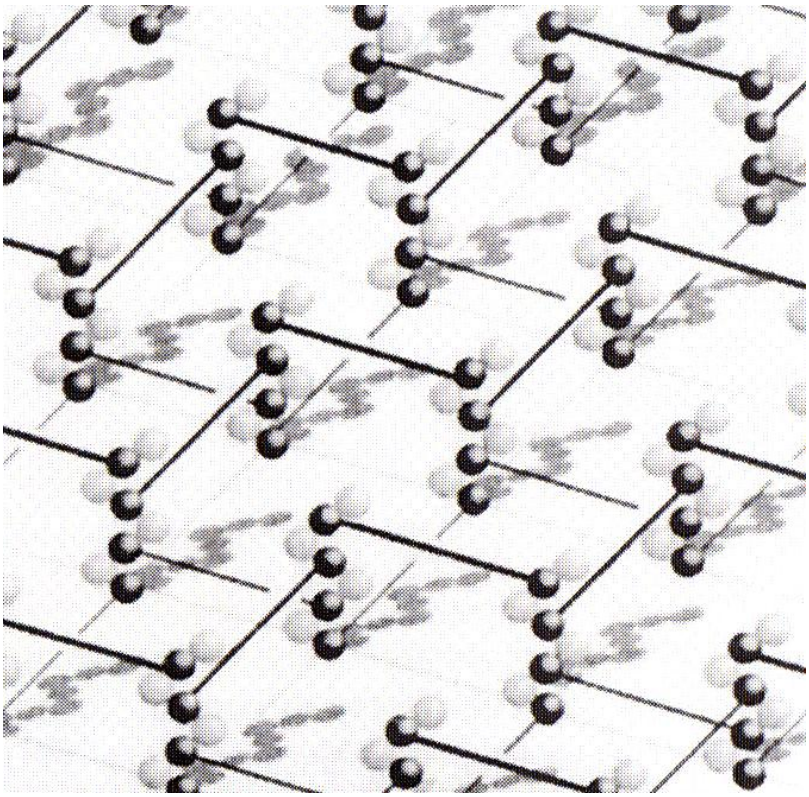

Figure 16: *Model of the peptidoglycan proposed by Dimitriev et al.* **Black balls** MurNAc; **white balls** GlcNAc; **straight lines** peptide bridges in the upper turn of the helix. For reasons of clarity, only the short saccharide chains of the Gram –negative bacteria are outlined; those of the Gram – positive cell wall are much longer (100 – 200 disaccharides). [36]

In the Gram-positive bacteria the glycan strands comprise 100-200 disaccharide units and are cross-linked throughout the entire length. In this way, a thick matrix with helix-shaped channels is formed that harbor either teichoic acids or lipoteichoic acids piercing outwards through the wall. According to this model, the thickness of the layer in Gram – negative bacteria corresponds to the height of one turn of polysaccharide helix (four disaccharide units; 3,92 nm), which is necessary to complete cross-linking.

1.1.3.4.2 Cell wall models of Gram – negative bacteria

Electron micrographs of Gram – negative bacteria show three or four electron-dense regions in the cell envelope (see Fig. 12). The innermost is cytoplasmic membrane. Outermost is outer membrane, and between them, in liquid periplasmic space, rigid peptidoglycan layer is placed. Sometimes, S-layer can be present at the surface of the outer membrane.

At the model of the Gram – negative cell envelope published by DiRienzo et al. (shown in Figure 17), a new concept of protein pores present in the outer membrane is developed. The pores consist of trimers of the so-called matrix proteins, which are stabilized by lipoproteins and arranged in such a manner that they form one membrane-spanning channel at its axis.[46]

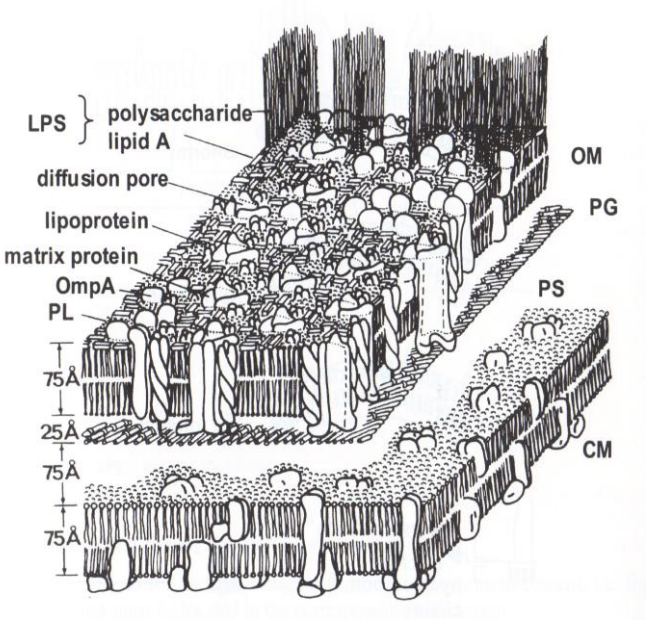

Figure 17: *Model of the Gram – negative cell envelope according to DiRienzo et al.* PL phospholipids, OM outer membrane, PG peptidoglycan, PS periplasmic space, CM cytoplasmic membrane.

It was postulated that the cell surface is not homogenously covered by the O-specific polysaccharide chains of LPS, but rather contains isle structures. Complex of Braun's lipoprotein with one of major proteins (OmpA) stabilize complete structure.

In the cell wall model of Hancock et al. (Figure 18.) proportions and the spatial arrangements of the individual cell wall components were exactly determined to the molecular dimensions.[47]

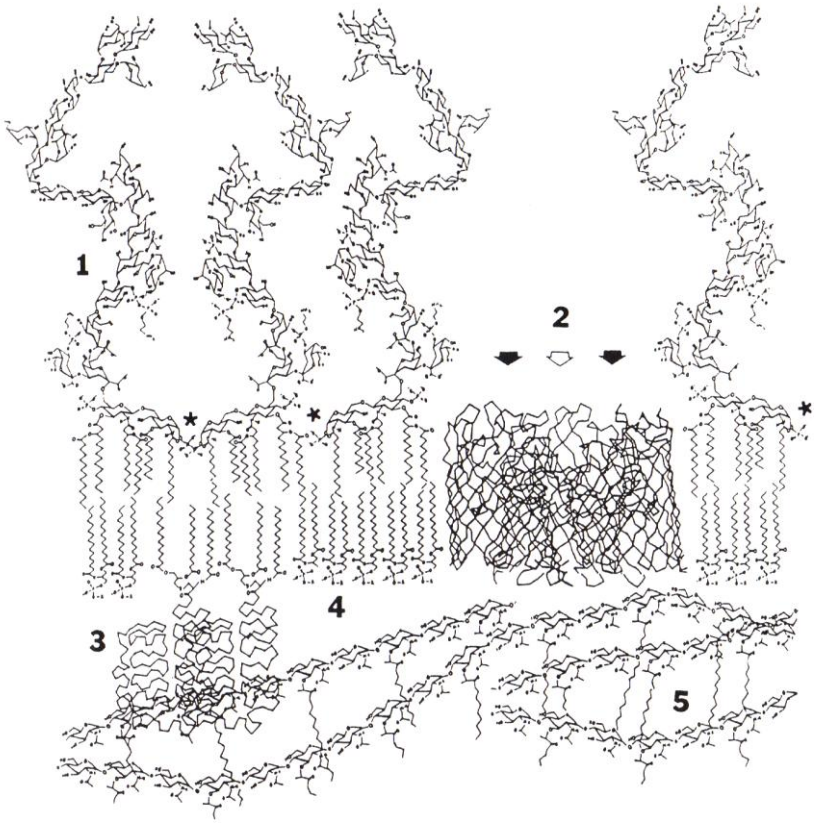

Figure 18: *Model of the Gram – negative cell envelope by Hancock et al.* 1 LPS, 2 trimeric OmpF-porin, 3 Braun's lipoprotein, 4 phospholipid, 5 peptidoglycan, * bivalent cation.

It should be kept in mind that those models are static by nature. Hydrocarbon chains in the lipid bi-layers adopt a number of spatial arrangements. Phospholipids in inner leaflet are fluid, while LPS layer furnishes a highly ordered quasi-crystalline structure with very low fluidity. Additionally, both components appear in two thermal phases: the ordered gel – like β – phase in which the fatty acid chains are all – *trans* arranged, and the more fluid liquid – crystalline α – phase, in which *gauche* conformations appears.

1.1.4 Other structures

1.1.4.1 S – layers

Surface layers (so called S – layers with S from surface) are composed of identical protein or glycoprotein molecules, aggregated to crystal – like planar structures, which cover the entire cell surface. Someone described it like "periodic macromolecular monolayer". [48] S – layers are wide – spread in both Gram – positive and Gram – negative bacteria. They form, depending on their origin, 5-25 nm thick square hexagonal or oblique – angled lattices on the cell surface (Fig.19).

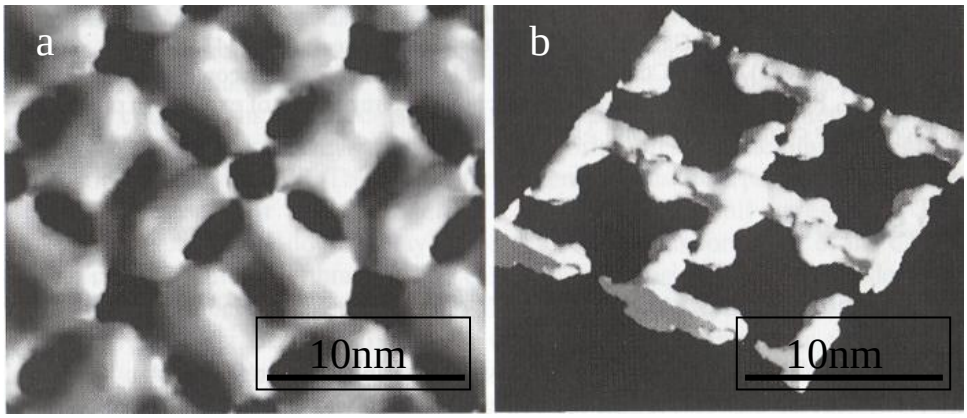

Figure 19: *Electronmicrograph images of different types of S-layers.* (Bar length 10nm) [49]

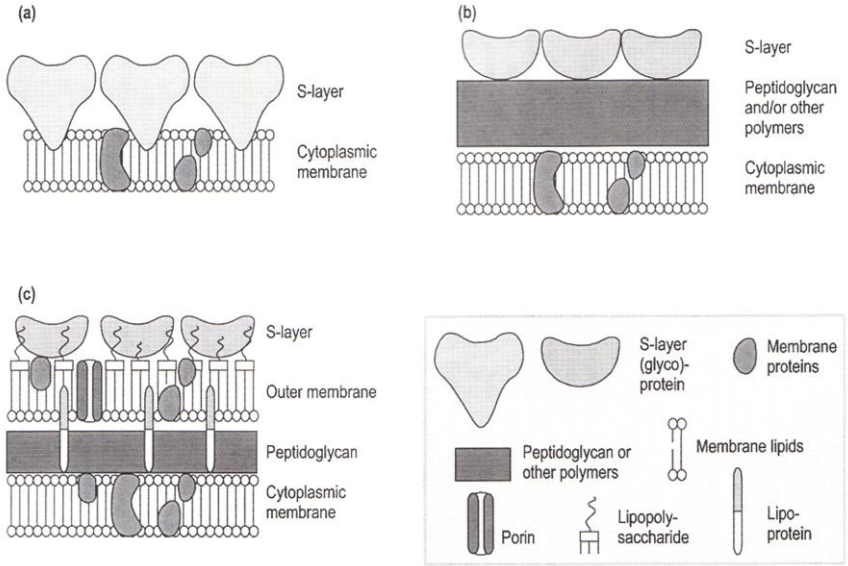

Figure 20: *Schematic illustration of the supramolecular architecture of the three major classes of prokaryotic cell envelopes containing S-layers.* a. Gram-negative Archaea; b. Gram - positive Archaea and Bacteria; c. Gram-negative Bacteria. [50]

They form pores, which in a given S – layer, are identical in size (diameters mostly between 2 – 8 nm) and the pores occupy up to 70% of the surface. Position of S layers and their supramolecular architecture at main types of bacteria is shown in Figure 20.

This structure is assembled by auto aggregation of mostly identical subunits, joined to each other and to the underlying layers (peptidoglycan, teichuronic acid, LPS…) by non-covalent bonds (electrostatic, hydrophobic or in the case of negatively charged S – layers also via Me^{2+} bridges). The functions of S – layers have not yet been revealed completely. It is supposed that they could serve as a mechanical and chemical protection, have stabilizing features, can create a kind of periplasmic space, bind small cations and cell – associated exo – enzymes etc.

1.1.4.2 Capsule

The general term for any network of polysaccharide or protein containing material extending outside of the bacterial cell is the glycocalix. Many bacteria produce such a coating on the outside of their cell, and they come in two types: capsules and slime layers. The structure can be pretty thick as shown in Figure 21a, or thin as shown in Figure 21b, rigid or flexible. The difference between the two is somewhat arbitrary. A capsule can be closely associated with cells and does not wash off easily, because it is fixed to the cell wall mostly through ionic and hydrophobic interactions. It seems that capsular polysaccharides (CPS) and LPS may interchelate and interact with each other on bacterial surface of Gram – negative bacteria. Some strains have Kdo or phosphatidic acid as linkage component for lipids of the cell wall. [26] A slime layer is excreted from bacteria and sometimes is more diffuse and easily washed away.

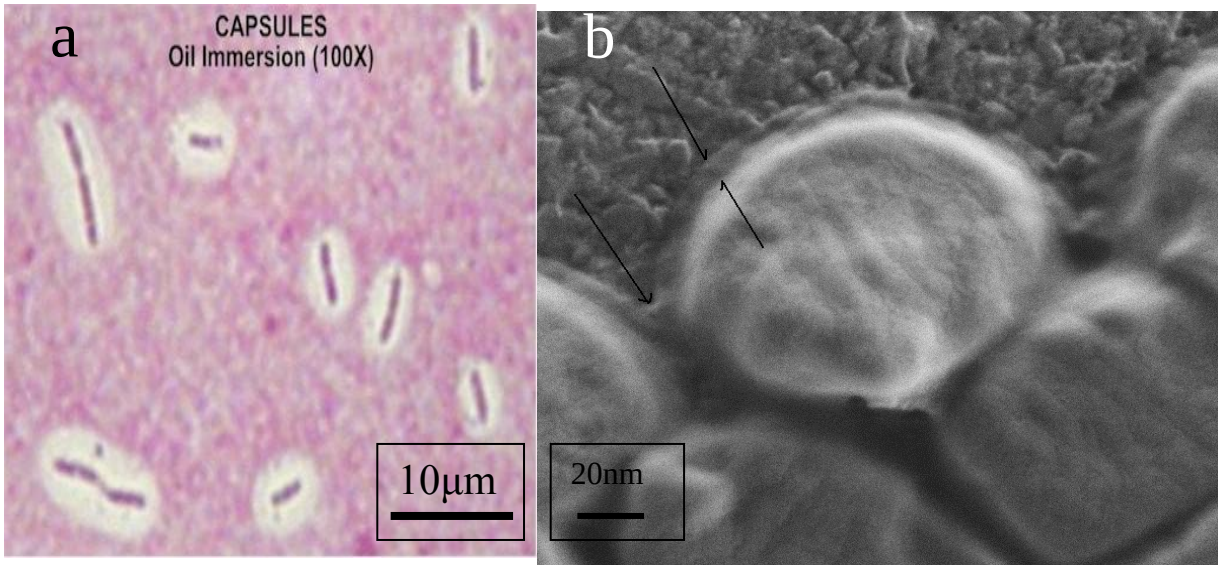

Figure 21: *The capsule structure.* **a.** Visible as colorless zone around bacterial cells by light microscopy, Gram stained, **b.** Visible as a thin zone around the cell in SEM microphotograph, all pointed with arrows.

Capsule has an adhesive and also a protective role. This layer of polysaccharides, in the most cases acid, (sometimes proteins, poly alcohols or amino sugars) protects the bacterial cell and is often associated with pathogenic bacteria because it serves as a barrier against attack by a host's immune system. [51] In addition, capsules and slime layers are negatively charged and largely hydrophilic, so they can bind extra water in the environment and contribute to the protection of the cell from desiccation. Capsules and slime layers can also provide protection from the loss of nutrients by holding them within the layer. These extra layers coating the surface of the cell may also potentially mask viral receptors, making it more difficult for viruses to attach.

Many of these functions manifest themselves in the form of bio-films, which allow for formation of communities of microorganisms all held together by glycocalyx.

1.1.4.3 Flagella and pili (fimbriae)

Many bacterial species have filamentous tubular proteinaceous appendages on their surface. They are different in size and function. Under certain conditions, bacterial cell may lose them without losing its own vitality.

Flagella are screw – shaped filaments up to 20 μm long and 10 – 30 nm thick (Figs. 22 and 23). Bacteria can have only one or more flagella, they can be localised polar or peritricheal, and these are type specific features. Flagellum consists of three parts: basal body, flagelar hook and filament. Function of flagella is locomotion.

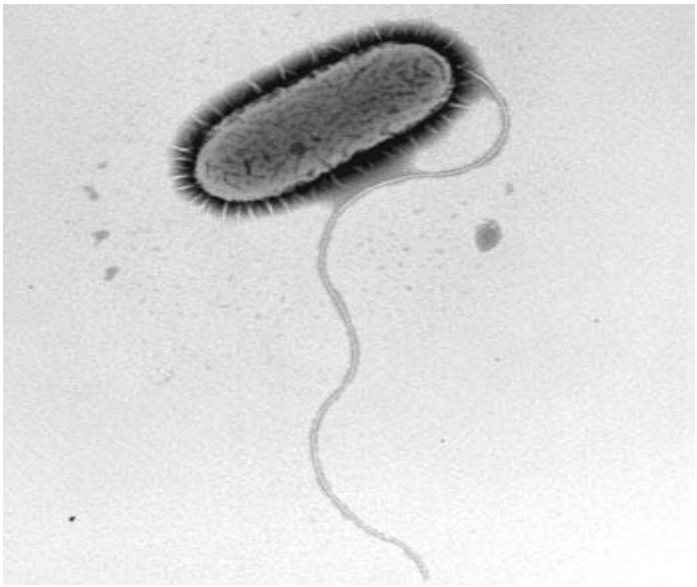

Figure 22: *Flagella and pili.* [52]

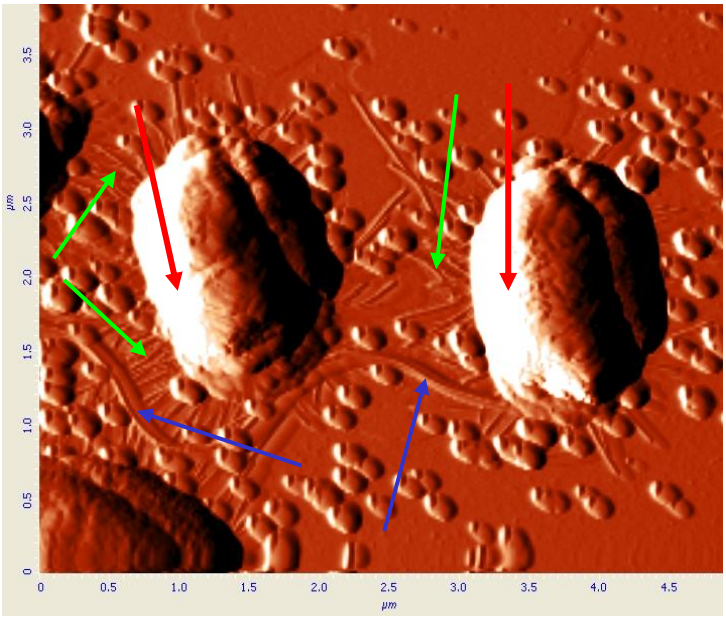

Figure 23: *AFM image of Escherichia coli with flagella and pili.* Bacterial cells red arrows pointed, flagella blue arrow pointed, pili green arrows pointed.

Pili (fimbria) are hair – like appendages, 1 – 2 μm long and up to 10 nm thick (Fig. 23). Their number is significantly higher than flagella and they are dispersed across entire bacterial surface. There are several types of pili. Bacteria mostly use them for adhering to various surfaces, but some specific types serve for transfer of genetic material between two bacterial cells (sex pili).

1.1.4.4 Spore

Some bacteria, like *Clostridium* and *Bacillus*, form structures included in the vegetative bacterial cells, called spores (endospores), shown in Figure 24, which are highly resistant to drought, high temperature and other environmental hazards.

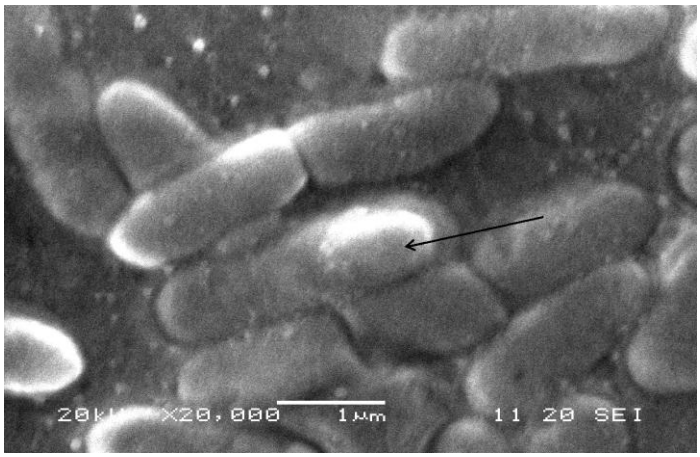

Figure 24: *SEM microphotograph of Bacillus stearothermophilus spore forming.* (arrow)

Endospores can be divided into several important parts. The center of the endospores contains the core and it consists of the cytoplasm, DNA, ribosomes enzymes and everything that is needed to function once returned to the vegetative state. The core is dehydrated, which is essential for heat resistance, long term dormancy and full chemical resistance. The cortex surrounds the core and is composed of two layers, a thin more densely staining layer that is similar in structure to the vegetative cell wall and a thicker less dense layer containing modified peptidoglycan. Outside of the cortex there is the spore coat containing several protein layers that are impermeable to most chemicals. The coat is composed of more than two proteins and these proteins are connected by cross-links.

Each single cell forms only one spore. That structure survives, in cases when the other components of bacterial cell are destructed. [53]

Endospores enable species to spread easily from one suitable environment to another and many endospore-forming bacteria are ubiquitous in the environment. Once the hazard is removed, the spore germinates to create a new vegetative cell, and consequently a new population. In case of using appropriate physical or chemical agents, spores can be destructed.

1.2 Damaging and destruction of bacteria

Although scientific application of antimicrobial agents is limited to past 150 years, empiric practices were more or less effective centuries ago. Though humans did not know anything about microorganisms, they had a need to protect themselves from disastrous illness, such as plague, cholera, variola etc. It has been known from ancient times that in such cases people were burning clothes, smoking the houses by sulphur, boiling water... All of these were usage of antimicrobial agents and application of antimicrobial procedures. Preservation of food by heating, drying, salting, acidifying, are procedures to prevent developing of microorganisms, and eventually killing them. Today, we are using these principles and procedures, too. All of them provide a failure to reproduce, and/or lack of vitality of microorganisms.

It is necessary to explain the term "death of bacterium". We can take Schmidt's statement: »The only single practical criterium is the failure to reproduce when, as far as known, suitable conditions for reproduction are provided. This means that any organism which fails to show evidence of growth when placed under what is considered, in the light of our present knowledge of bacterial nutrition and growth requirements, adequate growth conditions, is considered as death.« [54] This is the most common point of view in microbiology. However, in the destruction of bacterial cells and spores by some physical agents the final objective is to destroy the life processes. The lethal agent is capable of producing changes in the cell that prevent the cell from reproducing (whenever), either by direct effects on reproductive mechanism, by disrupting cellular structures or by disabling cellular metabolic systems that provide energy and chemical intermediates for reproduction.

Types of destruction of microorganisms can be chemical or physical, or combination of them, as shown in Table 3.

Table 3: *Types of antimicrobial processes.* [55]

Type of process	Agent	Application	Comments
Physical	Dry heath (≥160C°)<	Sterilization	less effective than moist heath
	Moist heath (≥120C°)	Sterilization	use of autoclave
	Moist heath (100C°)	Disinfection	inactivation of bacterial cells (56C°)in vaccine production
	Cold /freezing	Preservation	see text
	Ionizing radiation	Sterilization	
	Ultraviolet radiation	Disinfection	considered a surface steriliyer only
	Hydrostatic pressure	Disinfection (?)	activity dependent on concentration and temp.
Chemical (vapor phase)	Ethylene oxide	Disinfection	ethylene oxide also used as sterilizing agent
	Propylene oxide		
	Formaldehyde		possible carcinogenic activity of β-propionolactone
	β-propionolactone		
Chemical (liquid phase)	Acids and esters, alcohols, aldehydes, and aldehyde-Releasing agents, halogens (including chlorine-releasing agents), metals, phenols and cresols, quarterny ammonium compounds, biguanides	Disinfection or preservation	glutaraldehyde (pentanedial): has been considered a "chemosterilizer" quarterny ammonium compounds: also used as antiseptics chlorhexidine salts are importantant antiseptics, disinfectants, and preservatives
	Dyes (acridines, triphenylmethamine)	Antisepsis	now little used
	Metal chelate complexes	Antisepsis	
	Organic mercury compounds	Preservation or antisepsis	important pharmaceutical preservatives
	Silver compounds	Application to wounds	effective against *Pseudomonas aeruginosa*
Other	Bacterial vaccines and toxoids	Prophylaxis	subunit vaccines sometimes available
	Viral vaccines		
	Rikettsial vaccines		
	Antisera	Therapy	
	Antiviral protein (interferon)	Chemotherapy	
Combined processes	Heath + chemical	Sterilization	method at one time used in United Kingdom to sterilize certain iniections and eye drops
	Irradiation + chemical	Sterilization	
	Thermoradiation	Sterilization	use of lowered radiation dose in combination with substerilizing temperature
	Heath + hydrostatic	Sterilization (?)	
	Chemicals + ultrasonics	Sterilization (?)	

The exact mechanism of action of some antimicrobial agent is often not very clear. The reason for this is that more than one cell point can be targeted, and consequently the problem is to distinguish primary from secondary effects, which may contribute to the cell death.

Cellular targets of some conventionally used antimicrobial agents and their effects are shown in Table 4.

Table 4: *Cellular targets of antimicrobial agents.* [55]

Targets	Agents	Effect
Cell wall	Lysozyme	Attacks peptidoglycan (β 1-4 links)
	Adehydes	Interaction with $–NH_2$ groups
	Lysostaphin	Peptidase liberates N-terminal glycine and alanine
	Anionic surfactants	High concentration: lysis
Outer membrane	EDTA (and similar chelating agents)	Chelates cationes, induces release of up to 50% of lipopolysaccharide of outer membrane
	Lactoferrin, transferrin	Iron-binding proteins with effects apparently similar to EDTA
	Polycations (e.g. polylysine)	Displace cations
Cytoplasmic membrane	Moist heat, phenols, quarternary ammonium compounds, biguanides, parabens, hexachlorophene	Leakage of low-molecular-weight material; proton flux (for more specific information, see Table 3.4)
Nucleic acids	Acridines, dyes, alkylating agents, peroxygenes, hypochlorites, ionizing and ultraviolet radiations	Possible binding of chemical agents to nucleic acids extensively studied (see text and Table 3.5)
Enzymes or proteins	Metal ions	-SH groups of enzyms, which may be membrane associated
	Alkylating agents, oxidizing agents	May also combine with DNA or RNA

1.2.1 Effects of physical agents on bacteria

The most important physical agents are those shown in Table 3. Effects on bacterial cell of the most frequently used techniques are presented below.

1.2.1.1 Ionizing radiation

It is a process in which electrons are stripped from the atoms of material through which radiation passes. Types of ionizing radiation are X-rays, γ-rays, high – speed electrons (β-rays), protons, and α-rays (positively charged helium atoms). Actually, in practice, β-rays and γ-rays are used.

Ionizing radiation is believed to exert its effect by causing single- or double-strand breakages in DNA (the latter being more lethal). There are some bacteria fairly resistant to ionizing radiation. The most resistant of them is *Deinococcus radiodurans*, which exhibits an efficient repair process for both ionizing and UV radiations.

Bacterial spores are more resistant to ionizing radiation than vegetative cells.[56, 57] There are several reasons for it. These include the presence of radio-protective substances in the spore coat, the water content of the spore, the possible differences in the DNA of spore and vegetative cell, and ability of damaged cell to repair damage. [58] Irradiation injury is manifested as an inability to outgrow, or as an increased sensitivity to environmental stresses at the outgrow phase. Single-strand breaks can be repaired in dormant spores or during post-irradiation germination. [58,60]

1.2.1.2 Ultraviolet radiation

This type of radiation has a wavelength range between 210 and 328 nm with maximal bactericidal activity near 260 nm (peak absorption of DNA). This is important given that DNA is the target of UV radiation.[61,62] Exposure of non-sporulating bacteria to UV light results in forming of thymine dimers between adjacent thymine molecules in the some strand of DNA. Other dimers can be formed, such as an uracil- thymine heterodimer. The induction of dimers causes a death of bacterial cell. Inactivation can be rapid, and low doses can be used. [63] Some bacteria are capable to repair this damage, especially *Deinococcus radiodurans*. Repair mechanisms can be photoreactivation, excision repair, posteplication recombination repair and error-prone repair. [64] Bacterial spores are usually more resistant to UV light than vegetative cells. Small acid-soluble spore proteins (SASPs) appear to coat DNA in wild type spores of *Bacillus*. Spores lacking SASPs are significantly more sensitive to UV than normal types. [65]

1.2.1.3 Heat

Heat is one of most frequent used physical agents acting against microorganisms, especially bacteria. This agent can be used in two ways, as moist heat or as dry heat.

1.2.1.3.1 Moist heat

In this process the amount of humidity in atmosphere is almost 100%. [66] In practical applications, temperatures between 121 and 140°C are used.

When suspension of nonsporing bacteria is heated, several changes occur in the cells. These include leakage of low molecular appearance weight material, RNA and DNA breakdown, protein coagulation, and alterations in the appearance of the cell itself. [67,67] In *Staphylococcus aureus* Mg^{2+} is lost from theichoic acid in the cell wall. In *Escherichia coli*, structural damage occurs to the outer membrane, and the cells become more sensitive. In both bacteria, ribosomes from heat-injured cells have a different sedimentation coefficient than untreated ones. Single- and double- strand breaks of DNA occur, similar to those induced by ionizing radiation.

Mild heating causes an increase in mutation frequency. [55] Vegetative bacteria heated at sub-lethal temperatures may show enhanced resistance when exposed subsequently to higher temperatures. [69] Some bacteria such as *Bacillus stearothermophilus* can normally grow at 65°C or even higher temperature. [53]

Cell revival appears to be related to repair of DNA breaks. During heating at 50°C, *Escherichia coli* can synthesize a small number of so called "heat shock" proteins, which may demonstrate the cell's capability to express new information that may be needed to repair the multitarget damage induced by moist heat. [70]

The thermoresistance of spores depends of several factors affecting protoplast: a) dehydration, b) mineralisation, c) thermal adaptation, and d) protein thermotolerance.[71] When bacterial spores are lethally heated, intracellular constituents are released and there is a progressive loss of dipicolinic acid (DPA) and calcium, the rate of release being temperature-dependent, but it would appear that viability loss precedes DPA leakage (so leakage can not be considered a primary effect). [55]

Higher growth temperatures enhance the thermal resistance of spores and the ratio of total cation content to DPA content increases with increasing growth temperature. It is found that the heat resistance of spore was related directly to their calcium content and inversely to magnesium content. DPA does not appear to be directly involved in the heat resistance mechanism, although it might contribute by reducing or preventing thermally induced denaturation of proteins. DPA and almost all calcium, magnesium and manganese are located in spore core. [69] The water content of spore (much lower than in vegetative cell) is likely to be a controlling factor in its sensitivity to moist heat. [67,72]

SASPs lacking spores are more thermosensitive than wild type spores. [73] Maintenance of the integrity of the cortex is essential for the heat resistance of the spores, because removal of the cortex produce heat sensitive protoplasts (cell without cell wall e.g. after destruction by lysosime, suspended in isotonic solution). Deficiencies in DNA repair mechanisms may render spore more heat sensitive.

1.2.1.3.2 Dry heat

This is a much less efficient process than moist heat, and therefore much higher temperatures (up to 180°C) and longer exposing times must be used in practice. Oxidation probably plays an important role in this type of destruction of bacteria. [55] An effect on DNA is possible, too.

Sub-lethal temperature induce mutants in *Bacillus subtilis*, as a result of depurination, and dry heat sensitivity of spores could result from genetically determined differences in the water content or water retaining capacity of the spores.[74,75] The water content is an important factor in determining their inactivation by heat. [76]

1.2.1.4 Cold/freezing

Growth of microorganisms slows down and eventually, stops if they are exposed to low temperatures. Environmental factors such as nutrient status, pH, and water activity can alter minimal growth temperature. [55] Some bacteria can grow at temperatures approaching 0°C; these are termed psychrophillic.

Cold shock refers to a process in which microorganisms are suddenly chilled without freezing, and cell death has been shown to occur with Gram positive and Gram negative bacteria.[77] Difference between mesophiles (growing best near human body temperature; human pathogens belong to this group) and psychrophiles (growing best at near-zero temperatures) might be related to differences in membrane composition. Low-molecular weight material is released from chilled cell as a consequence of an increased permeability of the bacterial cell membrane, which in turn occurs because of a phase transition in membrane lipids. [55]

1.2.2 Effects of chemical agents on bacteria

The most important chemical agents used as antimicrobials are shown in Table 3. Sites of their action are shown in Table 4. Cellular uptake is a first step, and represents an early manifestation in effect of those agents. Several different models for uptake exist depending on chemical agent and point of acting.

1.2.2.1 Effects on bacterial cell wall and outer membrane

Some antibiotics such as β-lactams, d-cycloserine and vancomycin are active only against growing cells. Beside the antibiotics, there are other substances active against growing and non- growing cells.

EDTA (ethylenediamine tetraacetic acid) is not a powerfull bactericide agent on its own, but it has some effect to Gram-negative bacteria. It was found to be inhibitory (despite earlier claims) to Gram-positive bacterial cells, but mechanism is not clearly understood. [78] Its usefulness is in the fact that it can increase activity against Gram- negative bacteria of chemical unrelated antibacterial agents. For example, enzyme lysosime induces lysis of some Gram-positive bacteria, such as those from genera *Bacillus, Micrococcus and Sarcina*, which is effected by hydrolysis of the β,1-4 links between GlkNAc and MurNAc in peptydoglycan. *Staphylococcus aureus* (it can be lysed by lysostaphin), and typical Gram-negative bacteria are all resistant to its action. With Gram-negative bacteria, lysosime does not penetrate the outer membrane of the cell, but does so when the outer membrane is destabilized with EDTA. It is chelating agent, which combines with cations Mg^{2+} and Ca^{2+} associated with outer membrane of Gram-negative bacterial cell. At some time, large amounts of outer membrane lipopolysaccharide are released, so outer membrane is opened up and then another, chemically unrelated molecules can enter inside. [79] In contrary, despite the fact that EDTA has an effect against Gram-positive bacteria, it does not increase their sensitivity to antibacterial agents.

Polymixin, a polycationic antibiotic, disturbs outer membrane of Gram-negative bacteria cell wall thereby promoting its own entry to inner membrane, its ultimate point of action.

Mechanisms of acting glytaraldehyde (pentanedial) are not completely clear. In one way, it has the following effects on bacteria: a) cross-linking of peptidoglycan in Gram-positive bacteria, such that reduced lysis occurs with lysosime or lysostaphin b) interaction with protein in the cell wall of Gram-negative bacteria, so that lysis by EDTA – lysosime is reduced c) reaction with spore cortex constituents, this being assisted by the action of inorganic cations, and d) increased resistance to lysis of protoplasts and spheroplasts. [80] On the other hand, glytaraldehyde inhibits synthesis of protein, RNA, and DNA in Gram-negative bacteria, probably to arise from an inhibition of precursor uptake as a consequence of aldehyde – protein interaction in the outer structures of the cell. [81] More potent ortho-phthalaldehide (OPA) is recognised as a new chemical sterilant. [82]

1.2.2.2 Membrane-active antibacterial agents

These substances can damage the cell membrane and cause leakage of intracellular material. Several of them may act on the other sites, too.

Chlorhexidine and quaternary ammonium compounds (QACs) lyse bacterial protoplasts and spheroplasts. Chlorhexidine affects the outer membrane of Gram-negative bacterial wall with release of periplasmatic enzymes and disturbs the functionality of inner membrane by direct inhibition of membrane – bound and solubile Mg^{2+}, ATPase.[83] Cetyltrimethylammonium bromide affects proton moving pump through citoplasmatic membrane in *Staphylococcus aureus*. [84] Some agents such as tetrachlorsalycilanilide can uncouple electron transport (oxidative phosphorilation) and ATP synthesis in cytoplasmic membrane, consequently disturbing proton-moving force. [67] Binding of polyxexamethylene biguanide to negatively charged Gram-negative cell surface impairs to outer membrane, and interacts with inner membrane phospspholipides, so that the loss of potassium ions occurs, and eventually there is a complete loss of membrane function with precipitation of intracellular constituents. [85] A new sterilisant, a modified polyhexmethylabiguanide combined with silver iodide acts to outer membrane and internal structures, too.

1.2.2.3 Agents acting against cytoplasm's components

Mechanism of acting of chlorine has not yet been completely elucidated. It is known that this halogen acts by oxidation of sulfhydryl groups of vital enzymes in cytoplasm, as well as those bounded to the cell membrane. This reaction is apparently irreversible. Chlorine in minute concentration results in a destructive permeability of the cell wall. It is possible that hypochlorous (HOCl) deliberated in reaction of chlorine with water and formed by hydrolysis of N-chloro compounds, can be bactericidal.

However, inhibition of the essential cytoplasmic metabolic reactions is largely responsible for the destruction of bacterial cell. [67] Probably, similar effect has a new disinfectant, electrolyzing saline, which creates hypochlorous acid and free chlorine radicals.

1.2.2.4 Agents acting against nucleic acids

These agents can act on DNA as well as RNA. Acridines combine strongly to DNA, intercalates between adjacent base pairs, inhibit DNA synthesis although binding to other sites such as ribosomes, RNA and cell envelope. [67] Epoxides, such as ethylene oxide (CH_2CH_2O), interact by amino acids and proteins, causes hydroxyethylation of amino acids, with the phosphate group of nucleic acid to form triestar, and with guanine to give 7-(2'-hydroxyethyl) guanine. Alkylation of phosphated guanine in nonsporing bacteria has been proposed as the primary reason for the lethal effect of ethylene oxide. [86] Formaldehyde has been suggested to act by its alkylating effect, too. [87]

1.2.2.5 Sporocidal and sporistatic chemicals

A few chemicals are sporicidal. Those agents that include glutaraldehyde, formaldehyde, halogen – releasing agents, hydrogen peroxide, and ethylene oxide, have sporicidal activity, although mechanisms of their sporicidal action remain poorly understood. [88,89] Some agents such as phenols and QACs have little effect on viability of bacterial spores. Nevertheless, such agents are inhibitory at certain stages in overall life cycle, and consequently there are three ranges in which lethal or inhibitory effects may occur. These are during the various stages of sporulation, on the mature spore, and during germination or growth. Agents that are sporistatic inhibit germination or outgrow, although effects may be reversible.

1.2.2.6 Plasma

Influences of gas plasma on bacteria could be physical, chemical and, the most probably, combined.[90,91,92,93,94,95,96,97,98,99,100]

1.3 Plasma and plasma interactions

In recent years, plasma technologies are being intensively used for improved biomedical application of different materials, such as activation of polymer materials, modification of different implants, sterilization etc. [94] Low-pressure plasma is a non-equilibrium state of gas. Such a state of gas is usually obtained by placing a chamber containing gas at low pressure in an appropriate electric field (Fig.23).

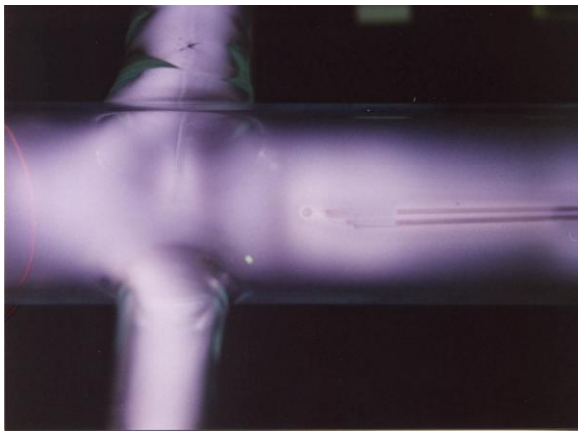

Figure 25: *Appearance of plasma in glow discharge chamber.*

Free electrons that are always presented in gas are accelerated in the electric field. If the electron kinetic energy is above the ionization threshold, they may cause molecule ionization. The electrons are thus multiplied at ionization collisions with neutral molecules. When the electric field is applied, electrons are rapidly multiplied until they are dense in the gas. The density of electrons depends on production and loss rates, and is typically of the order of $10^{16}m^{-3}$. The electron kinetic energy, again, depends on acceleration in the electric field and the energy loss at inelastic collisions. Since there are many elastic collisions between electrons themselves, they are thermal (have Maxwellian energy distribution function), so the electron temperature can be defined. Typical electron temperature in low-pressure plasmas is between 20.000 and 100.000^{o}C. [101]

Apart from ionization, the electrons with such a kinetic energy may cause other reactions at inelastic collisions. Since the dissociation threshold is lower than ionization one, the gaseous molecules are likely to be dissociated in plasma. The electrons may also cause excitation of both molecules and atoms. The excited molecules and atoms may or may not be de-excited by light quanta emission. In the latter case, the states are called metastable. The energy exchange at elastic collisions of electrons with heavy particles is poor, due to a low mass of electrons. There is usually also a lack of other effects that may heat gaseous molecules, so they usually remain at low kinetic energy. They are also thermal and the typical temperature (often called the neutral gas kinetic temperature) is close to the room temperature. [94, 101]

Generally, the following particles capable of interacting with bacteria are presented in low-pressure plasmas: neutral molecules and atoms, positively charged molecules and atoms, negatively charged molecules and atoms, and light quanta. Interesting for plasma interactions with biological mater are predominantly the neutral radicals that are chemically active. The density of these radicals depends on gas type and purity, gas pressure and flow, discharge power, type of discharge, frequency of discharge, shape of the discharge chamber, temperature of plasma facing materials. [94,101]

1.3.1 Influence of plasma on the microorganisms

There are several works [62,92,93,96,98,102,103,104] about acting of plasma against bacteria, but no much data about mechanisms of acting. It is found that exposing bacteria to low temperature gas plasma causes many negative influences on them, which finally lead to complete destruction and consequently, plasma can be used as antimicrobial agent. [92,93,94,96,98,104,105,106]

Until now, three basic mechanisms of plasma interactions with bacteria were identified:

1. Destruction by UV irradiation of the genetic material of the microorganism;
2. Erosion of microorganism, atom by atom, through intrinsic photodesorption. Photon induced desorption results from UV photons breaking chemical bonds in the microorganism material and leading to the formation of volatile compounds from atoms intrinsic to the microorganism. The volatile by-products of this non-equilibrium chemistry are small molecules (e.g. CO and CHX).
3. Erosion of microorganism, atom by atom, through etching. Etching stems from the absorption of reactive species from plasma (glow or afterglow) on microorganism with which they subsequently undergo chemical reactions to form volatile compounds (spontaneous etching). The reactive species can be atomic and molecular radicals, for example O and O_3 and excited molecules in a metastabile state, for example $^1O_2$ singlet state. This chemistry, which occurs under thermodynamic equilibrium conditions, yields small molecules (e.g. CO_2, H_2O) that are the final products of oxidation process. In certain cases, the etching mechanism is enhanced by UV photons (UV induced etching), the photons acting synergistically with the reactive species, thereby accelerating the erosion rate of microorganisms. This UV induced chemistry, which occurs under non-equilibrium conditions, can result in desorption of radicals and molecules, at both the intermediate and final stages of oxidation. [91]

Beside these elementary processes, thermal effects could be important, too, and synergistic with discussed mechanisms, since chemical reactions, recombination and relaxations are basically exothermic. Elementary processes listed above can be active in various plasmas, but due to their features, radiofrequency and microwave generated plasmas are especially appropriate for destroying of microorganisms.

1.3.2 Oxygen plasma effects on bacteria

Nonequillibrium oxygen plasma is a source of various reactive species with different kinetic and excitation energies. Its unique feature is extremely high probability for superellastic collisions between vibrationally excited molecules and neutral atoms. The result is a very low vibrational temperature, and moderate gas heating (the excessive energy is transformed to kinetic energy of colliding particles). The first excited state of O atom is metastable. The consequence is practically no radiation in UV range. The relatively strong emission occurs from higher excited states to lower excited states – in the red or IR part of spectrum. These features declare oxygen plasma as potentially very effective agent acting against bacteria.

Especially convenient could be neutral oxygen atoms generated in such plasma, because they are pretty benign to many polymers at room temperature but are supposed to interact with bacteria. From this point of view oxygen atoms may be used for sterilization of many modern biomedical devices that cannot be sterilized with conventional heat techniques. [92,93,94,95,96,97,98,103,104,105,106,107] This is why we decided to perform systematic research on interaction of oxygen atoms with several types of bacteria.

1.4 Methods for visualization surfaces of bacteria

Various methods can be used for investigation of interactions of plasma against bacteria. For visualization of changes on surfaces of bacteria the most convenient are some microscopy techniques. One of most powerful microscopy techniques today, especially in basic microbiology, is Atomic Force Microscopy (AFM). [108,109,110,111,112,113,114,115,116,117,118,119] More classical, but in some cases as suitable as AFM, is Scanning Electron Microscopy (SEM) [120,121,122,123,124]

1.4.1.1 Atomic Force Microscopy (AFM)

The atomic force microscopy (AFM) is a high-resolution type of scanning probe microscopy, with demonstrated resolution of fractions of a nanometer, more than 1000 times better than the optical difraction unit. [109] Binnig, Quate and Gerber invented the first Atomic Force Microscope in 1986. [125] The AFM is one of the foremost tools for imaging, measuring and manipulating matter at the nanoscale. Not only does AFM achieve molecular resolution but can be performed under fluids permitting samples to be imaged in near native conditions. The fluid may be exchanged or modified during imaging and therefore there is the potential for observing biological processes in real time, something which electron microscopy is not able to achieve.

An atomic force microscope is a unique instrument that has the characteristics of a high resolution SEM, a surface profiler, and a probe station. Because of these unique characteristics, the AFM has applications in all fields of science and technology. [109, 111] An AFM is a mechanical imaging instrument that measures the three dimensional topography as well as physical properties of a surface with a sharpened probe (see Figure 24). The information is gathered by "feeling" the surface with a mechanical probe.

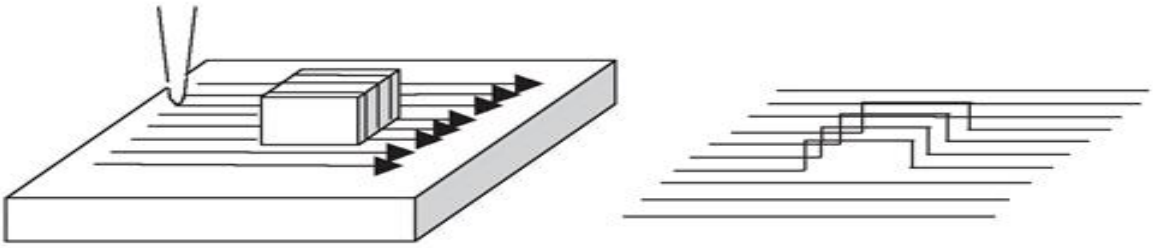

Figure 26: *The principle of creating AFM image*. [109]

The AFM consists of a microscale silicon cantilever with a sharp tip (probe) on its end, which is used to scan the specimen surface. Shape of the cantilever is usually triangular ("V" shaped) or long and rectangular (an "I" shape) as shown in Figure 30. Cantilevers are roughly 100 microns long and only a few microns thick. This makes them very flexible but strong enough to securely hold the tips on their end. The end of this tip is often slightly rounded, being around ten nanometers (0.00001 millimeters, or about 100 atoms) in radius.

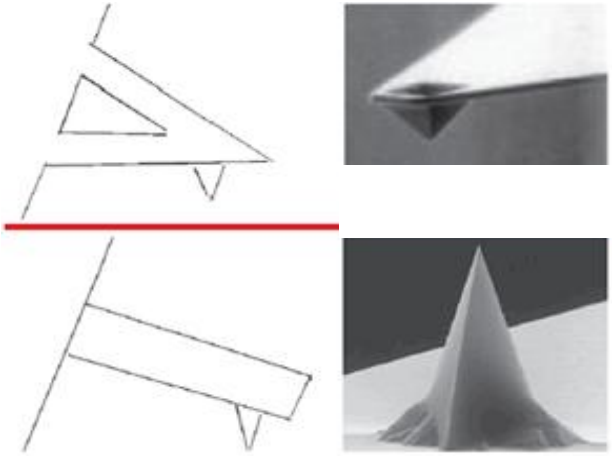

Figure 27: T*ypes of cantilevers and tip.* V-shape above, I-shape below. [109]

The areas scanned by the probe are around 100 - 150 μm. In practice, the heights of surface features scanned with an AFM are less than 20 um.

When the tip is brought into proximity of a sample surface, forces between the tip and the sample lead to a deflection of the cantilever according to Hooke's law ($F= -k_c$ d), where F is the force acting on the canteliver, k_c is spring constant of the cantilever, and d I s its deflection. [112]

Depending on the situation, forces that are measured in AFM include mechanical contact force, Van der Waals forces, capillary forces, chemical bonding, electrostatic forces, magnetic forces etc. Piezoelectric elements that facilitate tiny but accurate and precise movements on (electronic) command, enable very precise scanning.

AFM can generally measure the vertical and horizontal deflection of the cantilever with picometer resolution. To achieve this, most AFMs today use an optical lever. This device operates by reflecting a laser beam off the back of the cantilever (see Figure 31.). Angular deflection of the cantilever causes a twofold larger angular deflection of the laser beam. The reflected laser beam strikes a position-sensitive photodetector (PSPD) consisting of four side-by-side photodiodes. The difference between the four photodiode signals indicates the position of the laser spot on the detector and thus the angular deflection of the cantilever.

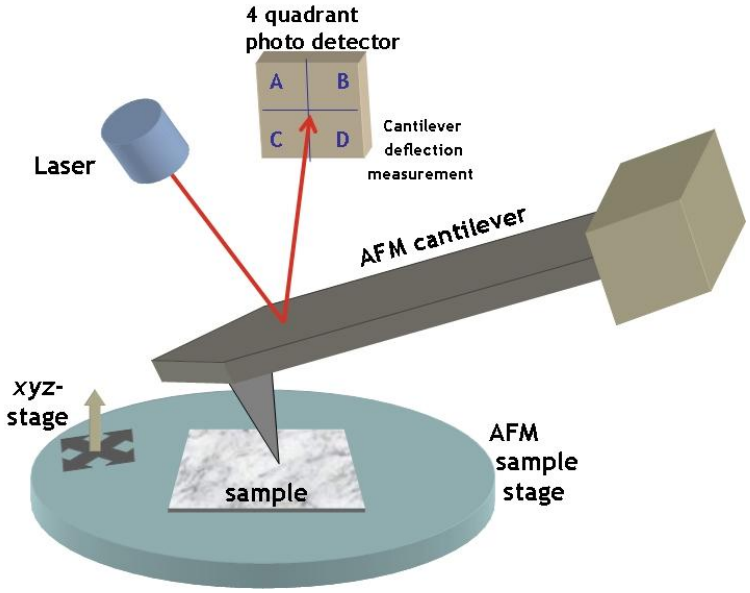

Figure 28: *The principle of AFM setup.* [111]

If the tip is scanned over the sample surface then the deflection of the cantilever can be recorded as an image, which represents the three – dimensional shape of the sample surface (deflection image). AFM uses a PSPD to detect the deflection of the cantilever and the cantilever´s twist.

The primary modes of operation are static (contact) mode and dynamic mode. Consequently, this technique is typically called 'contact mode'. Thus static mode AFM is almost always done in contact where the overall force is repulsive. In contact mode, the force between the tip and the surface is kept constant during scanning by maintaining a constant deflection. In the dynamic mode, the cantilever is externally oscillated at or close to its fundamental resonance frequency or a harmonic. The oscillation amplitude, phase and resonance frequency are modified by tip-sample interaction forces; these changes in oscillation with respect to the external reference oscillation provide information about the sample's characteristics. [108]

Atomic resolution is easily obtained on relatively robust and periodic samples. Soft samples – particularly biological samples – provide a more difficult surface to image because the forces exerted by the tip during imaging can cause deformation of the sample. The problem involved with imaging soft samples has been overcome to a large extent by the introduction of “tapping mode” AFM imaging. Instead of maintaining a constant tip-sample distance of a nanometer or so, the cantilever is oscillated in a direction normal to the sample resulting in only intermittent contact with the surface. This greatly reduces the lateral forces being applied in the plane of the sample, which are responsible for most of the damage as the tip is scanned. The AFM is capable of better than 1 nm lateral resolution on ideal samples and of 0.01 nm resolution in height measurement.[112]

In tapping mode (also called intermittent contact), the cantilever is oscillated such that the separation distance between the cantilever tip and the sample surface is modulated. In tapping mode the cantilever is driven to oscillate up and down at near its resonance frequency by a small piezoelectric element mounted in the AFM tip holder. The amplitude of this oscillation is greater than 10 nm, typically 100 to 200 nm. Due to the interaction of forces acting on the cantilever when the tip comes close to the surface, Van der Waals force or dipole-dipole interaction, electrostatic forces, etc cause the amplitude of this oscillation to decrease as the tip gets closer to the sample. An electronic servo uses the piezoelectric actuator to control the height of the cantilever above the sample. The servo adjusts the height to maintain a set cantilever oscillation amplitude as the cantilever is scanned over the sample. A Tapping AFM image is therefore produced by imaging the force of the oscillating contacts of the tip with the sample surface.[111]

Three types of data can be collected in this mode: height, phase and amplitude data. [109] There have been many studies of biological materials using AFM in the few years since its conception. Examples include nucleic acids and their complexes with proteins, two dimensional protein crystals and individual isolated proteins, membranes and membrane bound proteins, and living cells.[113,114,115,117,119]

1.4.1.2 Scanning Electron Microscopy (SEM)

The development of the Scanning Electron Microscope in the early1940’ and first commercial machines in the 1950's brought with it new areas of study in the medical and physical sciences because it allowed examination of a great variety of specimens.

The scanning electron microscope (SEM) is a type of electron microscope that images the sample surface by scanning it with a high-energy beam of electrons in a raster scan pattern. The electrons interact with the atoms that make up the sample producing signals that contain information about the sample's surface topography, composition and other properties such as electrical conductivity. The types of signals produced by an SEM include secondary electrons, back scattered electrons (BSE), characteristic x-rays, light (cathodoluminescence), specimen current and transmitted electrons. The signals result from interactions of the electron beam with atoms at or near the surface of the sample. [120]

In a typical SEM, an electron beam is thermionically emitted from an electron gun fitted with a filament metal (usually tungsten) cathode. The electron beam, which typically has an energy ranging from a few hundred eV to 40 keV, is focused by one or two condenser lenses to a spot about 0.4 nm to 5 nm in diameter. The beam passes through pairs of scanning coils or pairs of deflector plates in the electron column, typically in the final lens, which deflect the beam in the *x* and *y* axes so that it scans in a raster fashion over a rectangular area of the sample surface. (See Figure 32.)

When the primary electron beam interacts with the sample, the electrons lose energy by repeated random scattering and absorption within a teardrop-shaped volume of the specimen known as the interaction volume, which extends from less than 100 nm to around 5 µm into the surface. The size of the interaction volume depends on the electron's landing energy, the atomic number of the specimen and the specimen's density. The energy exchange between the electron beam and the sample results in the emission of secondary electrons by inelastic scattering, reflection of high-energy electrons by elastic scattering, and the emission of electromagnetic radiation, each of which can be detected by specialized detectors.

The most common imaging mode collects low-energy (<50 eV) secondary electrons that are ejected from the k-orbitals of the specimen atoms by inelastic scattering interactions with beam electrons. Due to their low energy, these electrons originate within a few nanometers from the sample surface. The electrons are detected by the detector which is a type of scintillator-photomultiplier system. The secondary electrons are first collected by attracting them towards an electrically-biased grid at about +400V, and then further accelerated towards a phosphor or scintillator positively biased to about +2000V. The accelerated secondary electrons are now sufficiently energetic to cause the scintillator to emit flashes of light (cathodoluminescence) which are conducted to a photomultiplier outside the SEM column via a light pipe and a window in the wall of the specimen chamber. The amplified electrical signal output by the photomultiplier is displayed as a two-dimensional intensity distribution that can be viewed and photographed on an analogue video display, or subjected to analog-to-digital conversion and displayed and saved as a digital image. This process relies on a raster-scanned primary beam. The brightness of the signal depends on the number of secondary electrons reaching the detector. If the beam enters the sample perpendicular to the surface, then the activated region is uniform about the axis of the beam and a certain number of electrons "escape" from within the sample. As the angle of incidence increases, the "escape" distance of one side of the beam will decrease, and more secondary electrons will be emitted. Thus steep surfaces and edges tend to be brighter than flat surfaces, which results in images with a well-defined, three-dimensional appearance. Using this technique, image resolution less than 1 nm is possible.

Backscattered electrons (BSE) consist of high-energy electrons originating in the electron beam that are reflected or back-scattered out of the specimen interaction volume by elastic scattering interactions with

specimen atoms. Since heavy elements (high atomic number) backscatter electrons more strongly than light elements (low atomic number), and thus appear brighter in the image, BSE are used to detect contrast between areas with different chemical compositions. Due to this fact, BSE images can provide information about the distribution of different elements in the sample. For the same reason BSE imaging can image colloidal gold immuno-labels of 5 or 10 nm diameter, that would otherwise be difficult or impossible to detect in secondary electron images in biological specimens.

The beam current absorbed by the specimen can also be detected and used to create images of the distribution of specimen current.

Electronic amplifiers of various types are used to amplify the signals which are displayed as variations in brightness on a cathode ray tube CRT). The raster scanning of the CRT display is synchronised with that of the beam on the specimen in the microscope, and the resulting image is therefore a distribution map of the intensity of the signal being emitted from the scanned area of the specimen. The image may be captured by photography from a high resolution cathode ray tube, but in modern machines is digitally captured and displayed on a computer monitor and saved to a computer's hard disc.[121]

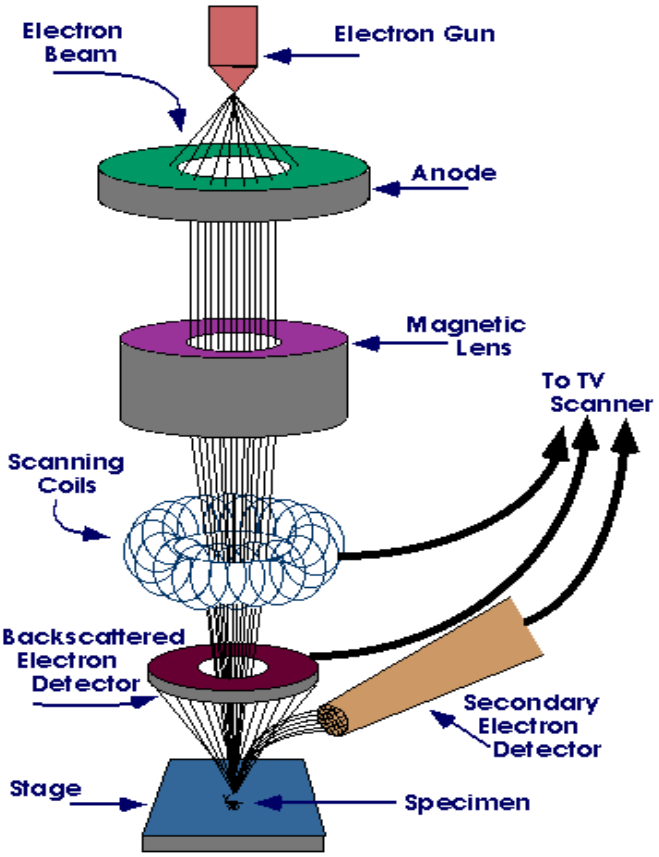

Figure 29: *Schematic wiev of the SEM function.* [122]

The spatial resolution of the SEM depends on the size of the electron spot, which in turn depends on both the wavelength of the electrons and the electron-optical system which produces the scanning beam. The resolution is also limited by the size of the interaction volume, or the extent to which the material interacts with the electron beam. The spot size and the interaction volume are both large compared to the distances between atoms, so the resolution of the SEM is not high enough to image individual atoms, as is possible in the shorter wavelength (i.e. higher energy) transmission electron microscope (TEM). The SEM has compensating advantages, though, including the ability to image a comparatively large area of the specimen; the ability to image bulk materials (not just thin films or foils); and the variety of analytical modes available for measuring the composition and properties of the specimen. Depending on the instrument, the resolution can fall somewhere between less than 1 nm and 20 nm. [120]

For conventional imaging in the SEM, specimens should be electrically conductive, at least at the surface, and electrically grounded to prevent the accumulation of electrostatic charge at the surface. Metal objects require little special preparation for SEM except for cleaning and mounting on a specimen stub.

Nonconductive specimens tend to charge when scanned by the electron beam, and especially in secondary electron imaging mode, this causes scanning faults and other image artifacts. They are therefore usually coated with an ultrathin coating of electrically-conducting material, commonly gold, deposited on the sample either by low vacuum sputter coating or by high vacuum evaporation. Conductive materials in current use for specimen coating include gold, gold/palladium alloy, platinum, osmium, iridium, tungsten, chromium and graphite. Coating prevents the accumulation of static electric charge on the specimen during electron irradiation. [120]

For SEM, a specimen is normally required to be completely dry, since the specimen chamber is at high vacuum. Hard, dry materials such as wood, bone, feathers, dried insects or shells can be examined with little further treatment, but living cells and tissues and whole, soft-bodied organisms usually require chemical fixation to preserve and stabilize their structure. Fixation is usually performed by incubation in a solution of a buffered chemical fixative, such as glutaraldehyde, sometimes in combination with formaldehyde [126] and other fixatives and optionally followed by postfixation with osmium tetroxide. The fixed tissue is then dehydrated. Because air-drying causes collapse and shrinkage, this is commonly achieved by critical point drying, which involves replacement of water in the cells with organic solvents such as ethanol or acetone, and replacement of these solvents in turn with a transitional fluid such as liquid carbon dioxide at high pressure. The carbon dioxide is finally removed while in a supercritical state, so that no gas-liquid interface is present within the sample during drying. The dry specimen is usually mounted on a specimen stub using an adhesive such as epoxy resin or electrically-conductive double-sided adhesive tape, and sputter coated with gold or gold/palladium alloy before examination in the microscope. However, it is possible to obtain pretty quality images from noncoated biological samples but using very low energies of electron beam in advanced SEM devices with digitaly enhanced signal.

1.4.1.3 Comparison of an AFM and SEM

The AFM has several advantages over the scanning electron microscope (SEM) for investigating biological samples. Unlike the electron microscope which provides a two-dimensional projection or a two-dimensional image of a sample, the AFM provides a true three-dimensional surface profile. Additionally, samples viewed by AFM do not require any special treatments (such as metal/carbon coatings) that would irreversibly change or damage the sample. While an electron microscope needs an expensive vacuum environment for proper operation, most AFM modes can work perfectly well in air ambient or even a liquid environment. This makes it possible to study biological macromolecules and even living organisms. In principle, AFM can provide higher resolution than SEM. It has been shown to give true atomic resolution in ultra-high vacuum (UHV) and, more recently, in liquid environments. High resolution AFM is comparable in resolution to Scanning Tunneling Microscopy and Transmission Electron Microscopy.

A disadvantage of AFM compared with the scanning electron microscope (SEM) is the image size. The SEM can image an area on the order of millimeters by millimetres with a depth of field on the order of millimetres. The AFM can only image a maximum height on the order of micrometres and a maximum scanning area of around 150 by 150 micrometres. Another inconvenience is that an incorrect choice of tip for the required resolution can lead to image artifacts. Due to the nature of AFM probes, they cannot normally measure steep walls or overhangs.

Table 5: *Comparison of an AFM and SEM.* [9afm url]

	SEM	AFM
Samples	Preferably conductive	Insulating/Conductive
Magnification	2 Dimensional	3 Dimensional
Environment	Vacuum	Vacuum / Air / Liquid
Time for image	0.1 - 1 minute	1 - 5 minute
Horizontal Resolution	5nm (FE-SEM)	0.2 nm
Vertical Resolution	n/a	.05 nm
Field of View	1mm	100 um
Depth of Field	Good	Poor
Contrast on Flat Samples	Poor	Good

In our work we used AFM and SEM techniques trying to take the best of both of them.Whenever it was possible, we compared images taken with AFM and SEM in order to get a clearer picture of some specific events.

2 Aims and Hypothesis

The aim of this work is to show clearly, which (if any) of the above stated three pictures of plasma induced degradation of bacteria is correct for the case of sterilization with two types of oxygen radicals, i.e. positive ions and neutral atoms in the ground state. The mechanisms are studied for two different types of bacterial cells, i.e. *Staphylococcus aureus* and *Eschericia coli* that belong to two main groups of bacteria (Gram – positive and Gram – negative). This work is, to the best of our knowledge, the first attempt to explain the interaction of neutral oxygen atoms with different constituents of bacterial cells.

2.1 Our hypothesis

According to our preliminary experimental results and relevant literature we developed following hypothesis:

- oxygen radicals can destroy bacterial cell by oxidation of organic compounds;
- oxygen atoms in the ground state are the most convenient radicals for slow degradation of bacteria at room temperature (which is preferred, if using this process for sterilization/disinfection, since many delicate biocompatible components do not stand heating to elevated temperature);
- doses of radicals necessary to destroy specific bacterial cell structures can be measured and well defined for different types of bacteria;
- etching is heavily un-isotropic process due to the complex structure of bacterial envelopes, and the etching rate depends on the type of bacteria;
- after receiving a certain dose of radicals, weak points appear on bacterial envelopes, the envelopes will be broken and spread all around bacteria, which will cause leakage of the cytoplasm and consequently death of bacterial cell.

3 Materials and Methods

Influence of radicals generated in oxygen plasma has been investigated on vegetative form of bacteria belongs to two main types, Gram-positive and Gram-negative, according to the composition of their cell wall. In our observations of influences of plasma radicals on bacterial structures, we made efforts to damage and destroy bacterial envelopes, followed by consequently degradation of bacteria.

3.1.1 Samples preparation

In our experiments typical representatives of these two main groups of bacteria were used. For Gram – positive, *Staphylococcus aureus* ATCC 25923 (MicroBioLogics, CE MN, USA) was chosen and for Gram – negative, it was *Escherichia coli* ATCC 10536, and 35218 (MicroBioLogics, CE MN, USA).

During preparation process, standard cultivation procedure has been performed. Both of the bacteria were cultivated on Columbia agar, culture medium reach in various nutrients, which allows expression of the typical (common) bacterial features. We used commercially prepared Columbia agar plates (BioMerieux, France), inoculated bacterial suspension on agar surface and incubated them for 24h at 37°C. After appropriate time of incubation, when bacterial colonies become visible on agar surface, bacteria are in logarithmic phase of growth and division. In this phase of growth, we get young cells, which express typical features for particular bacterial species. Bacteria are harvested carefully from the upper surface of the colonies, to pick up bacterial cells only. On that manner, we avoided eventual interference of substances from culture medium. Bacteria were dispensed in sterile distilled water, washed and shaken (on vortex), strong enough to obtain single cells. Density of that suspension was adjusted to approx. 10^8 CFU/ml, which correspond to 10^6 CFU/10μl used for preparing samples.

Bacteria were deposited on 10x10mm smooth, well oriented graphite, highly polished Al foil and highly polished silicon wafer substrates, shortly pretreated in plasma, with purpose to activate surface and consequently obtain better spilling effect and evenly distribution of bacterial cells in mono layer. Samples were slowly air dried at 30°C until water used for preparing suspension evaporated.

Samples made of *Staphylococcus aureus*, were sorted in three groups. Samples from the first group were not exposed to plasma radicals and were used as a comparative control. Samples from the second group were exposed to plasma in glow conditions. Samples from the third group were exposed to afterglow.

Samples made of *Escherichia coli* were sorted in three groups. Samples from the first group weren't exposed to plasma radicals and were used as a comparative control. Samples from the second group were exposed to plasma in glow conditions. Samples from the second third group were exposed to afterglow.

3.1.2 Experimental system and plasma setup

The experimental system suitable for generation of oxygen plasma has been elaborated in the thesis by Cvelbar [101]. Since the subject of this thesis is a study of bacteria degradation, and not the study of plasma generation techniques, we list here only some general features about the plasma and the particularities of experimental conditions used at degradation of bacteria. The plasma and its afterglow are thus represented by a "black box" – it is just a medium supplying oxygen radicals.

Oxygen plasma is created in an inductively coupled RF discharge described to details in the thesis of U. Cvelbar as well as in numerous scientific papers of our research group [102,106,127,128,129…]. A quick survey of the thesis and the papers reveals that the same experimental setup give plasma with different parameters. The reason for this is not just the statistical error, but also the fact that our plasma, as an example of an extremely non-equilibrium state of gas, is very sensitive to small details in the experimental

setup. The plasma parameters depend on the following conditions:

- The exact position of the RF coil
- The condition of the electrical connection between the coil and the generator
- The ambient temperature
- The humidity of the ambient air
- The history of the experimental chamber
- The conditions of the trap between the plasma or afterglow reactor and the oil rotary pump
- The size of the substrate
- The number of bacteria placed on the substrates
- The exact position of the substrates in the reaction chamber
- The accuracy of the vacuummeter, catalytic and Langmuir probes
- Etc.

We made all our best efforts to keep the conditions that we can influence as soon as stable and repeatable. It is well known, that the history of plasma reactors plays an important role in reproducibility of experimental conditions. To this end, we pretreated the vacuum system in the following way: The molecular sieves in the trap between the plasma reactor and the pump were replaced with fresh ones. The system was left running for several hours with a small leak of air in order to obtain a suitable adsorption of the water vapour on the sieves. This procedure assured a negligible pumping effect of the sieves for water vapour (the adsorption was equal to the desorption). Once the sieves were stabilized, the so-called ultimate pressure was about 7 Pa. As always, the ultimate pressure is something, which is difficult to define since the pressure keeps decreasing with increasing pumping time. This effect, however, was hardly detectable after the stabilization of the sieves. Still, the pumping time often defines the desorption of gases and vapours from the walls of the plasma reactor. In order to overcome this possible influence on our results, we left the system loaded with a sample pumping always for the same period of time before turning on our plasma. This time was always 3 minutes.

The samples themselves often represent a source of gases, especially water vapour. As mentioned above, the samples with bacteria were first dried at 30^{o}C in air in order to remove excess water in which bacteria were suspended, to overcome this problem. Namely, a 10 μl water drop as placed on our substrates would give an almost 1m^3 water vapour at 1 Pa. Taking into account the pumping speed of our rotary pump, i.e. 16 m^3 per hour, we can see that this amount of water is far from being negligible. That's why we dried our samples before mounting into the vacuum system.

The source of water vapour is also humid air inlet into the system after each treatment. We could not influence the humidity of air in our laboratory. In order to avoid possible uncertainties due to this effect, the vacuum system was filled with oxygen from flask (it should be dry) up to the ambient pressure before opening the plasma reactor.

RF plasma is well known to be cold, i.e. the kinetic temperature of heavy particles is close to the room temperature. In reality, however, the neutral gas temperature in plasma can never be maintained at ambient temperature due to heating of the plasma reactor. Relaxation of metastables, recombination of atoms, and neutralization of charged particles is heating the reactor. In order to minimize the heating of the reactor chamber, the discharge tube was forced air – cooled. By this, we managed to keep the outer walls of the tube close to the room temperature, but the inner walls (glass has a poor thermal conductivity) remain at somehow higher temperature. This effect, however, is supposed to be small so it is usually neglected. The substrates, on the other hand, should be kept at floating potential so active cooling is not possible. The samples are thus heated in plasma. All efforts were made to minimize this effect including application of rather small substrates and application of smooth materials with a low recombination coefficient as substrates.

In electrical discharges most of the gas volume is quite luminous, which is why one speaks of glow discharge. When the discharge takes place in a flowing gas, some of the species (e.g. neutral atoms) produced in the glow region can be soon carried away into an electric field free vessel, and one obtains what is called a flowing afterglow. The gas in the afterglow chamber is near (at) room temperature and rich with oxygen atoms, while there are no charged particles and no radiation. Effects on bacteria should be achieved in glow as well as in afterglow. Time to achieve these effects is usually shorter in glow discharge than in its afterglow. The reasons are probably synergistic effects of various particles and higher temperature in reaction vessel.

Any thermal effects are absent in the afterglow region, which is almost free from charged particles and

excited atoms and molecules. From this point of view, more controlled conditions are obtained in the afterglow. Still, due to completeness of this thesis, experiments were performed both in afterglow and plasma itself.

Oxidation of organic material is a heavily exothermic process and contributes to sample heating in plasma as well as in the afterglow. This effect was minimized using small number of bacteria on the substrates. Happily enough, the oxidation probability is small at room temperature.

Finally, in order to be able to get accurate results, plasma parameters were measured simultaneously during the experiments with bacteria. The Langmuir probe was placed at the same spot as the samples were, while the catalytic probe was mounted into the afterglow chamber, again at the same spot where the samples are mounted. The density of ions in plasma was determined with the Langmuir probe and was 1.4×10^{16}. The absolute accuracy of this value is estimated to about 30%. The density of neutral atoms, as determined by the catalytic probe, was 3.5×10^{21} m^{-3} in the afterglow chamber at the position of the samples. This value is pretty accurate (absolute accuracy of the probes is about 20%) for the case of the afterglow chamber. The density of O atoms in plasma itself was then calculated taking into account the loss of atoms on the way from plasma to the afterglow. Obviously, the value for O atom density in plasma is not as accurate as that in the afterglow. Still, it represents a valuable tool used for quantification of the results on bacteria degradation. The O density in plasma is 1×10^{22} m^{-3}. The absolute accuracy of this value is estimated to about 50%. The relative accuracy (i.e. when identical probe is applied at identical condition) is, of course, much higher. Systematic measurements (results are published in our scientific paper) showed the relative accuracy of few %. We are using plasma created with an RF generator working at the frequency of 27.12 MHz and power of about 250W.

A photo of the plasma glow discharge chamber is shown in Figure 33, while that of the afterglow chamber is shown in Figure 34. Both chambers are made from borosilicate glass with the commercial name Schott 8250.

Figure 30: *Glow discharge chamber.* Borosilicate glass Schott 8250.

Figure 31: *Afterglow chamber.* Borosilicate glass Schott 8250.

Prior to any experiments with plasma radicals, a few samples of both types of bacteria were exposed to vacuum for eight hours, to check for any visible eventual effects of vacuum on bacterial cells. After that time of vacuum treatment, the samples of both types of bacteria were investigated with AFM and SEM. There were no visible changes on the bacterial cells neither on the capsule, as compared to cells, which were not exposed to vacuum. Here, it is worth mentioning, however, that the SEM itself uses vacuum conditions. The typical exposure time to vacuum in SEM is less than an hour. Obviously, the AFM results are more trustable in this sense. Some samples that were evacuated for 8 hours were placed in appropriate liquid culture medium (GN broth Hajna, Hi Media Laboratories Ltd. India) incubated for 24 h and transferred to the Columbia agar plates. After 24 h of further incubation visible colonies of both types of bacteria were observed on the agar plate surfaces. So, we can conclude that vacuum doesn't damage bacterial cells in that period of time (8 hours) and consequently will not affect results obtained with oxygen radicals.

To achieve desired effects on bacteria, samples prepared and sorted as mention above, were placed in plasma or afterglow chambers. The following two types of bacteria plasma treatment experiments were performed in:

I. PLASMA GLOW: In these experiments we investigated changes on bacterial cells of *Staphylococcus aureus* and *Escherichia coli* caused by all types of particles capable of interacting with bacteria (neutral molecules and atoms, positively charged molecules and atoms and light quanta). Exposure times for *Staphylococcus aureus* samples varied from 5 s up to 120 s, as follows: 5 s, 10 s, 15 s, 20 s, 30 s, 45 s, 60 s, 90 s and 120 s. Exposure times for *Escherichia coli* samples varied from 1 s up to 60 s, as follows: 1 s, 5 s, 15 s, 20 s, 60 s.

II. PLASMA AFTERGLOW: In these experiments we investigated changes on bacterial cells caused by neutral atoms in the ground state only. Exposure times for *Staphylococcus aureus* varied from 1s up to 500 s, as follows: 1 s, 5 s, 20 s, 30 s, 45 s, 90 s, 120 s, 180 s, 300 s and 500 s. Exposure times for *Escherichia coli* samples varied from 5 s up to 360 s, as follows: 5 s, 10 s, 15 s, 20 s, 30 s, 45 s, 90 s,120 s, 180 s, 360s and 500s.

Since the density of atoms is perfectly constant during treatment of bacteria, the flux of O atoms on the surface of our samples is also constant and the dose is calculated usin the following equation

$$D = \tfrac{1}{4} n v t, \qquad (1)$$

where **n** is the atom density, **v** its average of the absolute value of the thermal velocity (i.e. v = 630 m/s) and **t** is the treatment time.

3.1.3 Visualization of changes on bacterial cells

After treatment, some samples were investigated with Atomic Force Microscope (AFM) Solver MDT mod. Nova pro 47. Samples for AFM investigation were prepared on 10x10mm smooth, well oriented graphite, and highly polished silicon wafer substrates. The tapping operation mode was used. Samples were scaned with a standard silicon cantilever with spring constant 0,2 N/m and at resonance frequency 184 KHz. All measurements were done in the air, on areas 5x5 μm, 3x3 μm, 2x2 μm, 1.5x1.5 μm, 1x1 μm and 500x500 nm. Images were processed to obtain height, phase and amplitude data..

Some of the samples were investigated by SEM microscope with field emission of primary electrons CARL ZEISS, GEMINI series mod. Supra 35, at accelerating voltage of 1KeV. Samples for this visualization techniqe were prepared on 10x10mm Al substrates. We used no speciefic technique of sample preparation because we wished to keep them in the state made during oxygen radicals treatment.

4 Results

In the following text we present results of our study on the influence of oxygen radicals on Gram – positive bacteria *Staphylococcus aureus* and Gram –negative ones, *Escherichia coli*. Results are sorted in two groups: the first one contains images of both bacterial species treated in glow discharge conditions and the second images of bacteria treated in the afterglow. For comparison, we also present images of both bacteria from samples that were not exposed to plasma radicals.

Samples were investigated by high – resolution AFM and SEM and numerous images are taken and analyzed. For AFM, tapping (semicontact) operation mode is used. In this mode, images with information of shape (height) and composition (phase) of various materials are obtained.

4.1 Untreated samples of *Staphylococcus aureus* and *Escherichia coli*

Images of these samples serve for comparison of normal appearance of bacterial cells and we show them first. Both AFM and SEM images are shown. In these images, the morphology of substrates is visible, too.

4.1.1 Samples of *Staphylococcus aureus*

The normal appearance of untreated bacteria can be observed from Figs. 32 - 36. It is possible to see the very surface of our samples. As mentioned before, our bacteria are covered with capsule so the surface of capsule is observed. Deeper structures (cell wall, cytoplasmic membrane and cytoplasm) cannot be seen in these pictures. As shown in Chapter 1, *Staphylococcus aureus* are bacteria whose cells have spherical form. Many strains of these bacteria produce capsule, including the strain we used in our experiments.

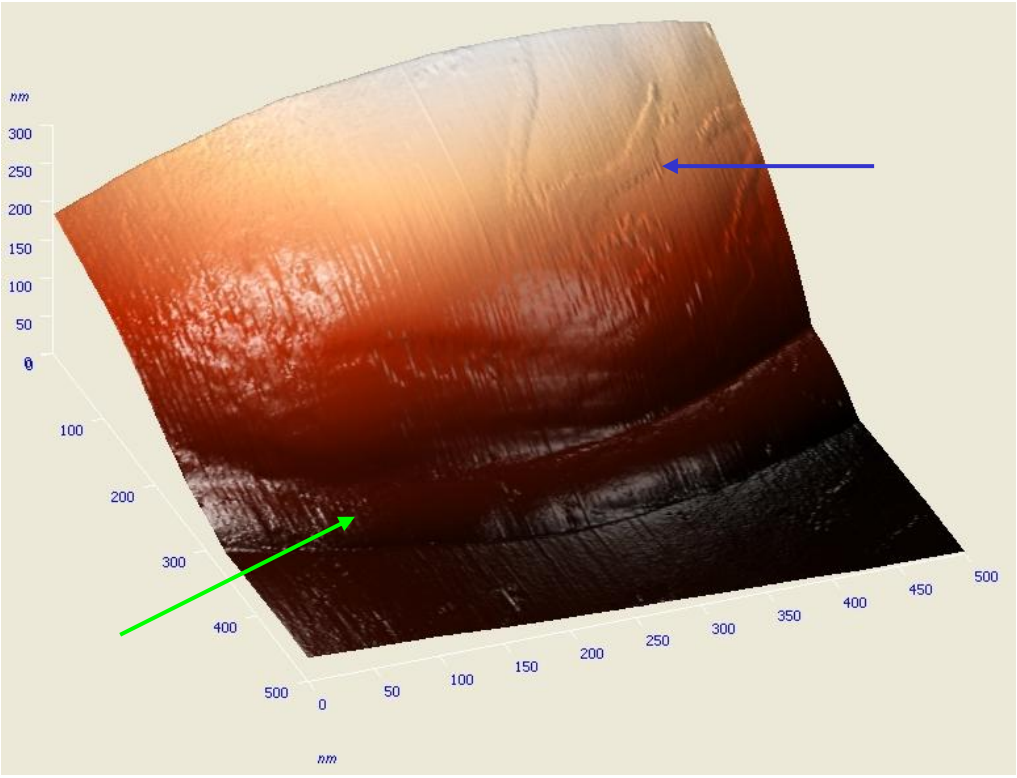

Figure 32: *AFM 0.5x0.5μm height 3D image of Staphylococcus aureus cell, untreated*. Clearly visible capsular material surrounds the cell (blue arrow) and tears down (green arrow).

Capsular substance surrounds the bacterial cell. As noticed from AFM images it slightly tears down and forms a ring around the bacterium. Small amount of this substance can be seen on the substrate around bacterial cell Such parts seem to be scattered in small quantities around bacterium. These observations are clearly visible, and pointed with arrows on Figures 32 – 34. In these images surface of bacterial cell is relatively smooth.

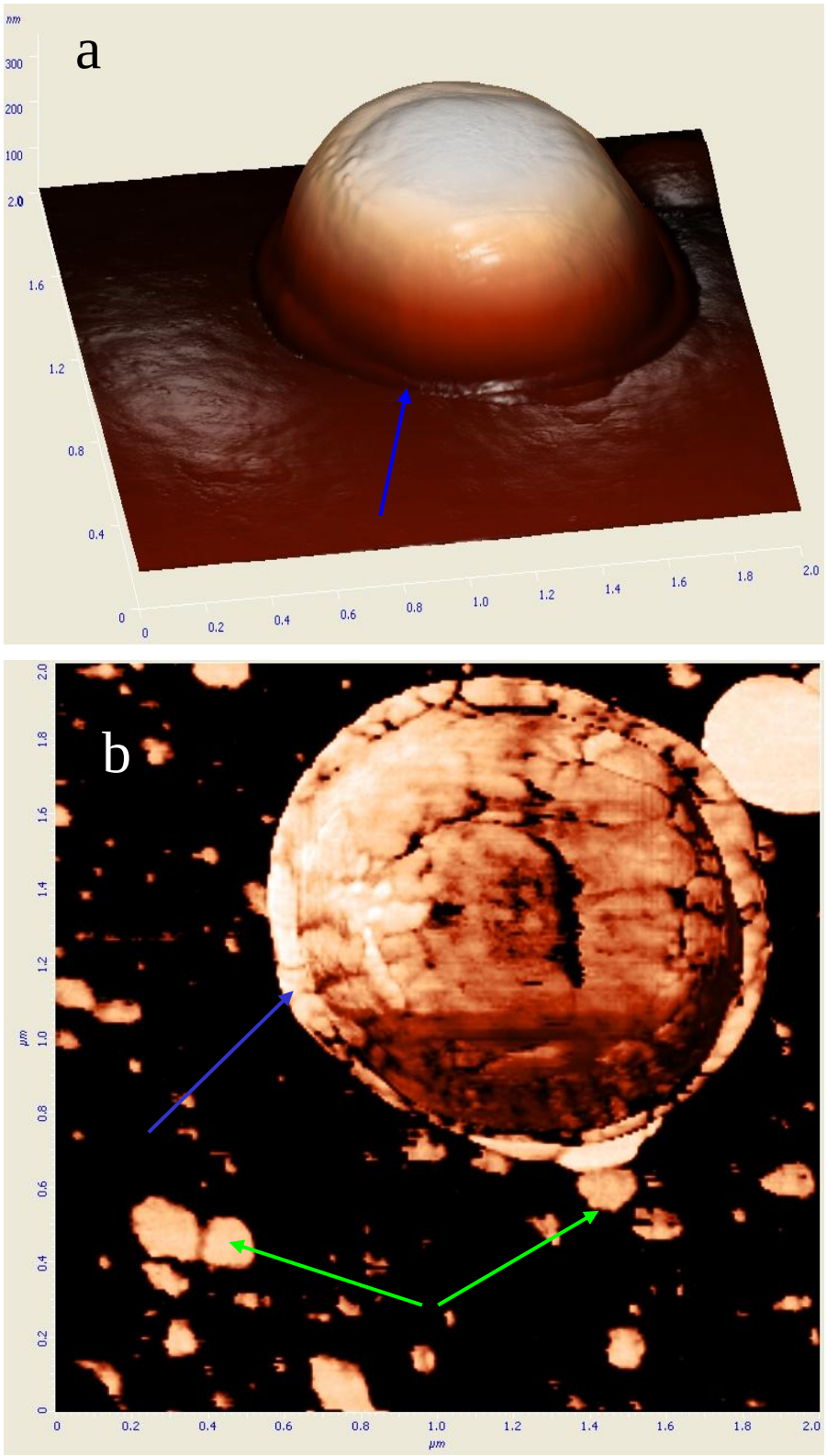

Figure 33: *AFM 2x2µm image of Staphylococcus aureus cell, untreated*. **a.** height 3D image; Smooth surface and clearly visible capsular material tears down (blue arrow), **b.** phase image; Clearly visible capsular material surrounds the cell (blue arrow) and slightly tears off (green arrows).

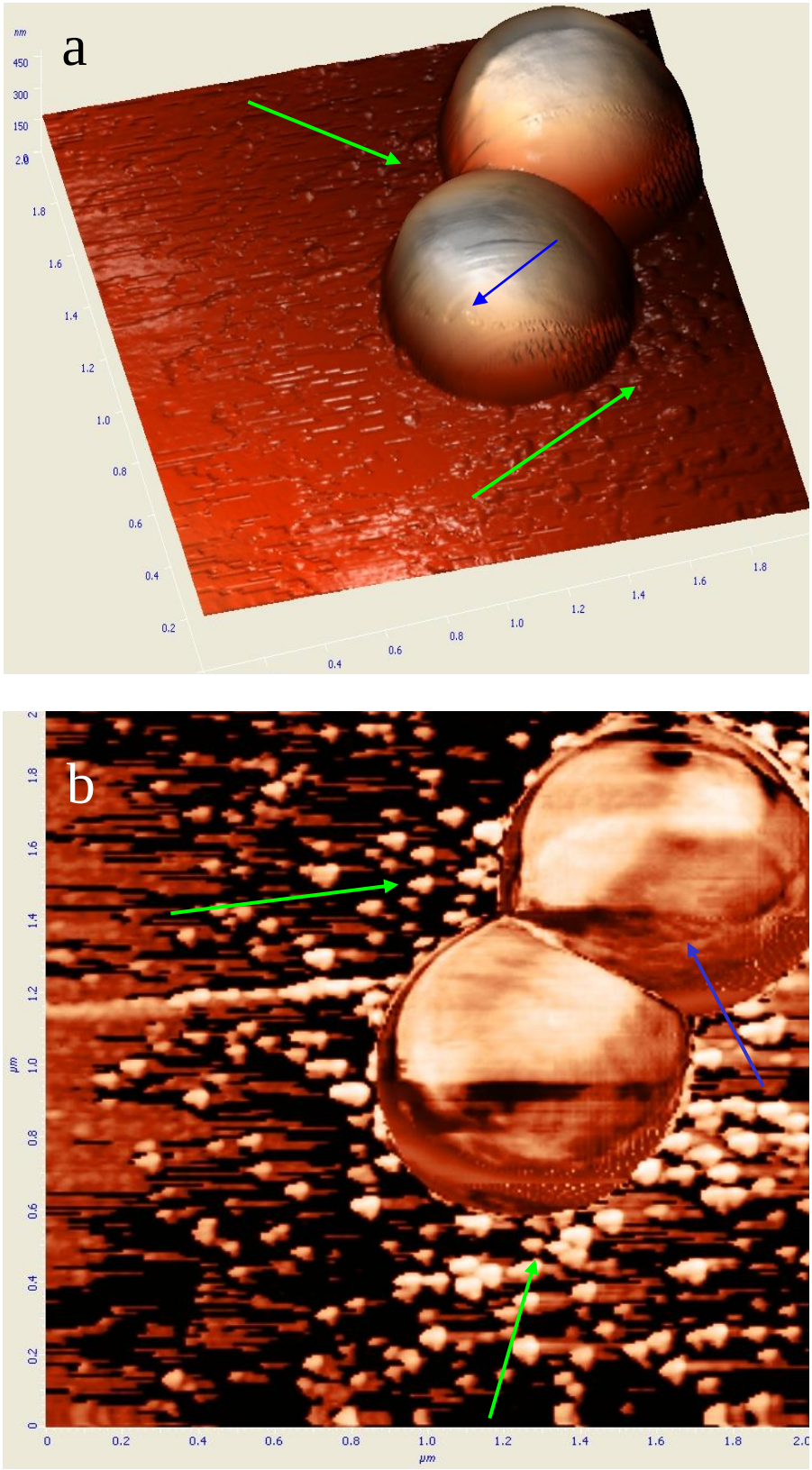

Figure 34: *AFM 2x2µm image of Staphylococcus aureus cells, untreated.* **a.** height 3D image; Relative smooth surface(blue arrow) and capsular material slightly tears down around bacterial cell (green arrows), **b.** phase image; Clearly visible capsular material surrounds the cells (green arrows) and slightly tears down (blue arrow).

In SEM images, capsular substance appears like a rather pretty transparent, smeared zone on the edges of bacterial cells. Tears of capsule can be seen as foggy areas off bacterial cells. So, in many cases, bacterial cells aren't very sharply demarcated from the surface. The morphology of Al substrate can be seen, too. This is visible in Figures 35 and 36.

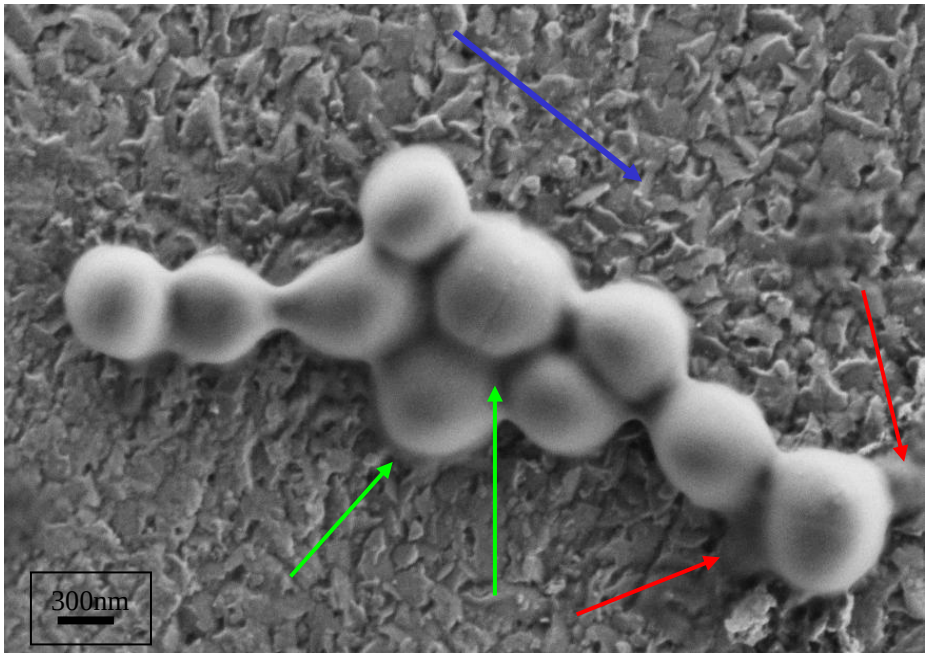

Figure 35: *SEM image of Staphylococcus aureus untreated*. Clearly visible capsular material surrounds the cells (green arrows) and slightly tears off (red arrows). Structure of Al substrate is visible, blue arrow pointed.

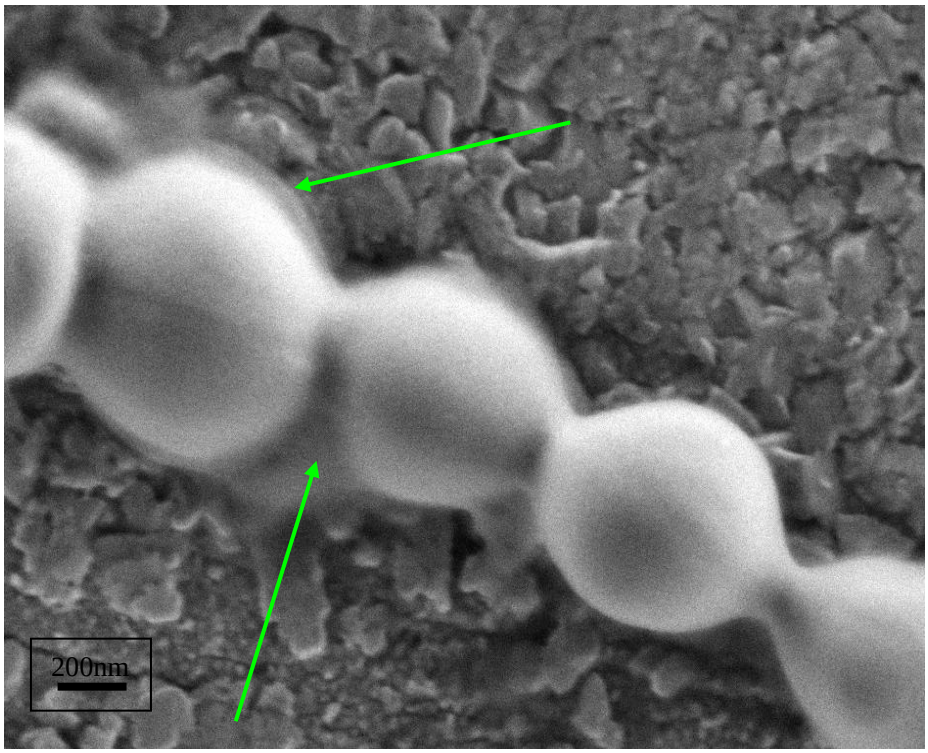

Figure 36: *SEM image of Staphylococcus aureus, untreated, for 8h vacuum exposed*. No visible changes on bacterial cells.

4.1.2 Samples of *Escherichia coli*

The cells of this bacteria can be found in bacilar (rod) or coccobacilar form. Almost all strains are surrounded with voluminous capsule, as well as strains we used in this experiments. Appearance of capsule of *Escherichia coli* in this images is very similar to those of capsule of *Staphylococcus aureus*.

In AFM images, capsule can be seen as bulky material surrounding bacterial cell, as well as small amount of rounded droplets on surface of the substrate. Flagella and pili can be seen, too. This is shown and pointed with arrows in Figure 37.

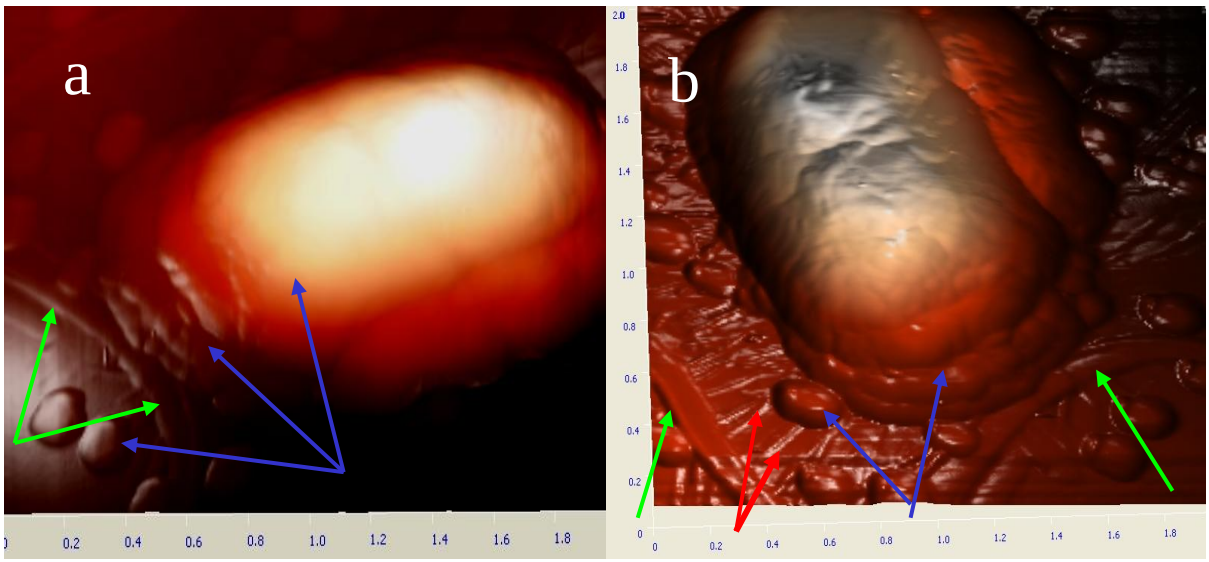

Figure 37: *AFM 2x2μm height 3D image of Escherichia coli cell, untreated.* **a.**Voluminous capsular substance coat bacterial cell and slightly tears off, blue arrows pointed, flagella (green arrows) and pili (red arrows) are visible. **b.** Capsular substance (glycocalix) coats bacterial cell and slightly tears off, blue arrows pointed.

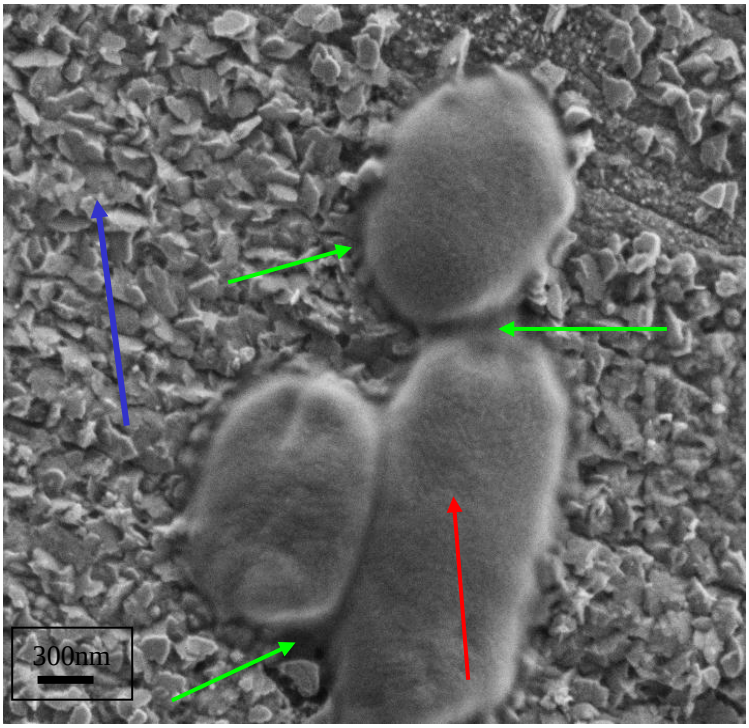

Figure 38: *SEM image of Escherichia coli cells, untreated.* Capsular substance is visible on surface of the cells (red arrow) and slightly tears down (green arrows). Morphology of Al substrate is visible, blue arrow pointed.

In SEM images, capsule is visible as transparent, foggy zone surrounding bacterial cells and filling spaces between them, showed in Figures 38, 39 and 40. Morphology of Al substrate is visible, too.

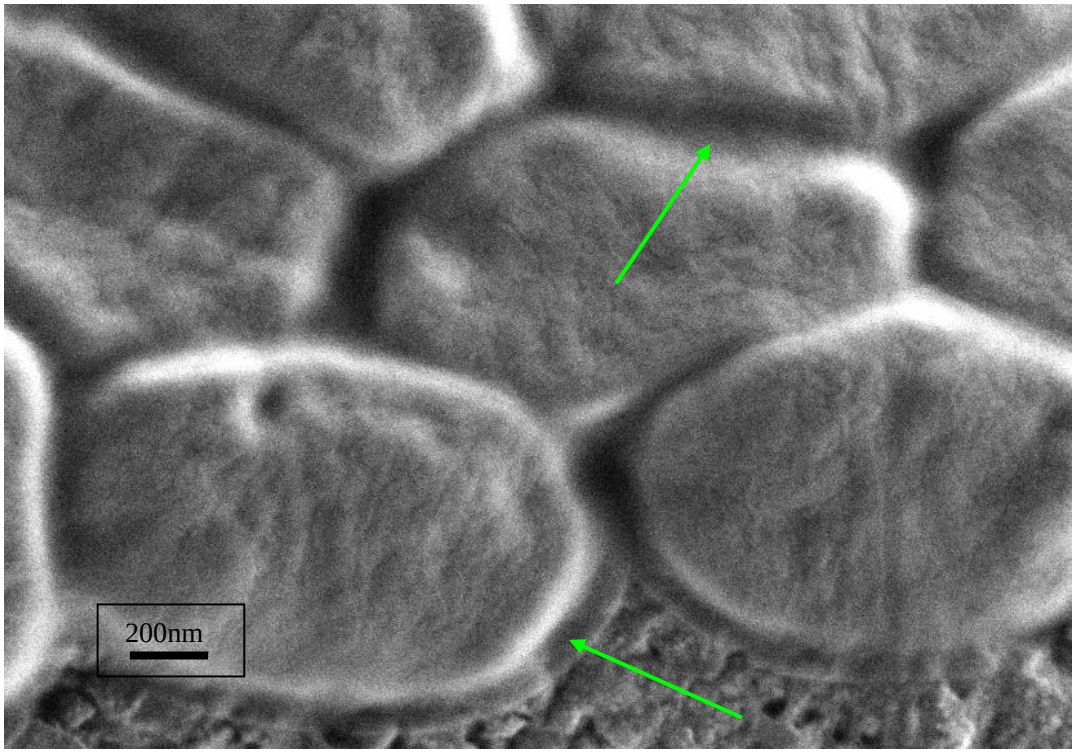

Figure 39: *SEM image of Escherichia coli cells, untreated.* Capsular substance is visible, green arrows pointed.

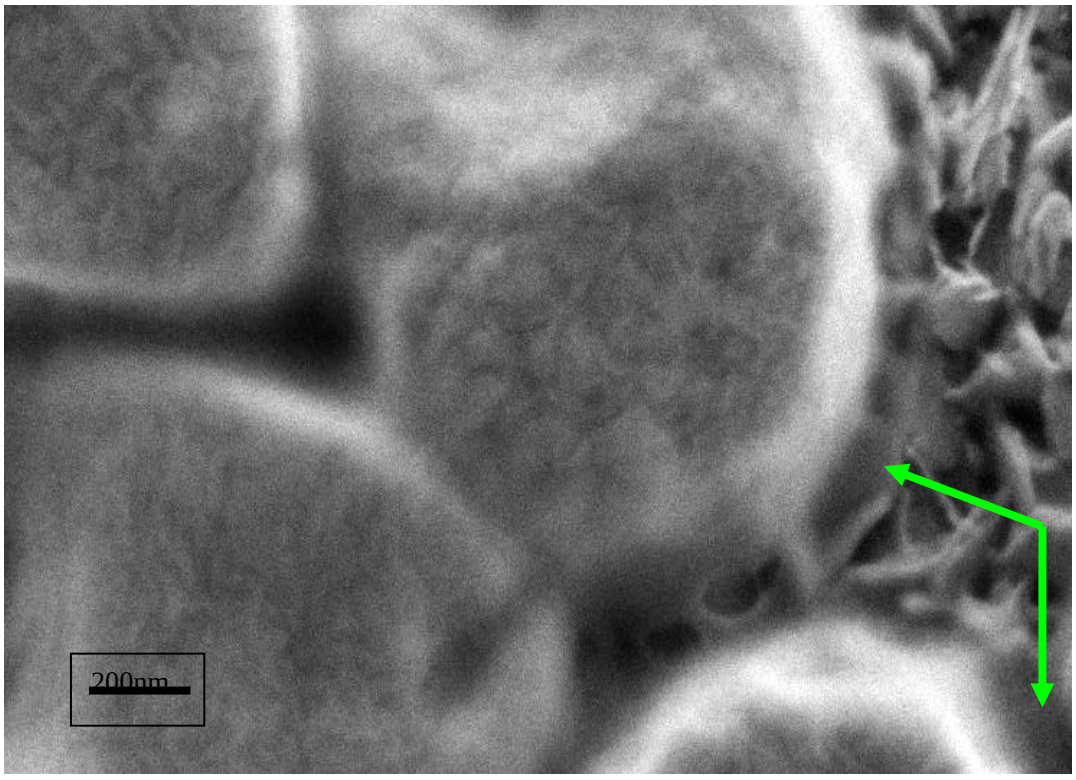

Figure 40: *SEM image of Escherichia coli cells, untreated, for 8h vacuum exposed.* No visible changes. Capsule pointed with arrows.

4.2 Samples treated in glow discharge conditions

Samples treated in glow discharge conditions were exposed to all oxygen radicals generated in plasma including neutral atoms as well as charged particles and metastable molecules. It was expected that modifications happen in relatively short period of time.

4.2.1 Samples of *Staphylococcus aureus*

Exposure time for *Staphylococcus aureus* samples was from 5 to 120 seconds, as follows: 5 s, 10 s, 15 s, 20 s, 30 s, 45 s, 90 s, and 120 s. After the treatment, samples were investigated with AFM and SEM.

For this type of bacteria that were exposed to glow discharge, the first visible changes has been observed after approx. 5 to 10 seconds of exposure.

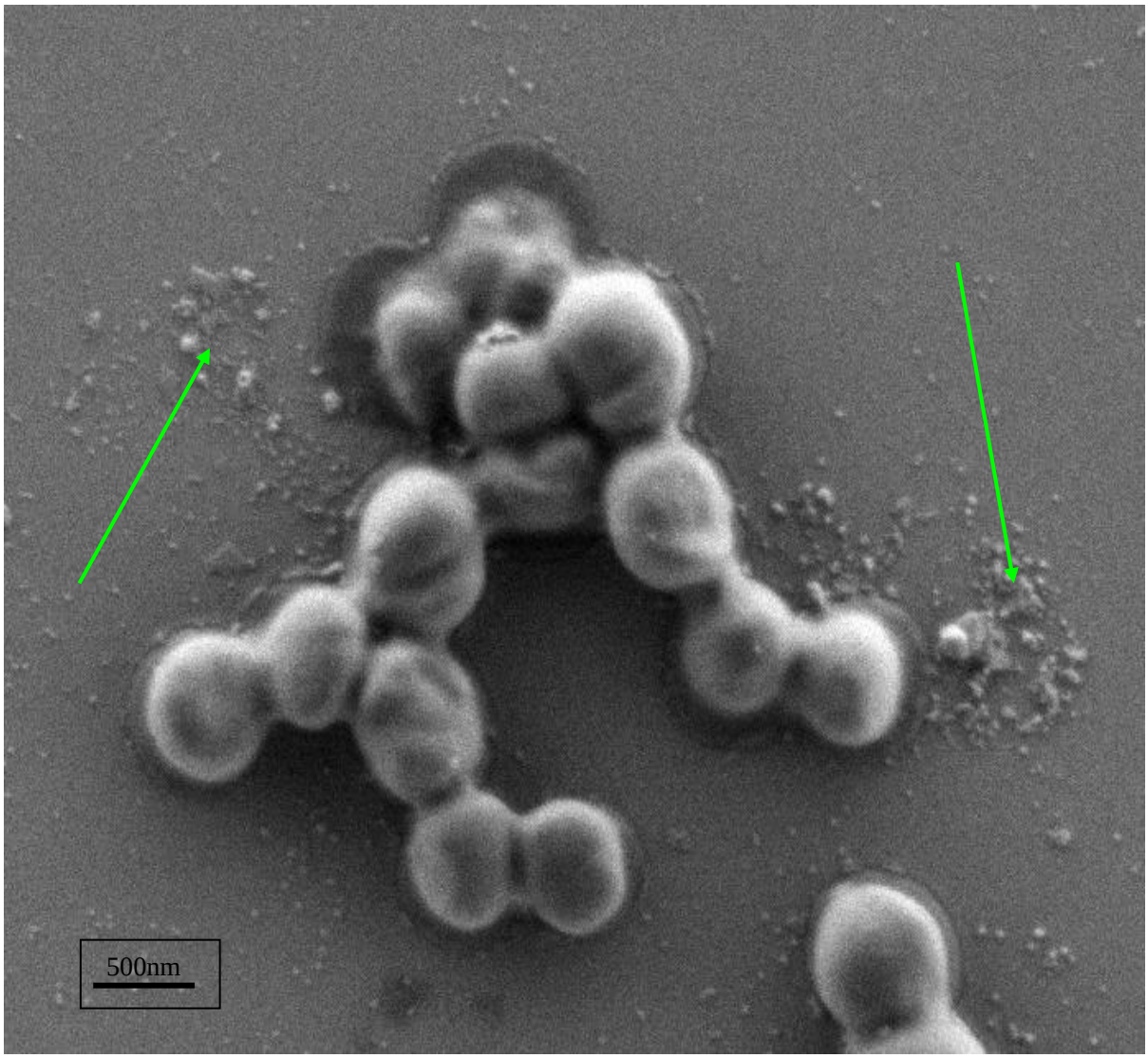

Figure 41: *SEM image of Staphylococcus aureus, glow discharge 5s treated.* Significant amount of capsular material scattered around the cells, green arrows pointed.

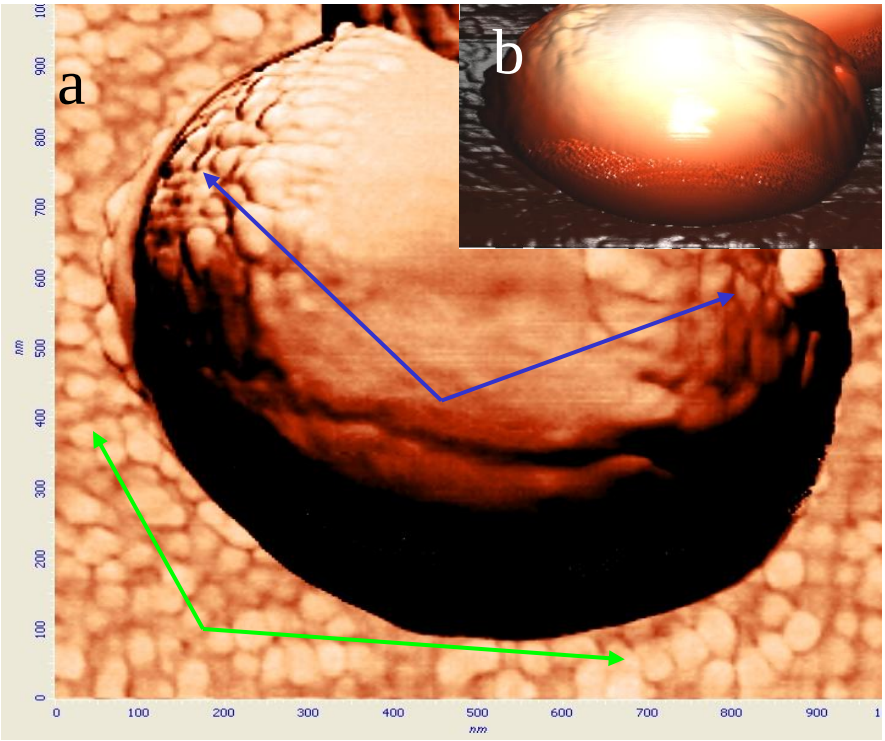

Figure 42: *AFM 1 x 1µm image of Staphylococcus aureus cell, 5s glow discharge treated*. **a.** phase image, **b.** height 3D image; Capsular structure is changed (blue arrows). A plenty of capsular material tears off around bacterial cell (green arrows).

In this period, changes in capsular substance happen (shown with blue arrows in Figure 42). A plenty of mostly round shaped capsular material (glycocalix) tears off and surrounds bacterial cells (Figs. 41 – 43) This is clearly visible, when comparing with bacterial cells of untreated samples (Figs. 32- 36).

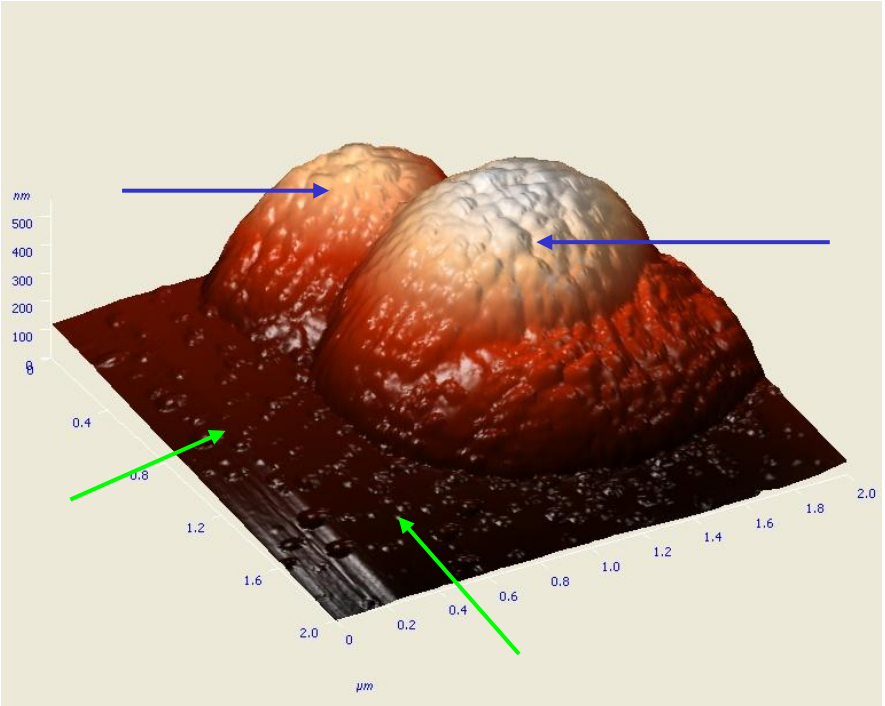

Figure 43: *AFM 2x2µm height 3D image of Staphylococcus aureus cells, 10s glow discharge treated*. Peptidoglycan rough structure is visible (blue arrows). A plenty of capsular material tears off around bacterial cell (green arrows).

After about 10 seconds of exposure, almost complete capsular material is removed. At this period, etching of peptidoglycan from the cell wall starts (Fig. 43). Appearance of particles scattered around bacterial cells is different if we compare them with particles on previous images. Segments of peptidoglycan, clearly visible by AFM, are different in size and polygonal irregular in shape (Figures 44 – 46).

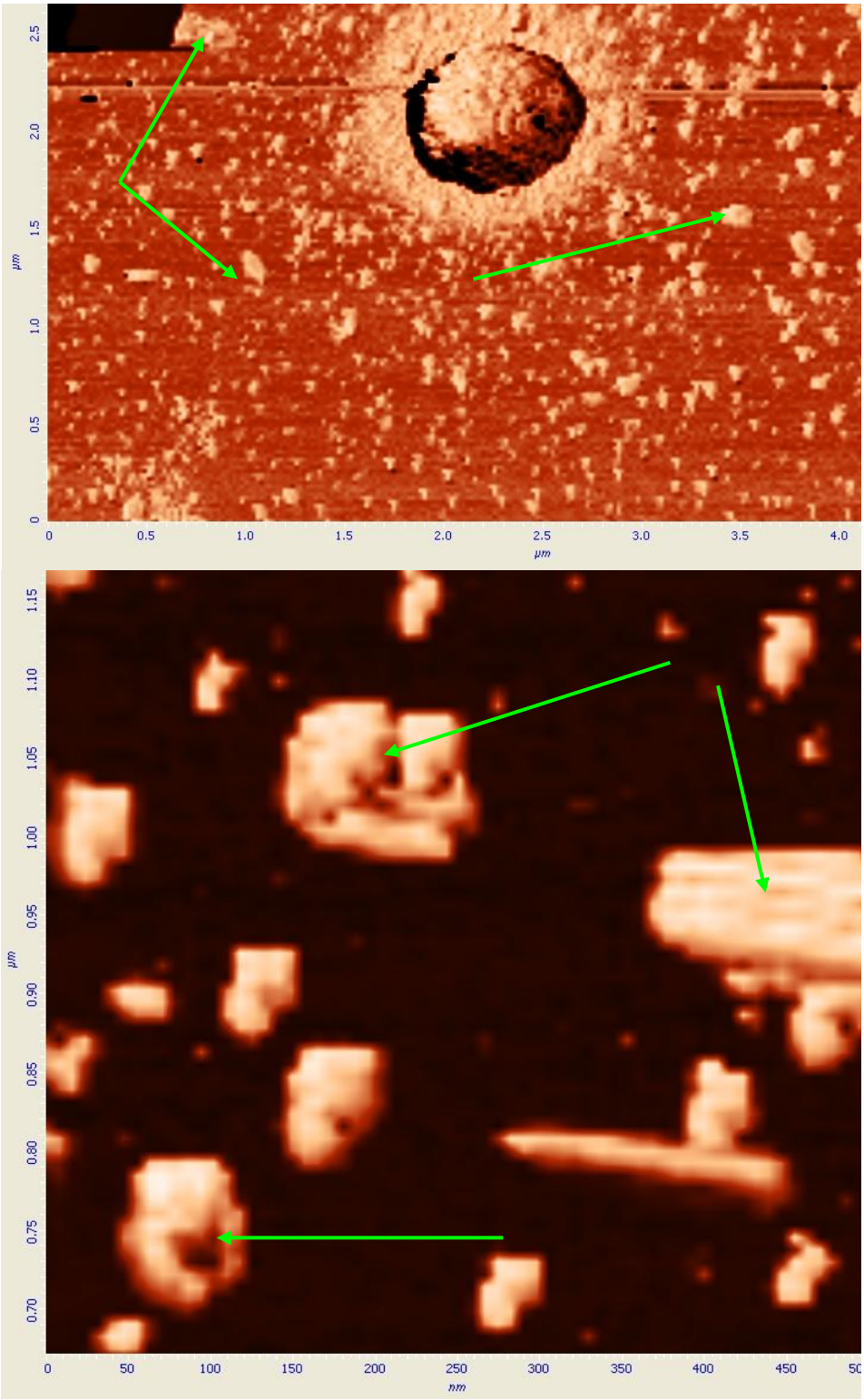

Figure 44: **a.** *AFM 5x5µm phase image of Staphylococcus aureus cell, 15s glow discharge treated.* A plenty of peptidoglycan material is scattered around bacterial cell (green arrows). **b.** *AFM 0,5x0,5µm phase image.* Pieces of peptidoglycan different in size and polygonal shape are visible, arrows pointed.

Some large particles of peplydoglycane are removed from the cell wall (green arrows on Figs. 44 and 45). Similarity of these pieces with structures on cell surface is clearly visible on phase images. This process continues approx. to 30 seconds exposure time (Figs. 47 – 48). In that period, strong disrupting of peptidoglycane domains starts. The process of disintegration of the cell wall rapidly accelerates.

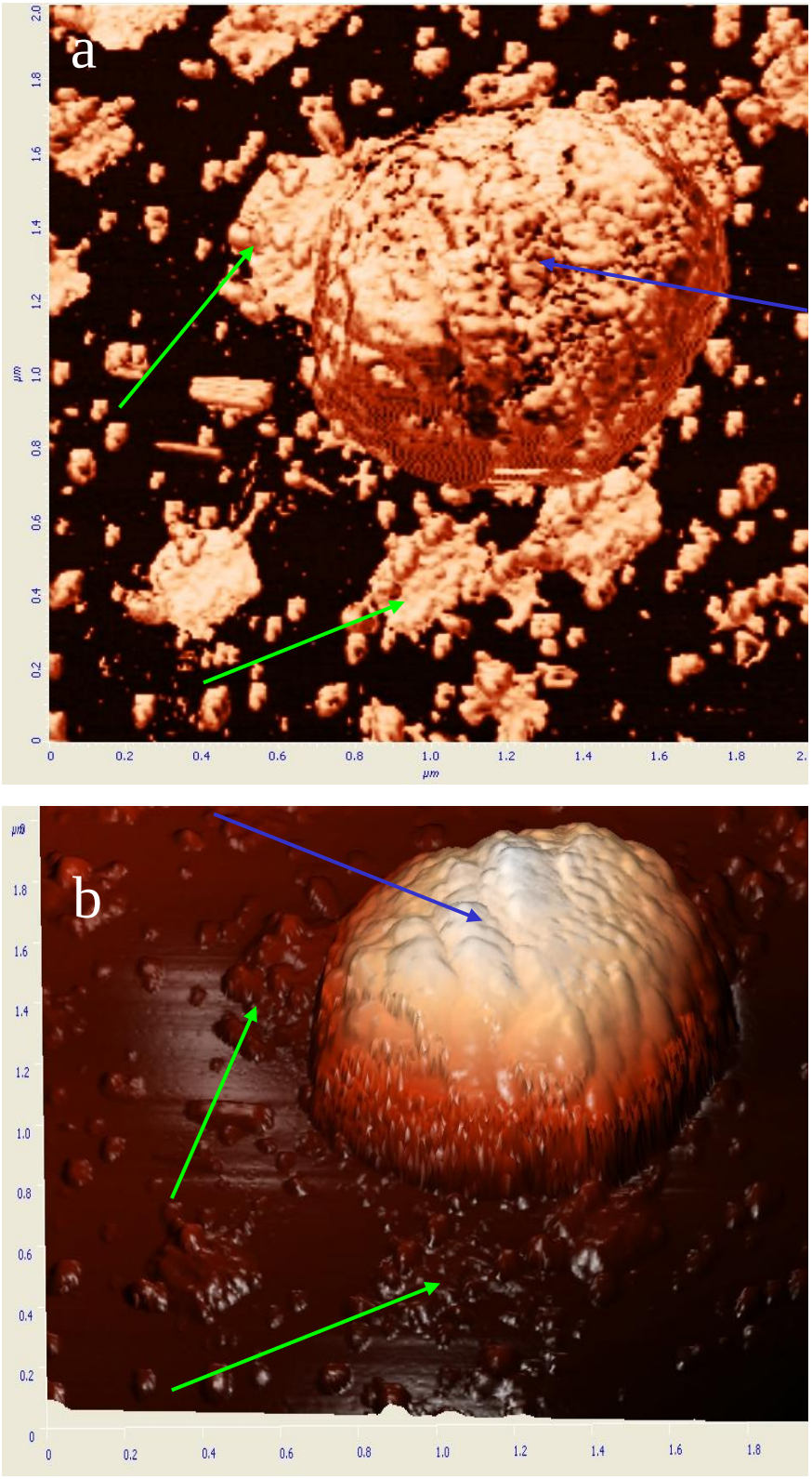

Figure 45: *AFM 2x2μm image of Staphylococcus aureus cell, 15s glow discharge treated.* **a.** phase image, **b.** height 3D image; Peptidoglycan rough structure on bacterial cell is visible (blue arrow). Peptidoglycan material scattered around bacterial cell (green arrows). Disrupting of peptidoglycan domains started.

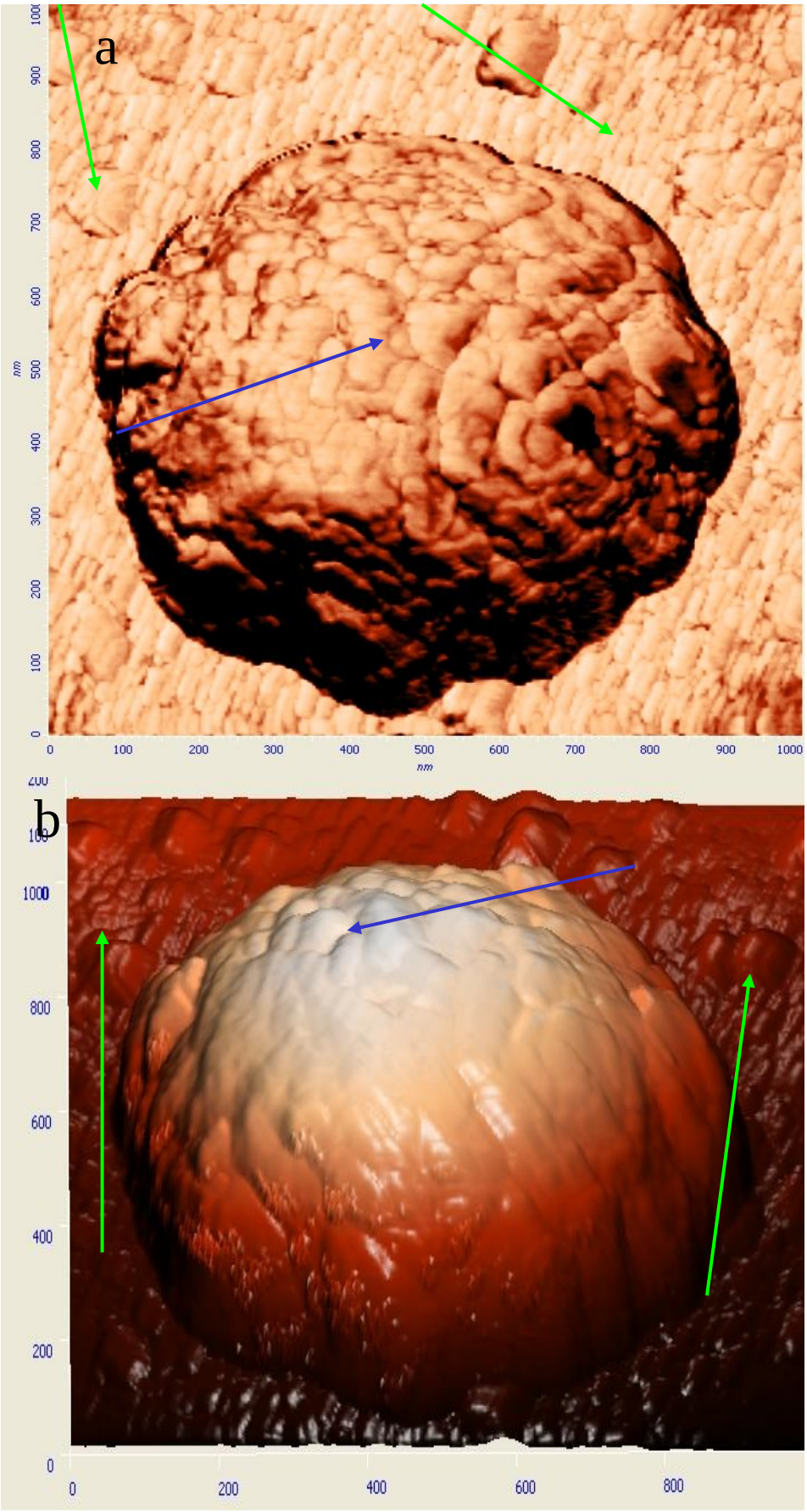

Figure 46: A*FM 1x1 μm image of Staphylococcus aureus cell, 20s glow discharge treated*. **a.** phase image, **b.** height 3D image; Peptidoglycan rough structure on bacterial cell is visible (blue arrows), a plenty of peptidoglycan material scattered around bacterial cell (green arrows).

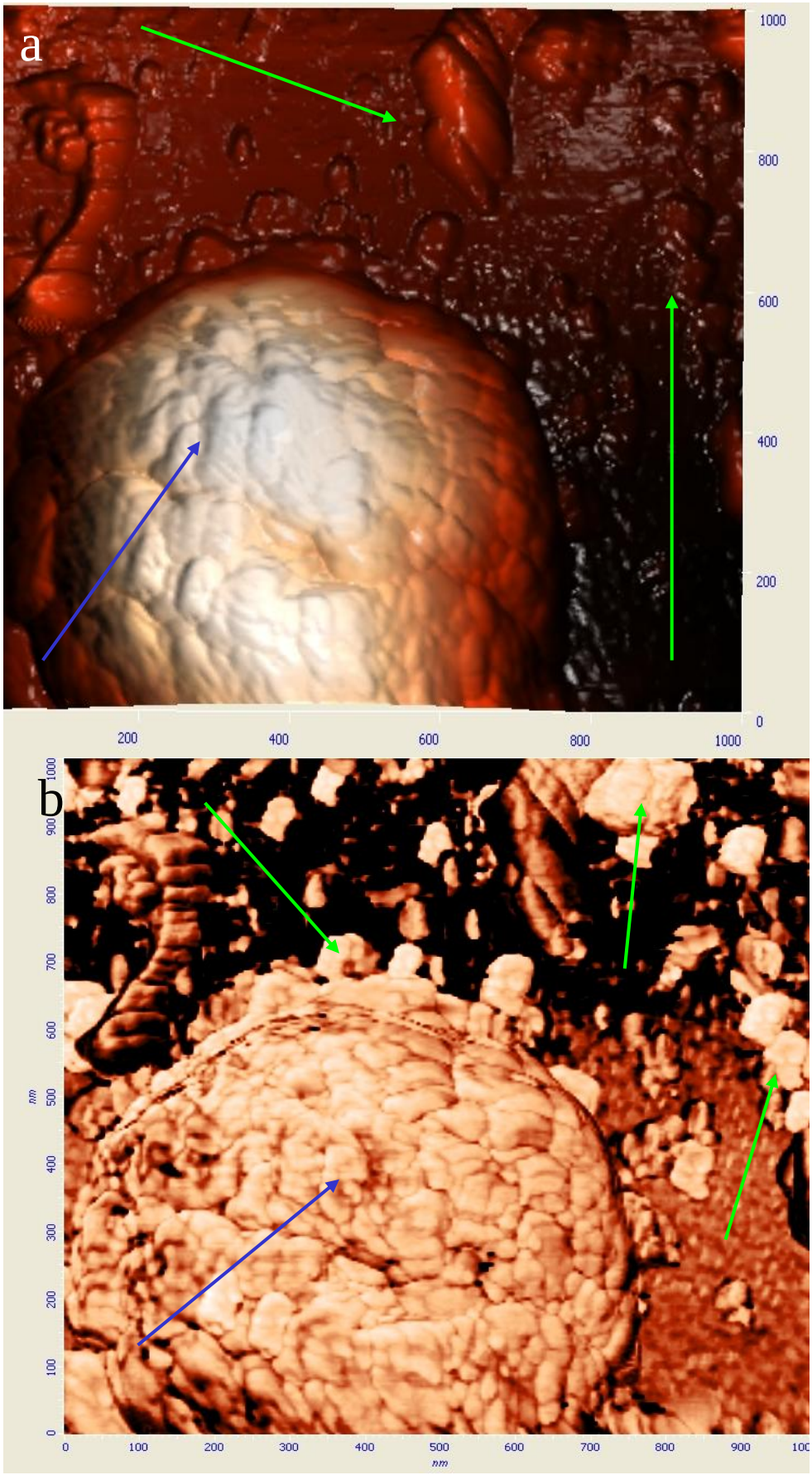

Figure 47: *AFM 1x1µm image of Staphylococcus aureus cell, 30s glow discharge treated.* **a** height 3D image, **b.** phase image; Peptidoglycan rough structure on bacterial cell is visible (blue arrows), a plenty of peptidoglycan material scattered around bacterial cell (green arrows).

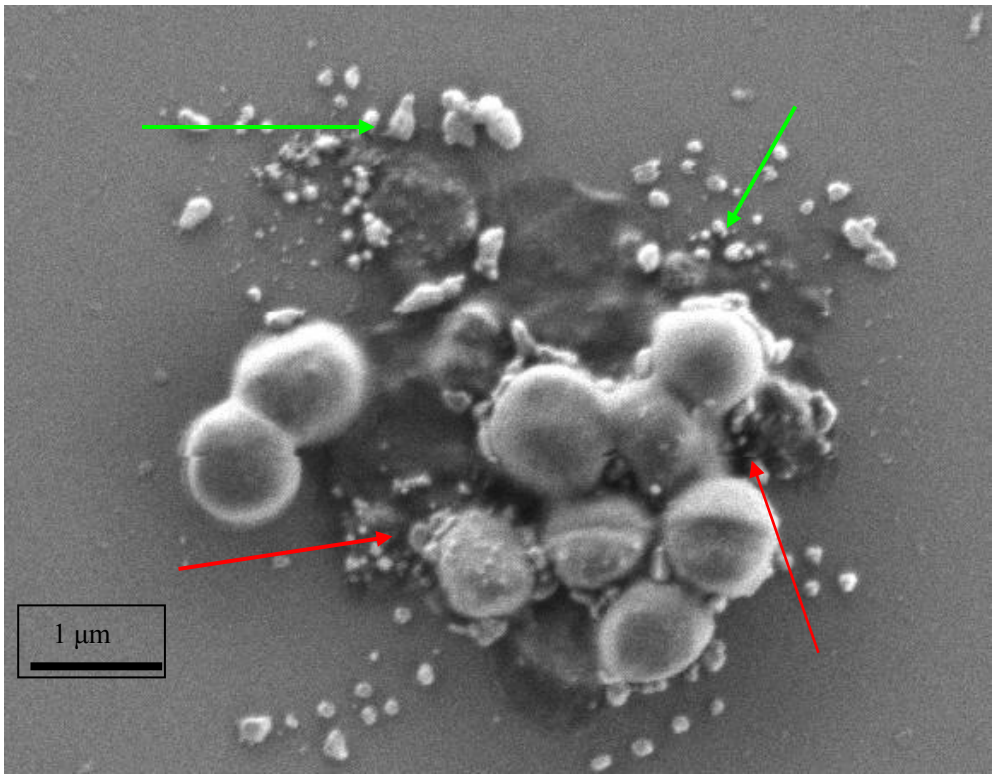

Figure 48: *SEM image of Staphylococcus aureus 30s glow discharge treated.* Clearly visible peptidoglycan scattered arounds the cells, green arrows pointed. Disrupting of peptidoglycan domains started, red arrows pointed.

After approx. 40 seconds most of bacterial cells are disrupted. There are clearly visible pieces of peptidoglycan and intracellular material scattered around the disrupted cells (Figs.49 – 50). Some pieces of peptidoglycan can still exist on cell surface (red arrow on Fig. 50b) and some traces of the cell wall can be observed (Fig. 50b, black arrow and Fig. 53, red arrows).

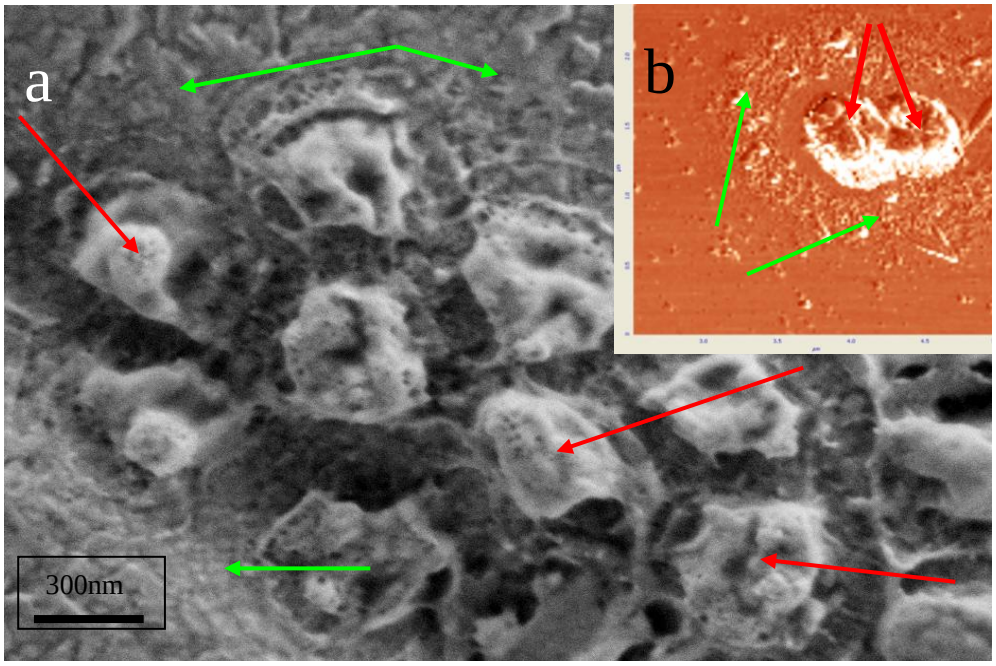

Figure 49: **a.** *SEM image of Staphylococcus aureus 40s glow discharge treated.* Disrupted cells, red arrows pointed, cellular material scattered around bacterial cells, green arrows. **b.** *AFM 5x5µm phase image of Staphylococcus aureus cells, 45s glow discharge treated.* Disrupted cells, red arrows pointed. Cellular material is scattered around bacterial cells, green arrows pointed.

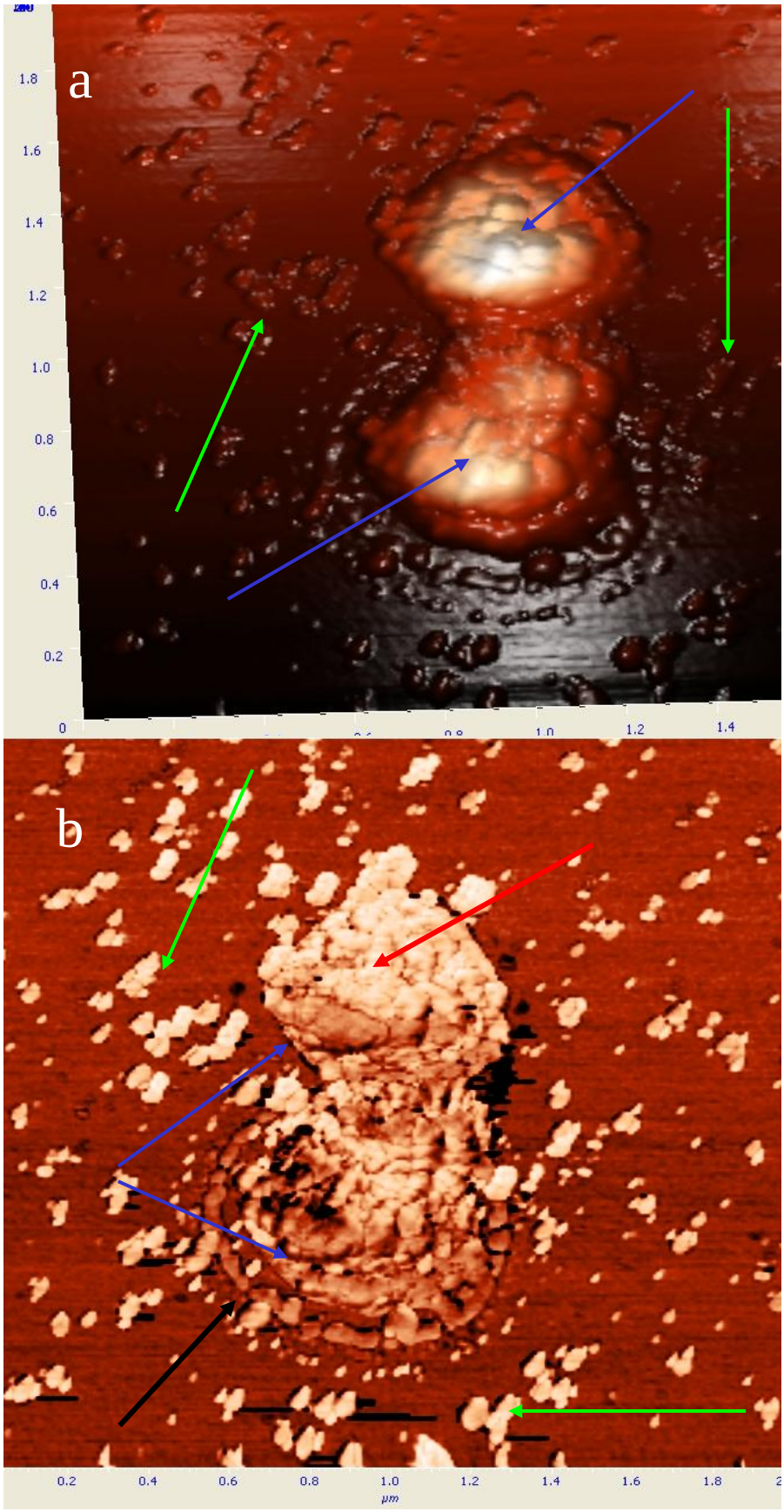

Figure 50: *AFM 2x2µm image of Staphylococcus aureus cells, 45s glow discharge treated.* **a.** height 3D image, **b.** phase image; Disrupted cells, intracellular structures are visible (blue arrows), but some peptidoglycan are still on cell surface (red arrow). A plenty of cellular material and peptidoglycan scattered around bacterial cells (green arrows). Traces of bacterial cell wall are visible (black arrow).

After these abrupt changes, the disintegrating process slows down. Degradation and removal of rough, irregular round shaped pieces of intracellular material (Figs. 51) keeps going on during the period longer than 120 seconds (Figs. 52 – 54).

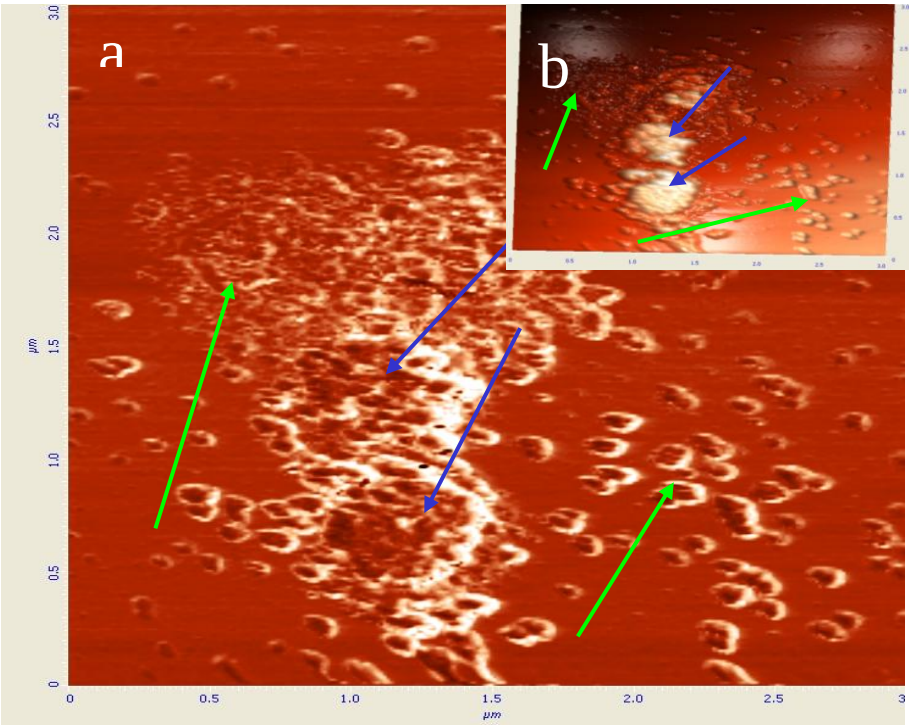

Figure 51: *AFM 3x3µm image of Staphylococcus aureus cells, 60s glow discharge treated.* **a.** phase image, **b.** height 3D image; Further degradation of disrupted cells (blue arrows) continues. Cellular material scattered around bacterial cells (green arrows).

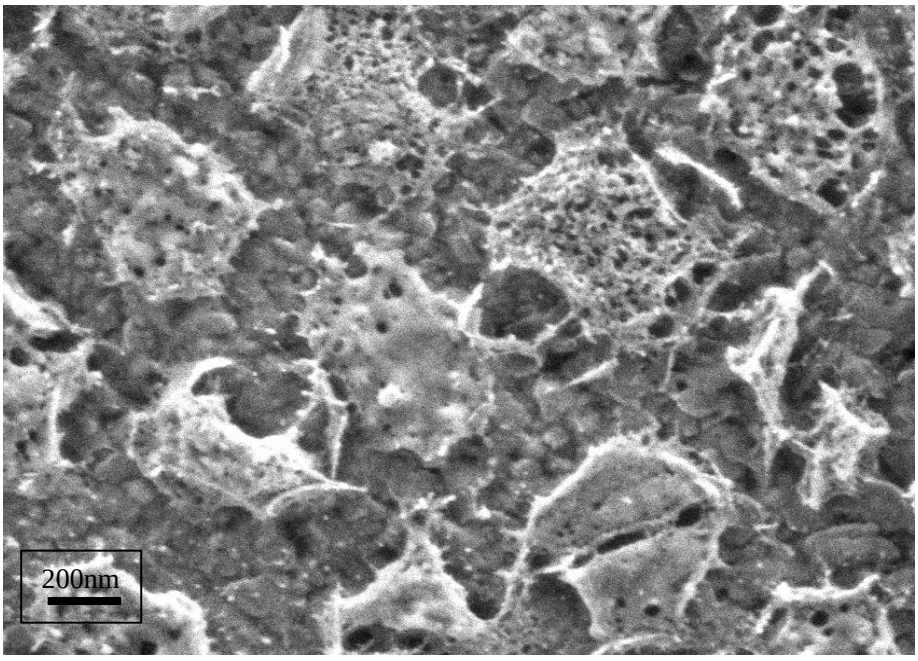

Figure 52: *SEM image of Staphylococcus aureus 60s glow discharge treated.* Disrupted cells, degradation of cellular substance continues.

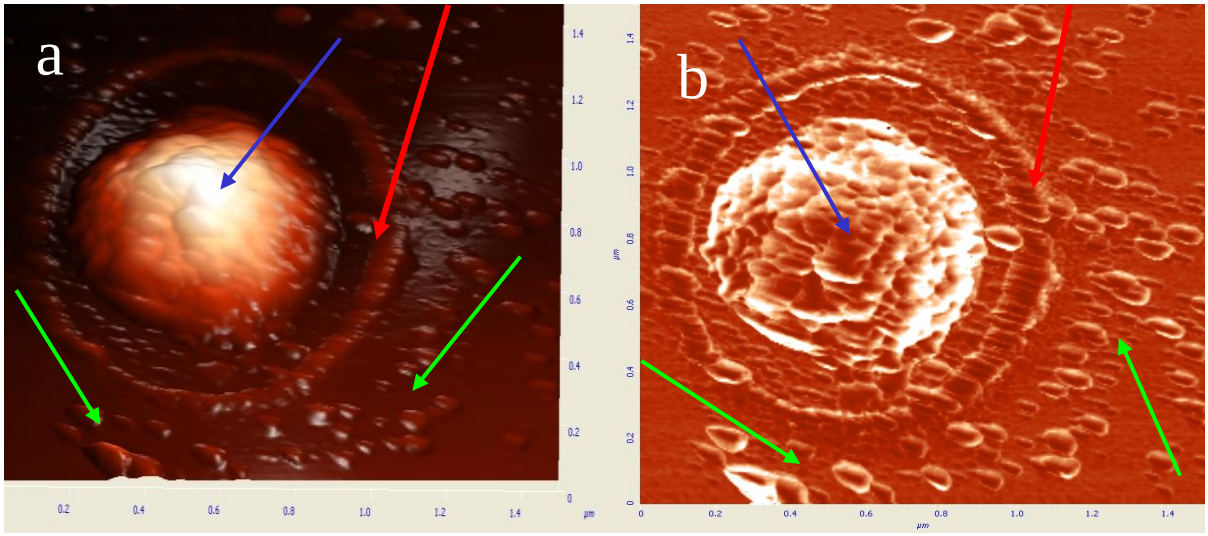

Figure 53: *AFM 1.5x1.5µm image of Staphylococcus aureus cell, 90s glow discharge treated.* **a.** height 3D image, **b.** phase image; Disrupted cell (blue arrows), residuals of bacterial cell wall are visible (red arrows). Cellular material scattered around bacterial cells (green arrows).

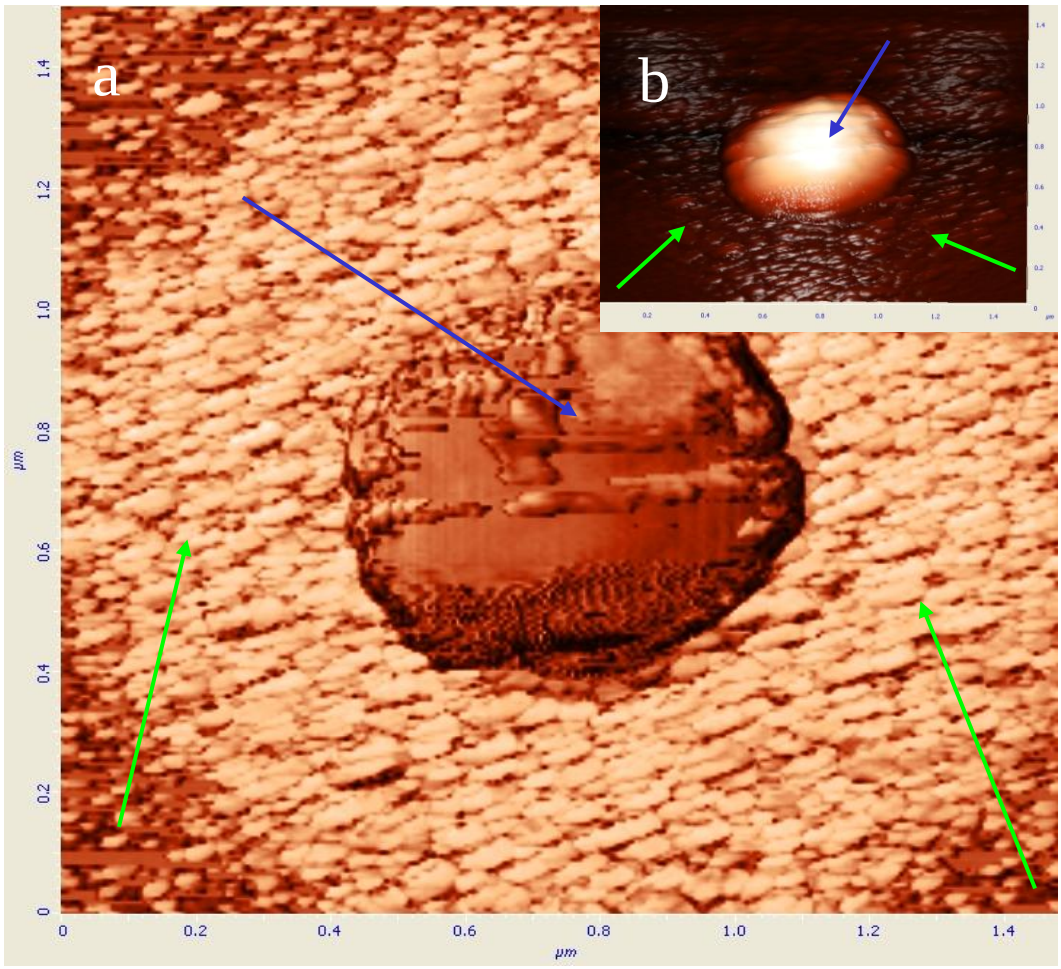

Figure 54: AFM *1.5x1.5µm image of Staphylococcus aureus cell, 120s glow discharge treated.* **a.** phase image **b.** height 3D image, Further degradation of disrupted cell (blue arrows), cellular material scattered around bacterial cell (green arrows).

4.2.2 Samples of *Escherichia coli*

Exposure time for E*scherichia coli* samples was from 1 to 60 seconds, as follows: 1 s, 5 s, 10 s, 15s, 20 s, 40 s and 60 s. After treatment, samples were investigated with SEM and images were taken.

On bacterial cells of this species exposed to glow discharge for 1 second, changes on capsular structures are visible (Fig. 55), if comparing them against untreated bacteria (Figs. 38 – 40). Modified capsular material tears down (red arrows) and is clearly visible around bacterial cell, as irregular round shaped particles, what is pointed with green arrows in Fig.55. At this period, sharp granular morphology of Al substrate, observed on untreated samples, is not visible.

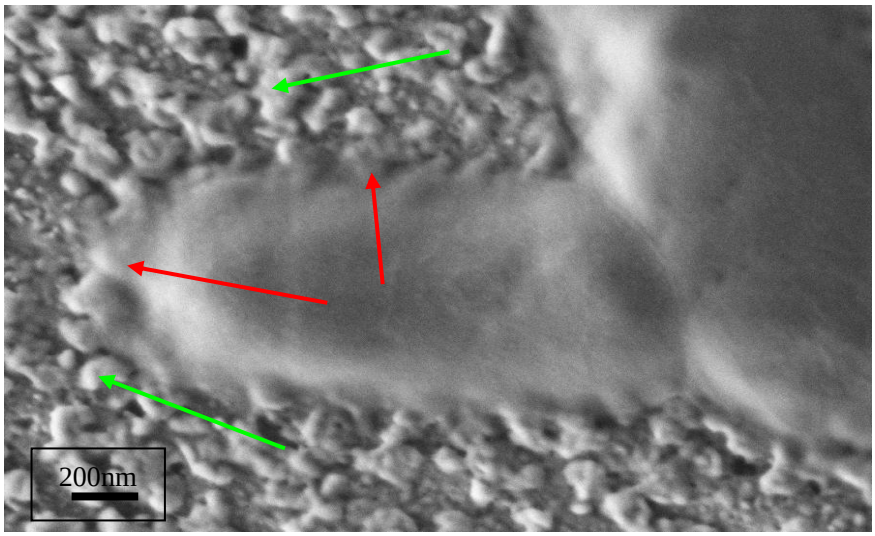

Figure 55: *SEM image of Escherichia coli 1s, glow discharge treated.* Modified capsular material tears down (red arrows) and is clearly visible around bacterial cell (green arrows).

After 5 seconds exposure, etching of capsular substance starts. Visible spaces between the cells, filled with capsular material earlier, become noticeable and, no transparent zone of capsule visible on SEM images of non treated cells (see Figs. 38 – 40), all pointed with green arrows in Fig. 56. After removal of capsule, granular structure of Al substrate is visible again (blue arrow in Fig. 56).

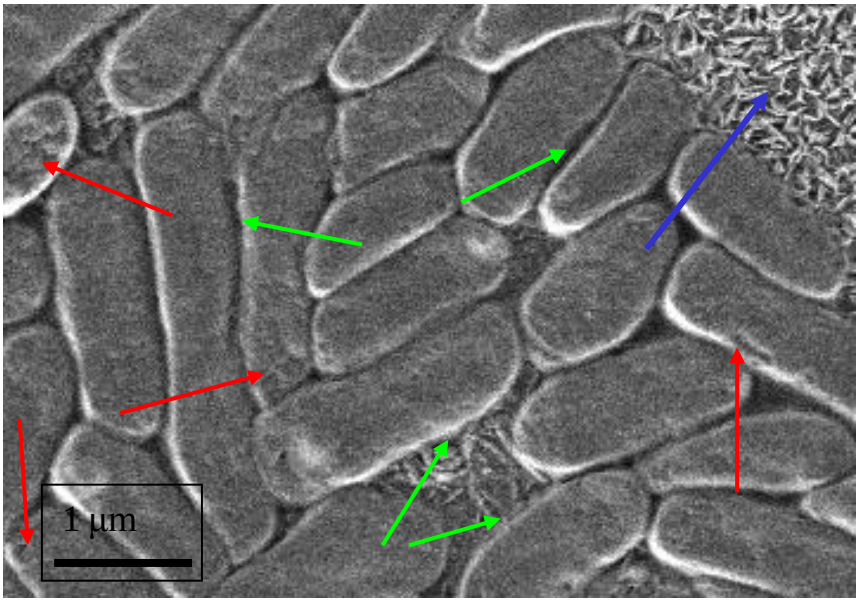

Figure 56: *SEM image of Escherichia coli, 5s glow discharge treated.* Empty spaces between bacterial cells are visible, capsular substance missing (green arrows). Some damages of bacterial cell wall are visible (red arrows). Sharp granular structure of Al substrate is visible (blue arrow).

At this period some damages on bacterial cells become visible, what is pointed with red arrows in Fig. 56.

Treatment in glow discharge for 10 seconds cause serious damages on the cell surface, in form of irregular holes and cracks, pointed with red arrows in Fig. 57, which mean that bacterial cell wall must be seriously damaged. Probably, it means the death of bacteria.

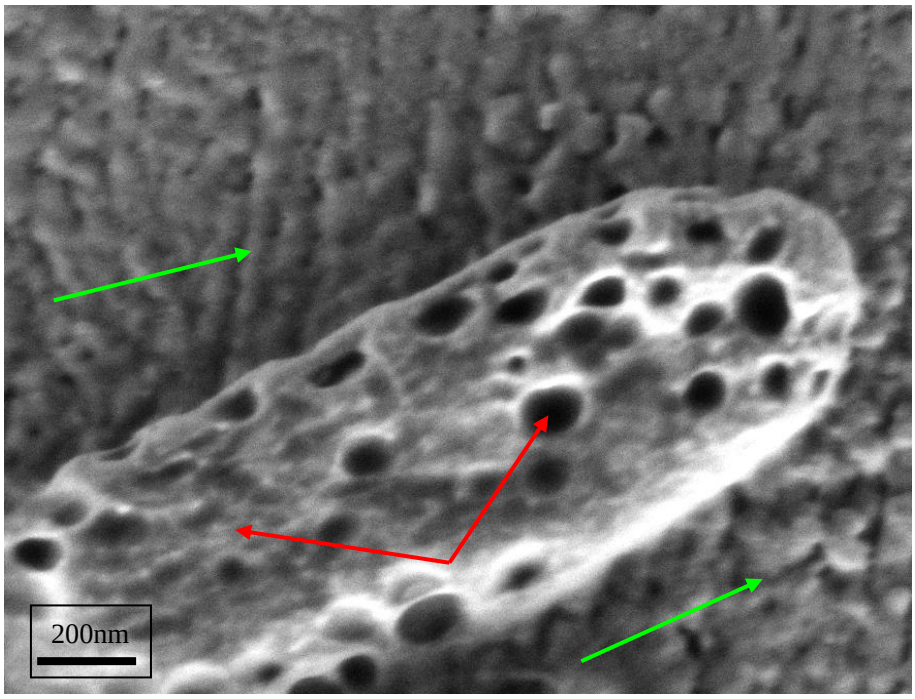

Figure 57: *SEM image of Escherichia coli, 10s glow discharge treated.* Massive cell wall damages are visible (red arrows). Material from bacterial cell wall scattered all around the cell (green arrows).

Material from bacterial cell wall is scattered all around the cell, what is pointed with green arrows in Figs. 57 and 58. Pieces are rounded, not likely to pieces from Gram – positive bacteria. After 20 seconds exposure, whole bacterial cell is totally destructed. Degradation continues (Figs. 59 – 60) until some ashes are left.

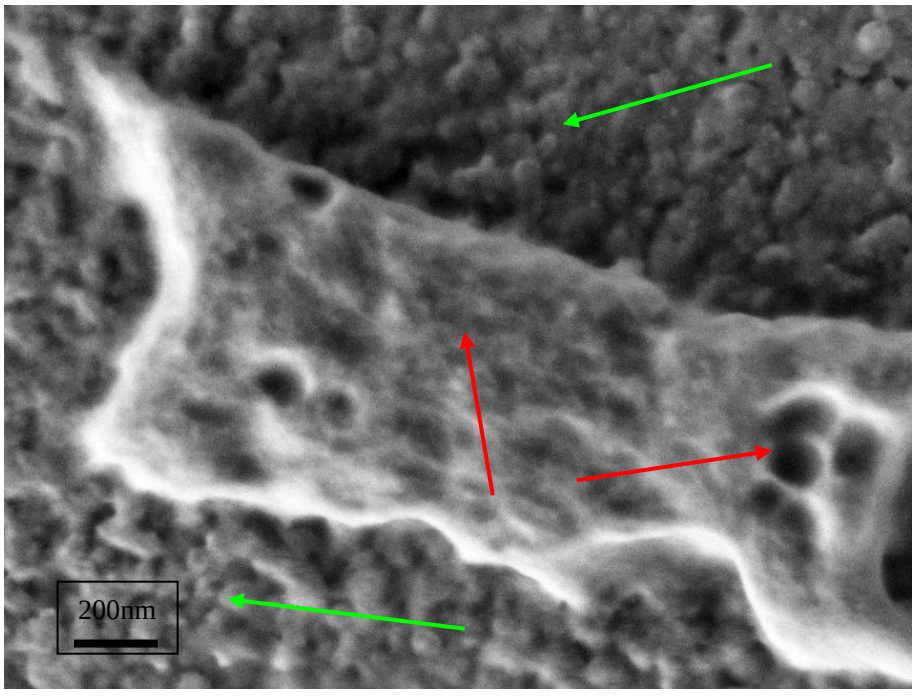

Figure 58: *SEM image of Escherichia coli, 15s glow discharge treated.* Massive cell wall damages are visible (red arrows). Material from bacterial cell wall scattered all around the cell (green arrows).

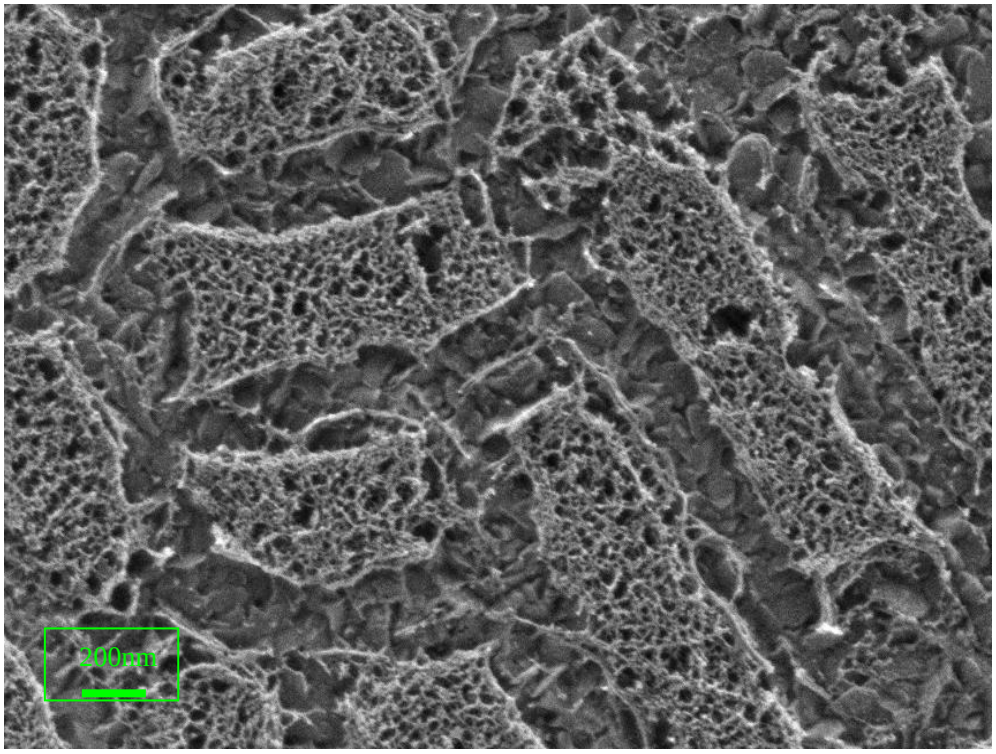

Figure 59: *SEM image of Escherichia coli, 20s glow discharge treated*. Bacterial cell is destructed totally.

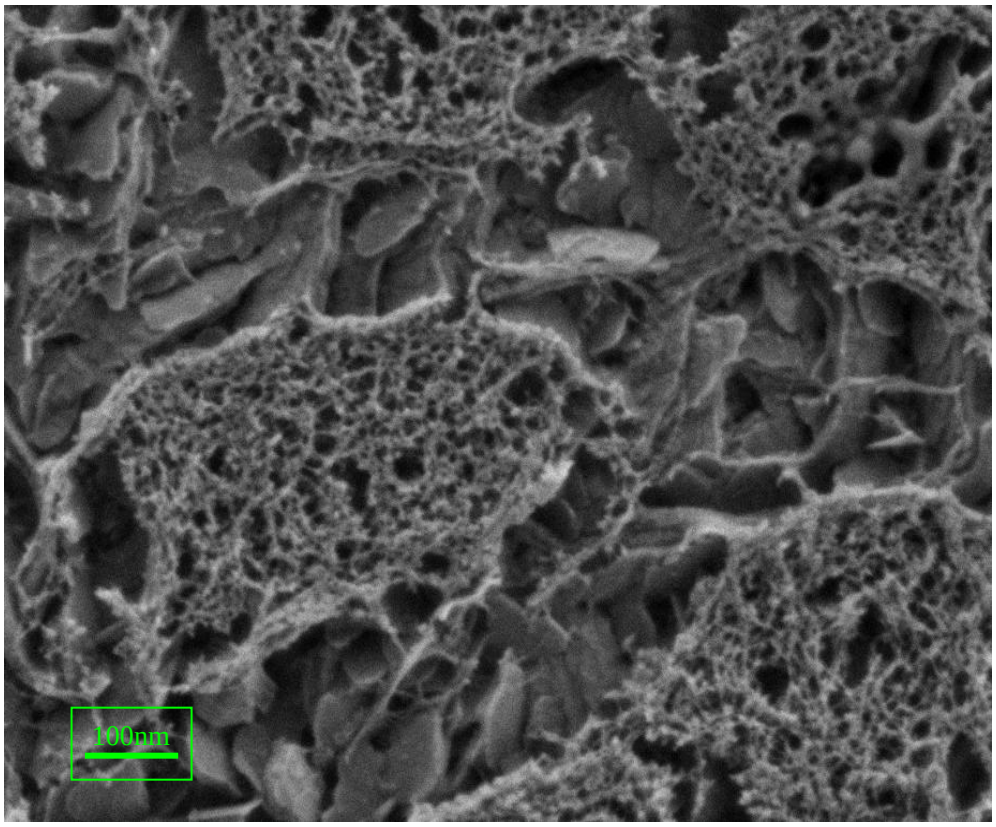

Figure 60: *SEM image of Escherichia coli, 60s glow discharge treated.* Bacterial cells are disintegrated and some ashes left.

4.3 Samples treated in afterglow conditions

Samples whose images are shown below were treated in afterglow conditions and consequently exposed to neutral oxygen atoms only. Temperature in the afterglow chamber is near the room temperature. At these conditions, any side effect would be neglected and influence of neutral oxygen atoms should be a single effect.

4.3.1 Samples of *Staphylococcus aureus*

Exposure time for *Staphylococcus aureus* samples was from 1 up to 500 seconds, as follows: 1 s, 5 s, 20 s, 30 s, 45 s, 90 s, 120 s, 180 s, 300 s and 500 s. After the treatment, samples were investigated with AFM and SEM and images were taken.

There are no clearly visible changes on bacterial cells up to about 5 seconds of exposure time (Figs. 61 - 62), if we compare these images with images of untreated cells (Figs. 32 – 36). Voluminous capsular coat is visible on surface of bacterial cells and only some small amount of particles of capsular material can be observed around the cells.

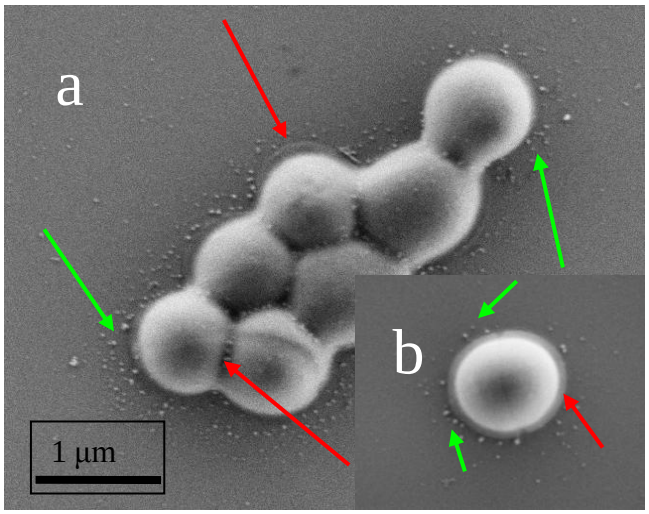

Figure 61: *SEM image of Staphylococcus aureus cell 1s afterglow treated.* Visible capsular layer (red arrows) and capsular material slightly tears off (green arrows). No clearly visible changes.

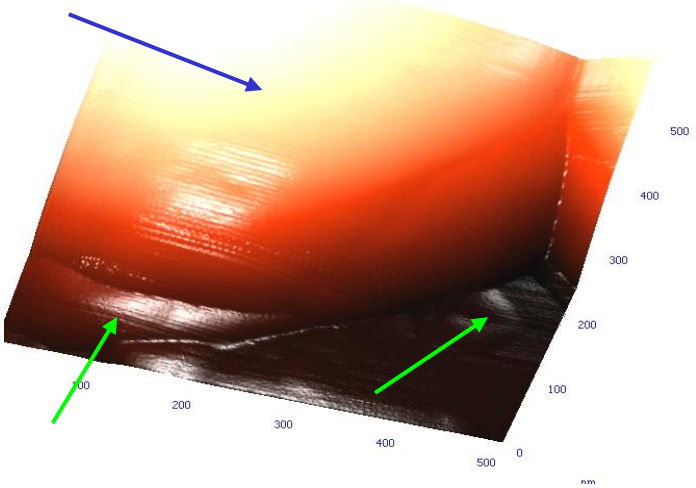

Figure 62: *AFM 0,5x0,5µm height 3D image of Staphylococcus aureus cells, 5s afterglow treated.* Visible capsular layer (blue arrow) and capsular material, slightly tears off (green arrows). No clearly visible changes.

After about 20 seconds of exposure, capsule still coats bacterial cell, but structural changes of capsular material appear (blue arrows in Fig. 63). In the period of 30 seconds, structural changes become intensive and modified capsular material appears on cell surface (Fig. 65). Some amount of the same, round shaped, material also tears off, as clearly visible on AFM phase images in Figure 63b and Figure 65. Scattered capsular material is clearly visible on SEM image in Figure 64, too.

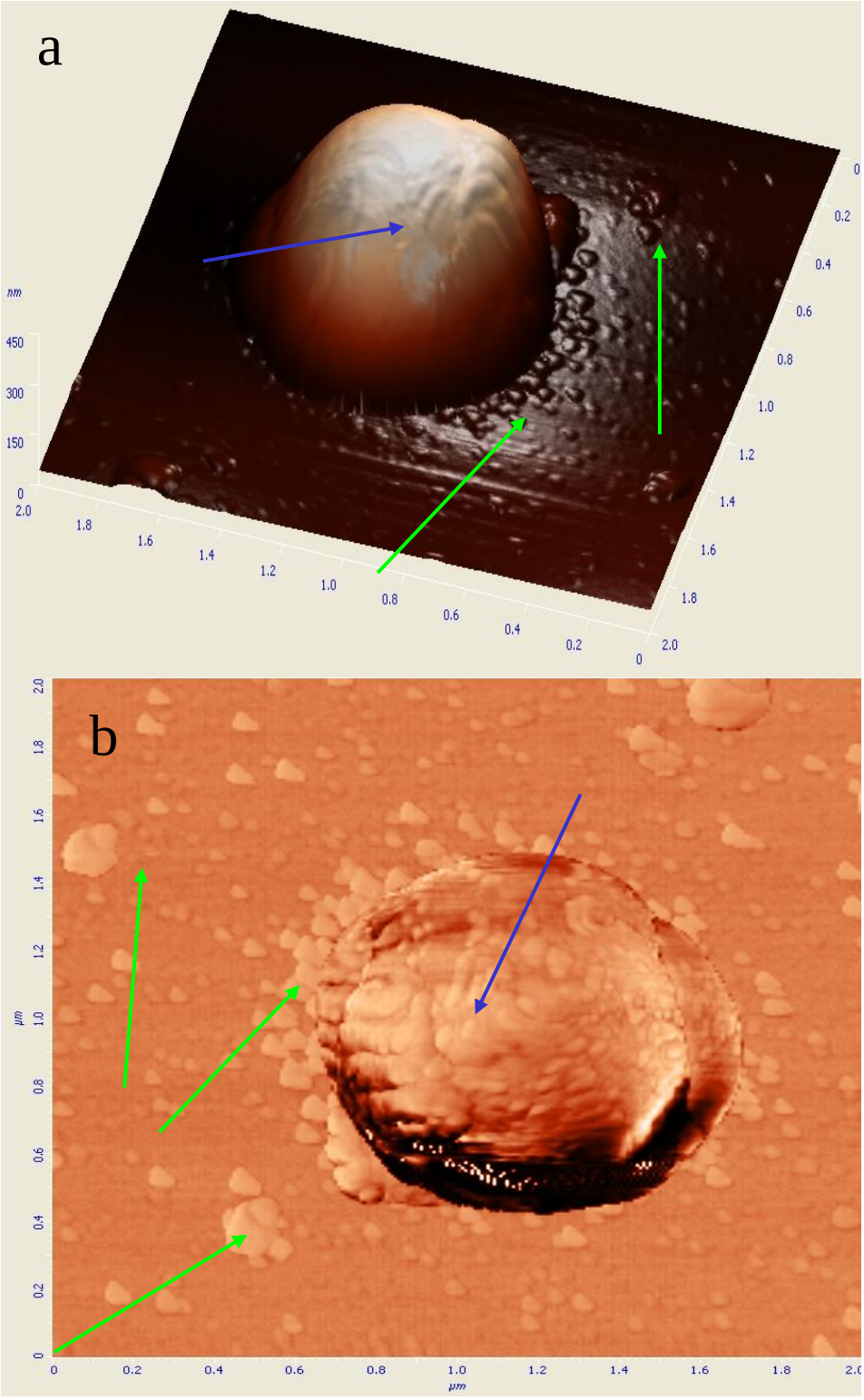

Figure 63: *AFM 2x2µm image of Staphylococcus aureus cell, 20s afterglow treated.* **a.** height 3D image; Relative smooth, but modified surface and clearly visible capsular material which tears off around bacterial cell (green arrows). **b.** phase image; Clearly visible capsular material on cell surface (blue arrows) which tears off (green arrows).

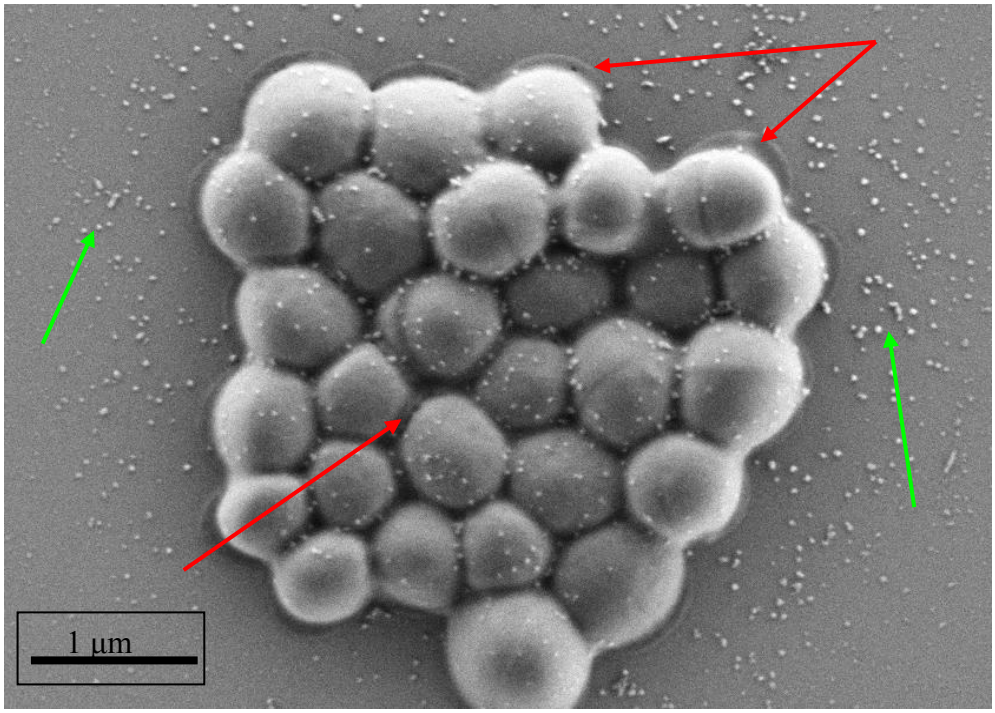

Figure 64: *SEM image of Staphylococcus aureus cells, 20s afterglow treated.* Clearly visible capsular material surrounds the cell (red arrows) and slightly tears off (green arrows), too.

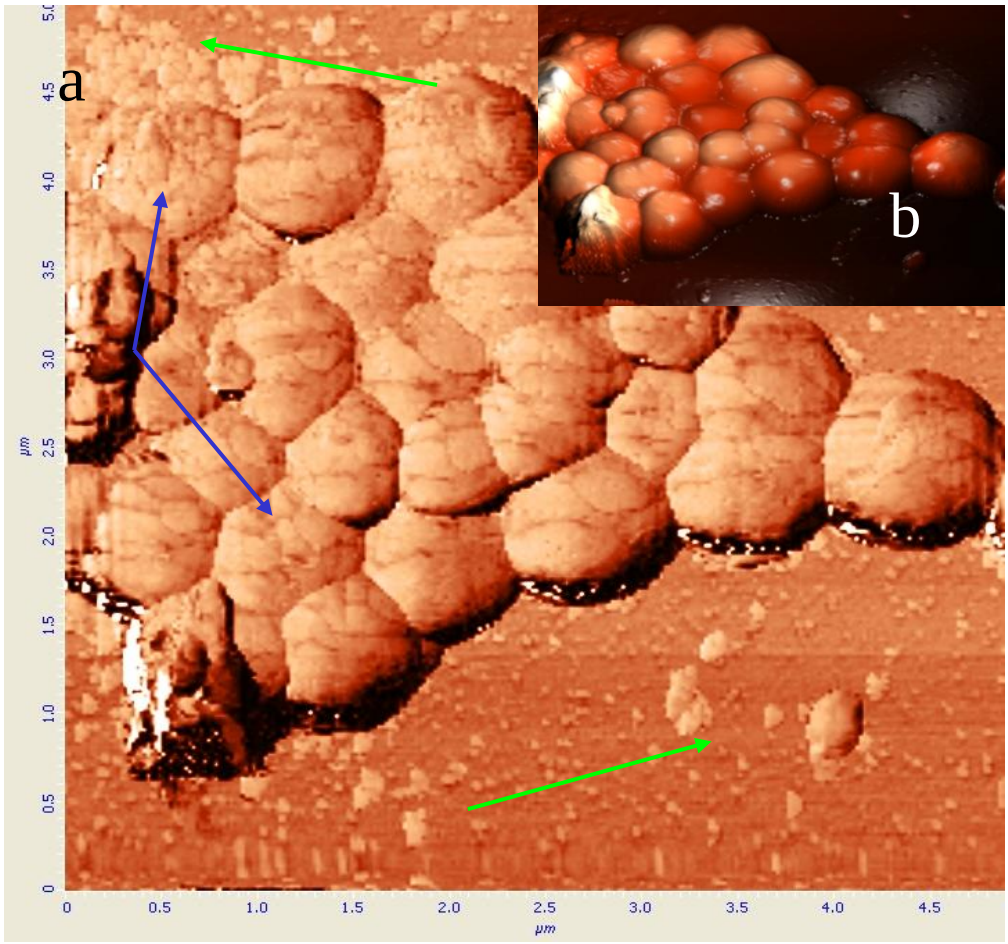

Figure 65: *AFM 5x5µm image of Staphylococcus aureus cells, 30s afterglow treated.* **a.** phase image, **b.** height 3D image; Visible changes in capsular material on cell's surface (blue arrows) which tears off around bacterial cell (green arrows).

The process is progressive, so if we compare SEM images in Figure 64 and Figure 66, changes are visible. After 45 seconds of exposure, majority of capsular coat is removed and only traces (ghosts) are visible as pointed with red arrows in Figure 66. In this period peptidoglycan is exposed to oxygen radicals, and etching starts.

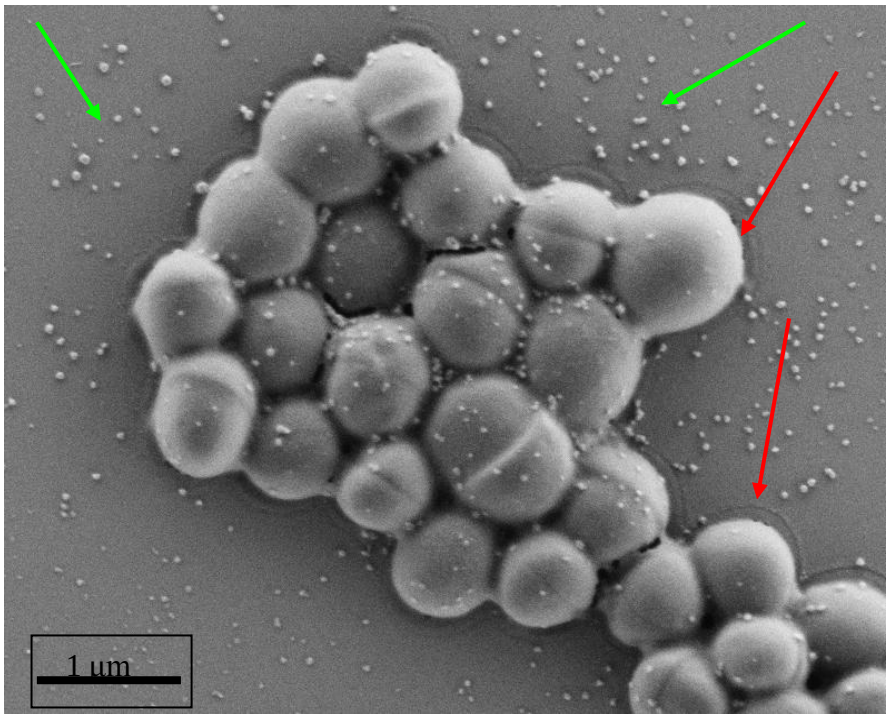

Figure 66: *SEM image of Staphylococcus aureus cells, 45s afterglow treated.* Capsular material scattered around the cells (green arrows). Traces of capsule (ghosts) are visible (red arrows).

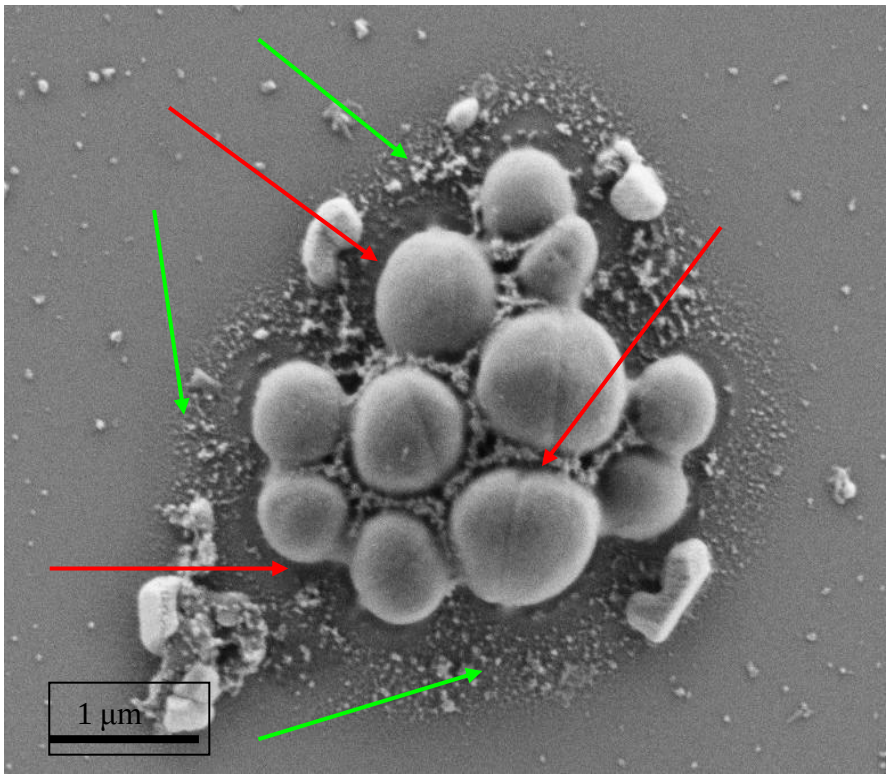

Figure 67: *SEM image of Staphylococcus aureus cells, 90s afterglow treated.* Capsular material disappeared from the cells surfaces (red arrows) and scattered around a cell (green arrows).

After about 90 seconds of exposure, almost all capsular material has been removed from the cell surface and can be seen scattered around bacterial cells (Figs. 67 and 68). Surface of bacterial cell is still pretty smooth, as can be seen on SEM image in Fig. 67.

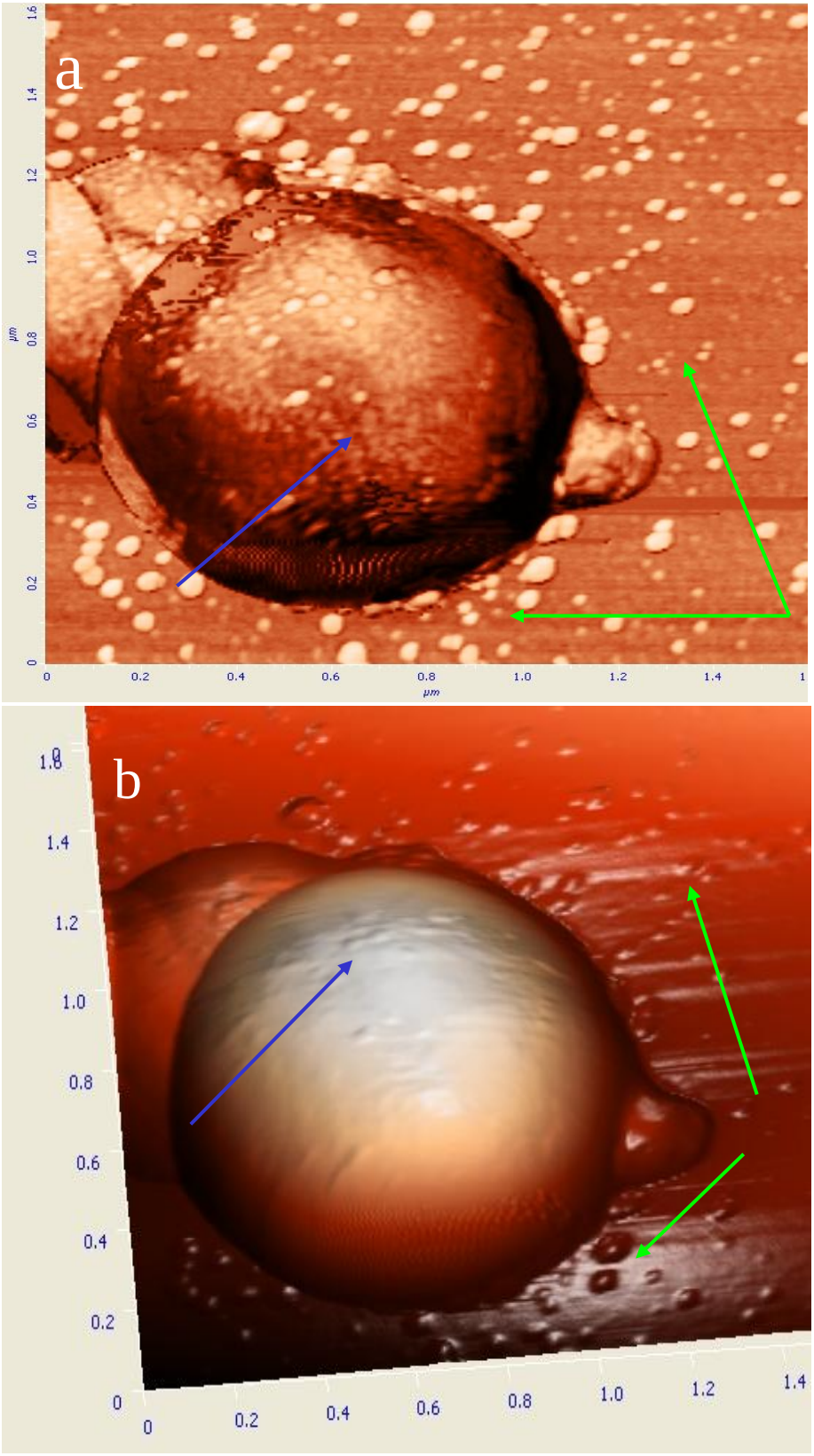

Figure 68: *AFM 1,5x1,5µm image of Staphylococcus aureus cells, 90s afterglow treated.* **a.** phase image **b.** height 3D image; Capsular material disappeared from cell's surface (blue arrow) and scattered around bacterial cell (green arrows).

In the next period, up to about 120 seconds round shaped pieces of capsular substance are widely scattered all around, what is very well visible on AFM phase image in Figure 69 **b.** and SEM image in Figure 71. Only some traces of capsular material are still visible on cell surface, as shown on images in Figure 70. Rough peptidoglycan structure is in great extent exposed to oxygen radicals (Figs. 69 – 71).

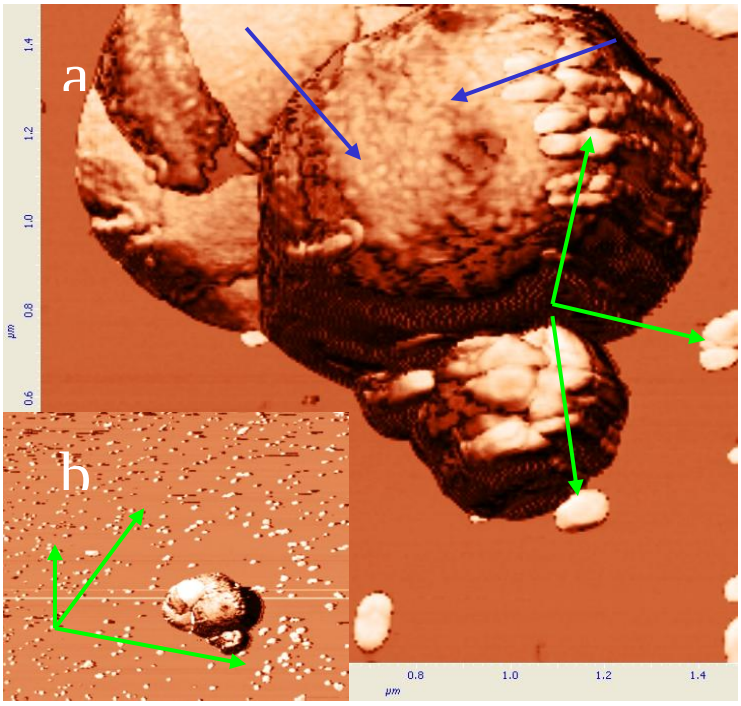

Figure 69: **a.** *AFM phase image 1.5x1.5µm image of Staphylococcus aureus cells, 120s afterglow treated.* Traces of capsular substance are visible (green arrows). Peptidoglycan rough structure is visible (blue arrows). **b.** *AFM phase image 5x5µm image of Staphylococcus aureus cells, 120s afterglow treated.* Capsular material scattered around bacterial cell (green arrows).

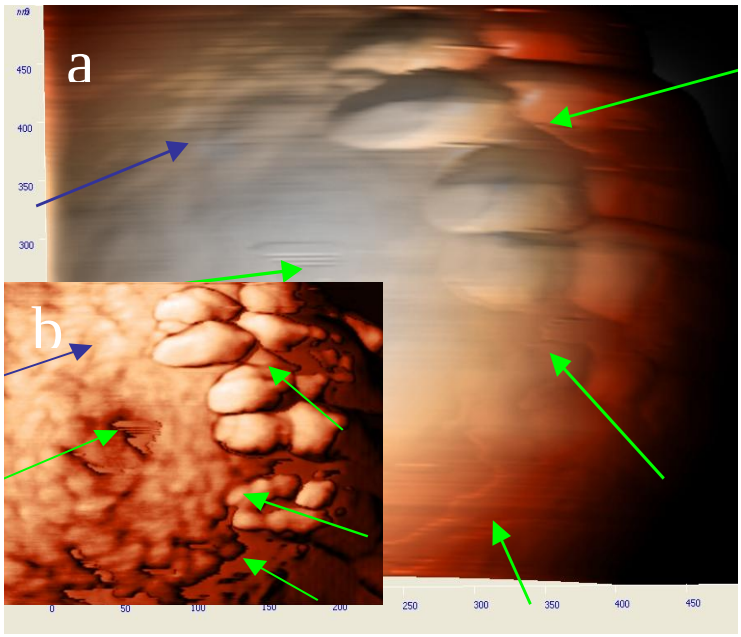

Figure 70: *AFM 0.5x0.5µm image of Staphylococcus aureus cell, 120s afterglow treated.* **a.** height 3D image, **b.** phase image; Rough structure of peptidoglycan is visible (blue arrows). Traces of capsular substance are visible (green arrows).

Cell surface is not smooth any more, if we compare SEM images in Fig. 67 and Fig. 71. It looks like being etched. Nevertheless, some of scattered pieces could be peptidoglycan.

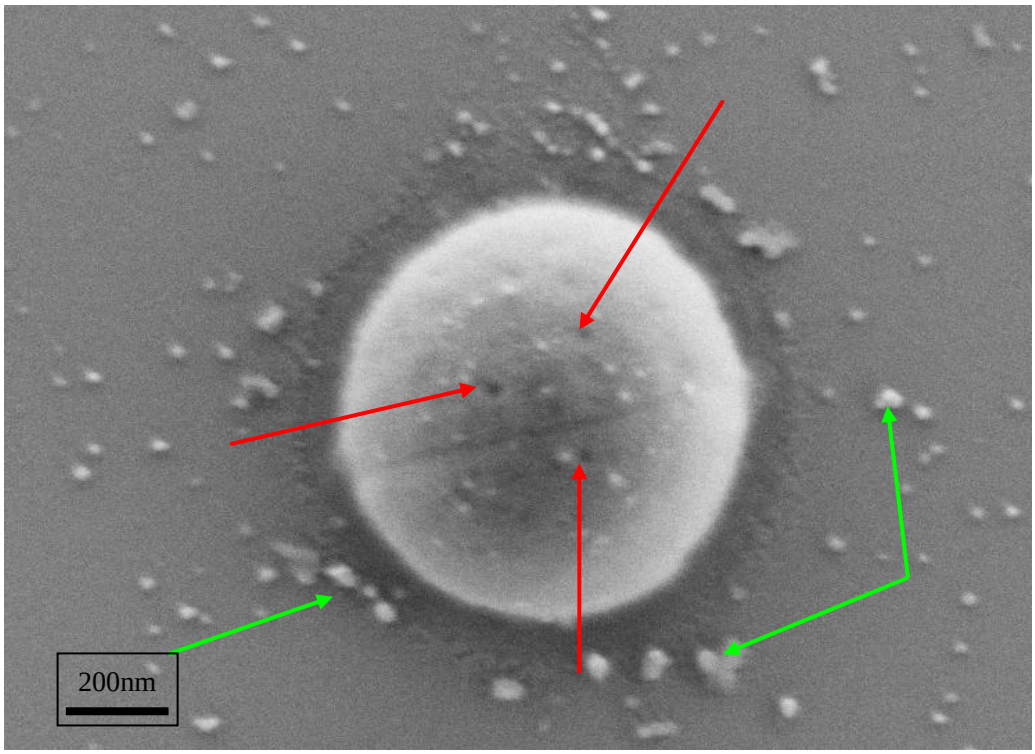

Figure 71: *SEM image of Staphylococcus aureus cels, 120s afterglow treated.* Pieces of capsular substance scattered around a cell (green arrows). Peptidoglycan rough structure is visible. Disruption of peptidoglycan started, red arrows pointed.

In the further minute (exposing time of 180 seconds)**,** massive disruption of peptydoglycan from cell wall is observed (Figs. 72 - 74). A lot of pieces, of the same composition as on the cell surface disrupt from bacterial cells. This is especially well shown on phase image in Figure 72b. Wholes in bacterial cell wall and roughness of the surface are clearly visible in Figures 73 and 74.

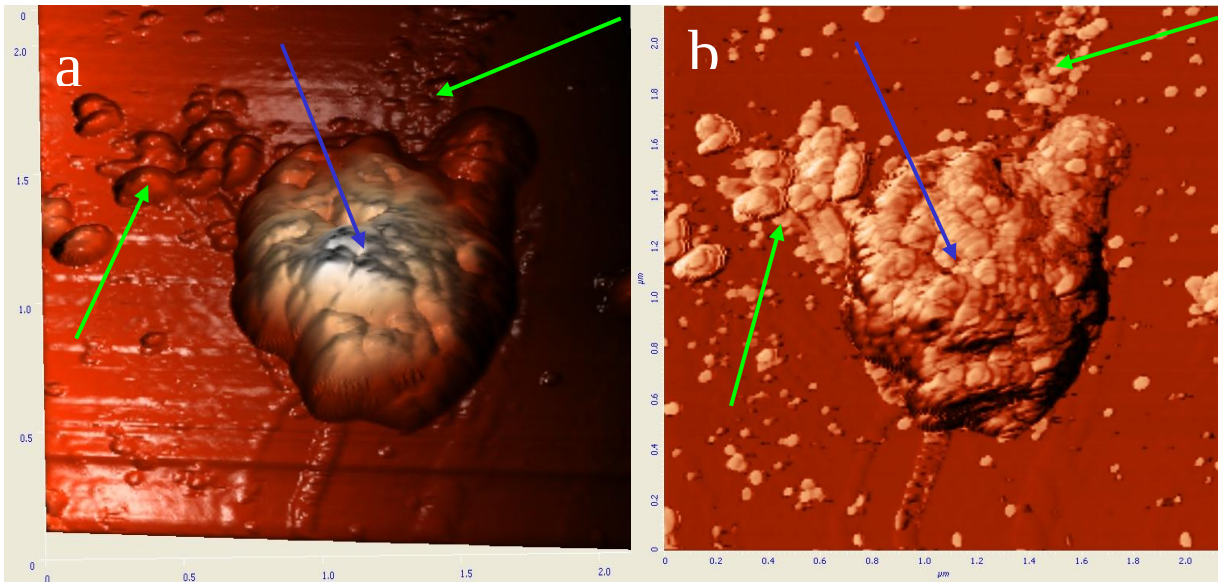

Figure 72: *AFM 2x2µm images of Staphylococcus aureus cell, 180s treated.* **a.** height 3D image, **b.** phase image; Peptidoglycan rough structure is visible (blue arrows). Massive disruption of peptidoglycan continues (green arrows).

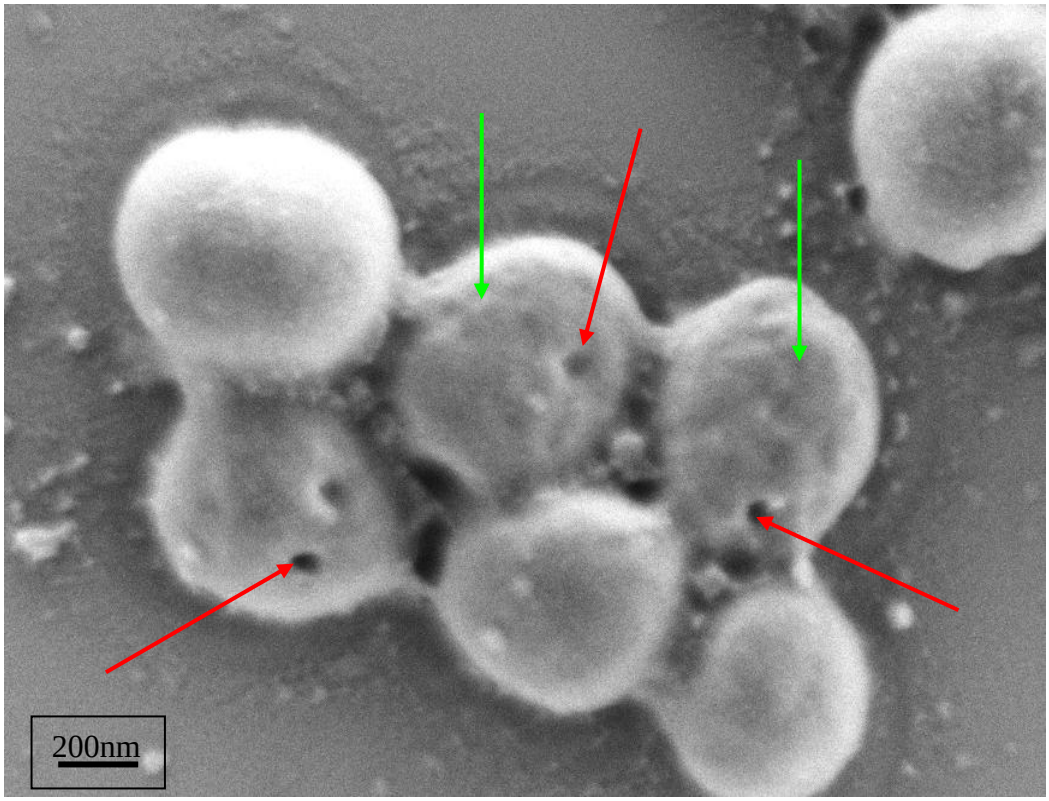

Figure 73: *SEM image of Staphylococcus aureus cells, 180s afterglow treated.* Peptidoglycan rough structure is visible (green arrows). Disruption of peptidoglycan continues (red arrows).

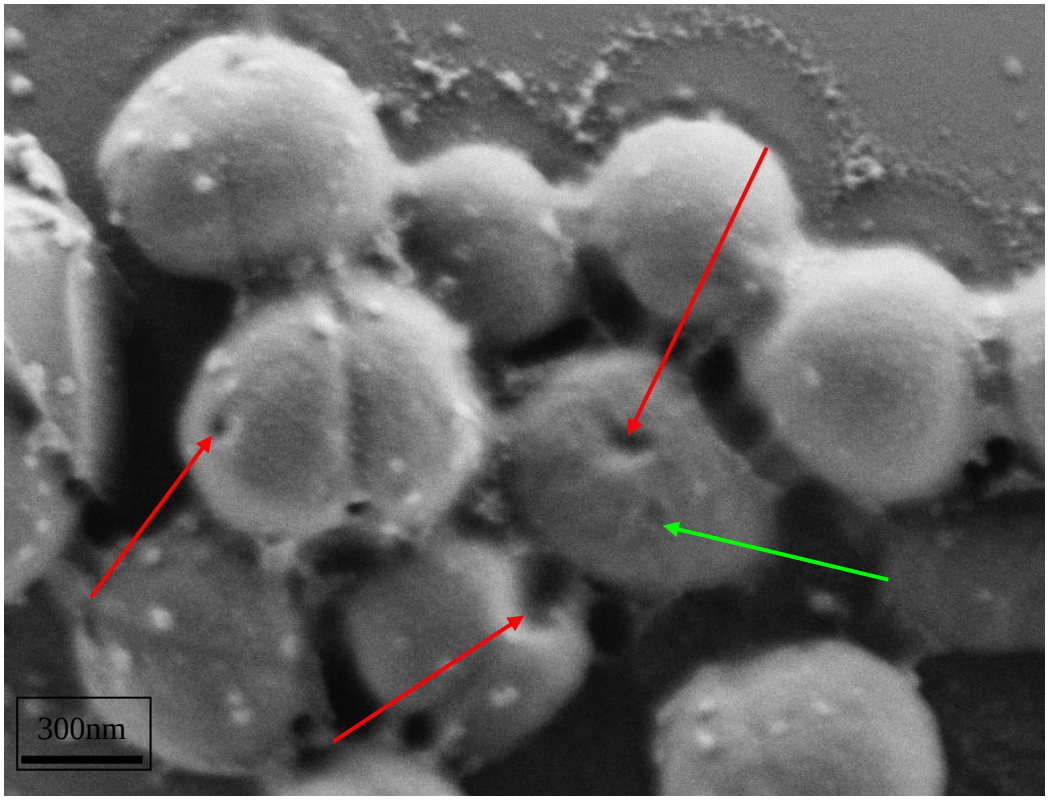

Figure 74: *SEM image of Staphylococcus aureus cells, 180s afterglow treated.* Peptidoglycan rough structure is visible (green arrow). Disruption of peptidoglycan continues (red arrows).

After up to 300 seconds, at our experimental conditions, cell wall disrupts. Domains of peptidoglycan are removed at some parts of bacterial cell wall, as shown on AFM images in Figure 75. Numerous holes and cracks can be observed on the surface of bacterial cells and large pieces of peptidoglycan beside the bacterial cells. This is clearly visible on SEM image in Figure 76.

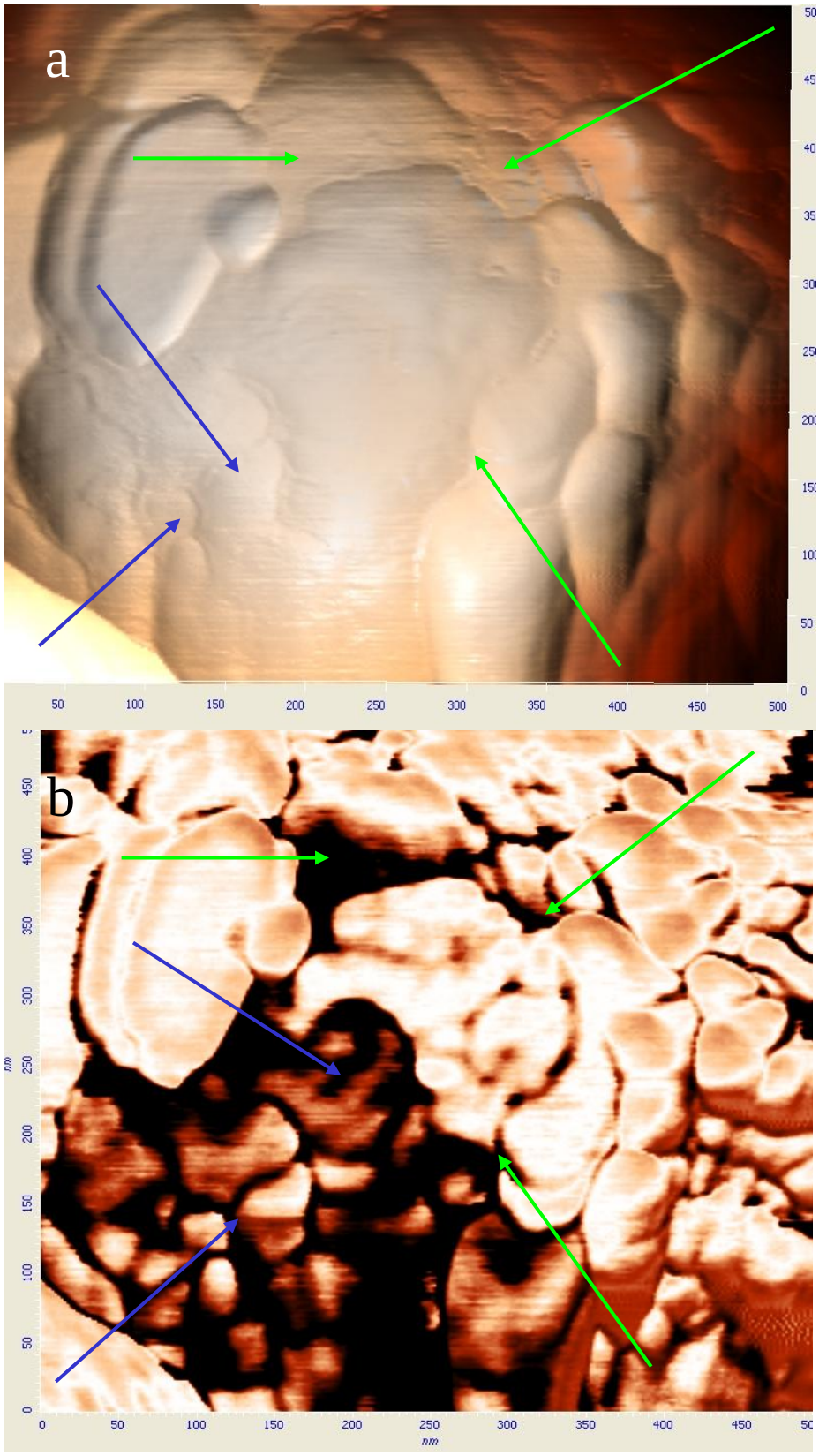

Figure 75: *AFM phase mode 0,5x0,5μm image of Staphylococcus aureus cell, 300s afterglow treated.* Massive disruption of peptidoglycan is visible (green arrows). Intracellular structures are visible (blue arrows).

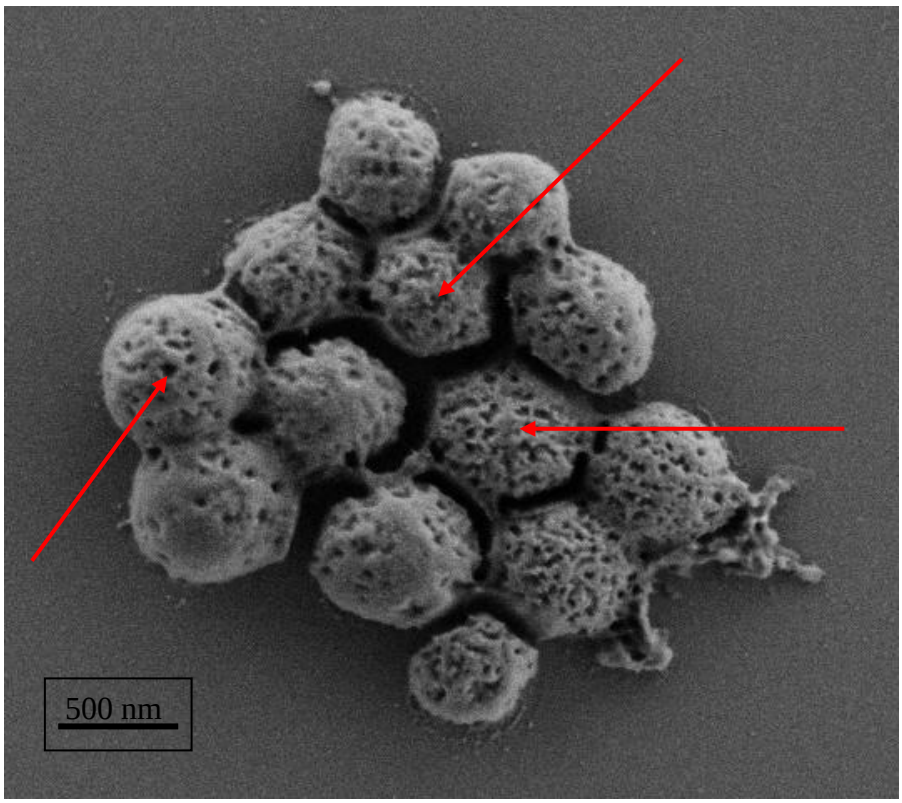

Figure 76: *SEM image of Staphylococcus aureus cells, 300s afterglow treated.* Disruption of peptidoglycan continues (red arrows). Bacterial cell wall is badly damaged.

Bacteria are devitalized now and cytoplasm internal structures become visible (Fig.75 - 77). Removing of intracellular material and traces of peptidoglycan from disrupted cell wall continues slowly, in a period longer than 500 seconds (Fig 77 and 78).

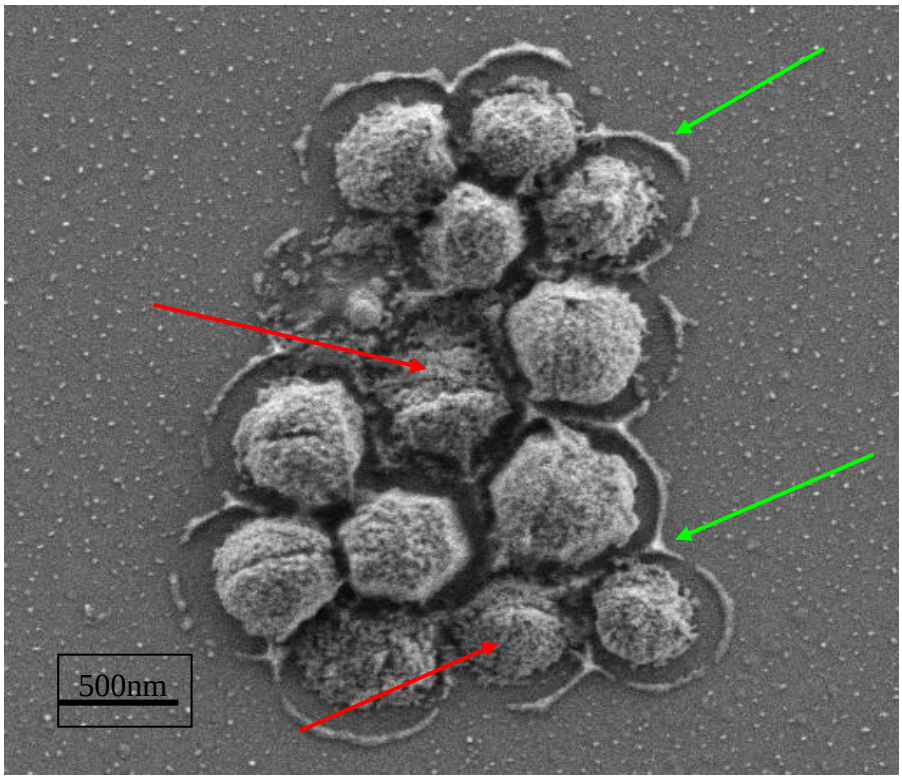

Figure 77: *SEM image of Staphylococcus aureus cells, 500s afterglow treated.* Intracellular cytoskeletal structures are visible (red arrows). Traces of cell wall still exist (green arrows).

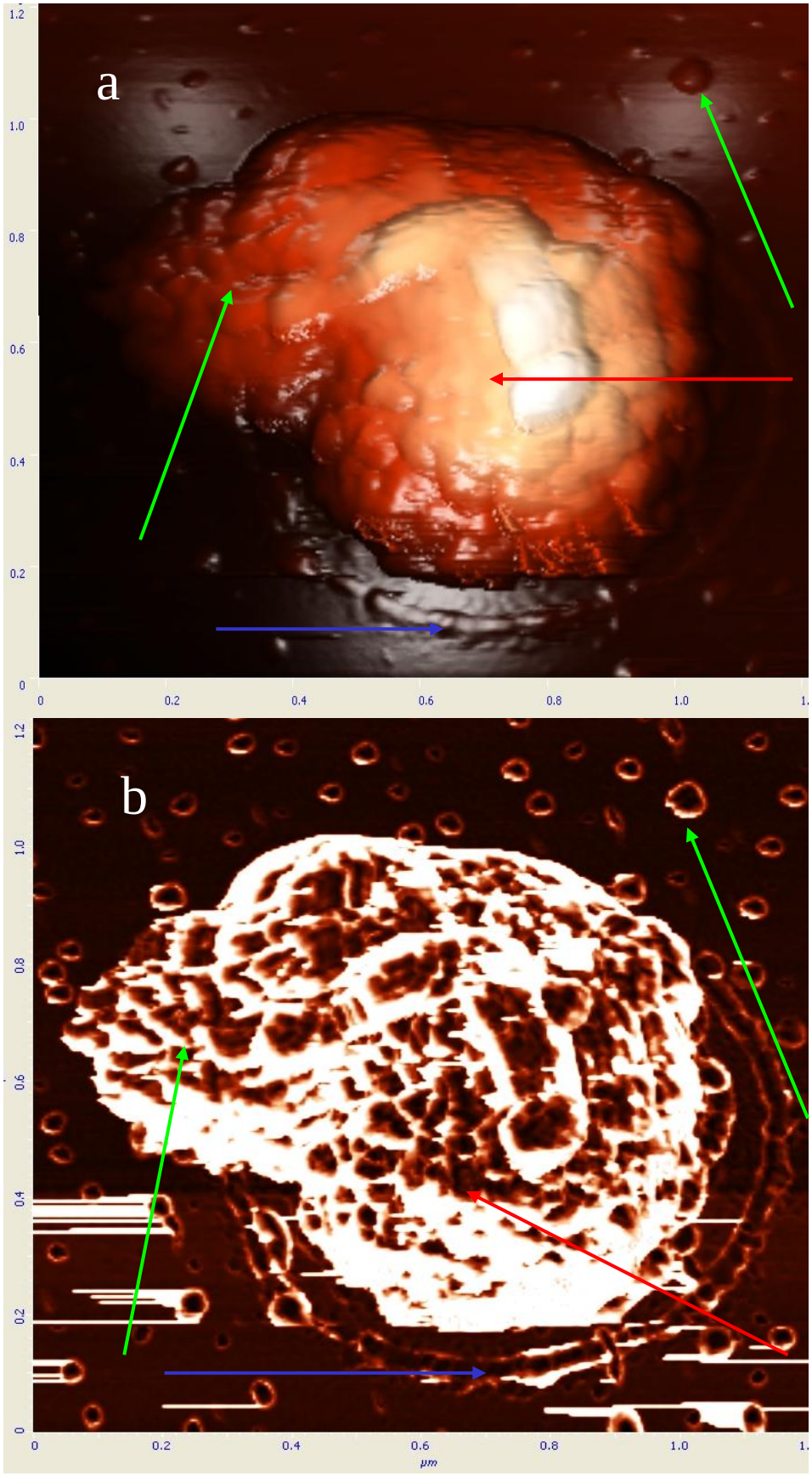

Figure 78: *AFM 1.5x1.5µm images of Staphylococcus aureus cells, 500s treated.* **a.** height 3D image **b.** phase image; Disrupted cells, red arrows pointed, cellular material spilled around bacterial cell (green arrows). Some traces of bacterial cell wall are still visible (blue arrows).

4.3.2 Samples of *Escherichia coli*

Exposure time for *Escherichia coli* samples was from 5 up to 500 seconds, as follows: 5 s, 10 s, 15 s 20 s, 30s, 45 s, 90 s, 120 s, 180 s, 360 s and 500 s. After the treatment, samples were investigated with AFM.

At our experimental conditions there are no visible changes in short period of time about 5 seconds (Fig. 79), comparing with non treated samples in Fig. 37, what is similar to process happening in the case of *S. aureus*.(See Fig. 62)

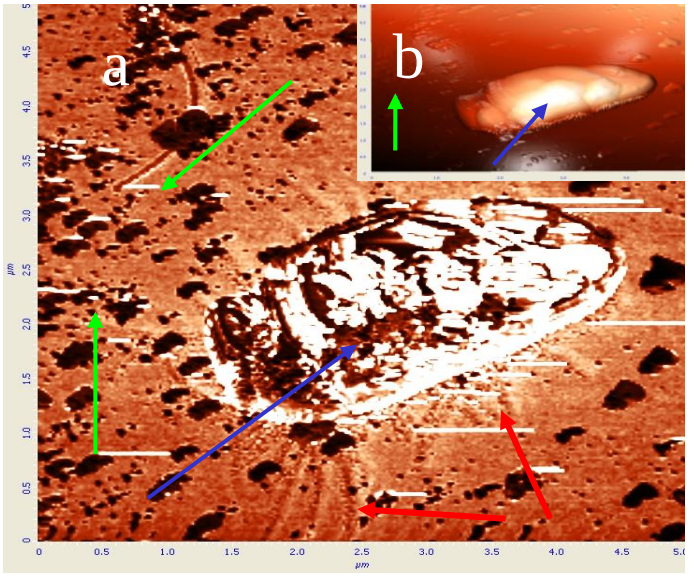

Figure 79: *AFM 5x5μm image of Escherichia coli cell, 5s afterglow treated.* **a.** phase image, **b.** height 3D image; Voluminous capsule coats bacterial cell (blue arrows) and slightly tears off (green arrows). Pili around bacterial cell are visible (red arrow). No visible changes on bacterial cell.

Visible changes in capsular material of *Escherichia coli* become noticeable after approximately 10 seconds exposure to neutral oxygen atoms, when intensive tearing off the capsular substance becomes visible and particles are found all around bacterial cells. (Figs. 80 and 81) In this phase, pili are still visible as shown on Figs. 79 and 81.

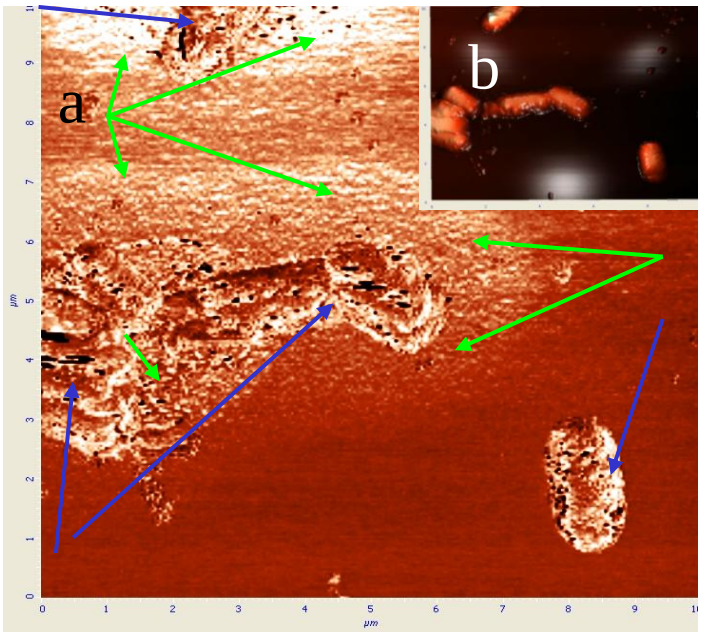

Figure 80: *AFM 10x10μm image of Escherichia coli cells, 10s afterglow treated.* **a.** phase image **b.** height 3D image; Voluminous capsule coats bacterial cells (blue arrows), capsular material intensively tears off and scattered around (green arrows).

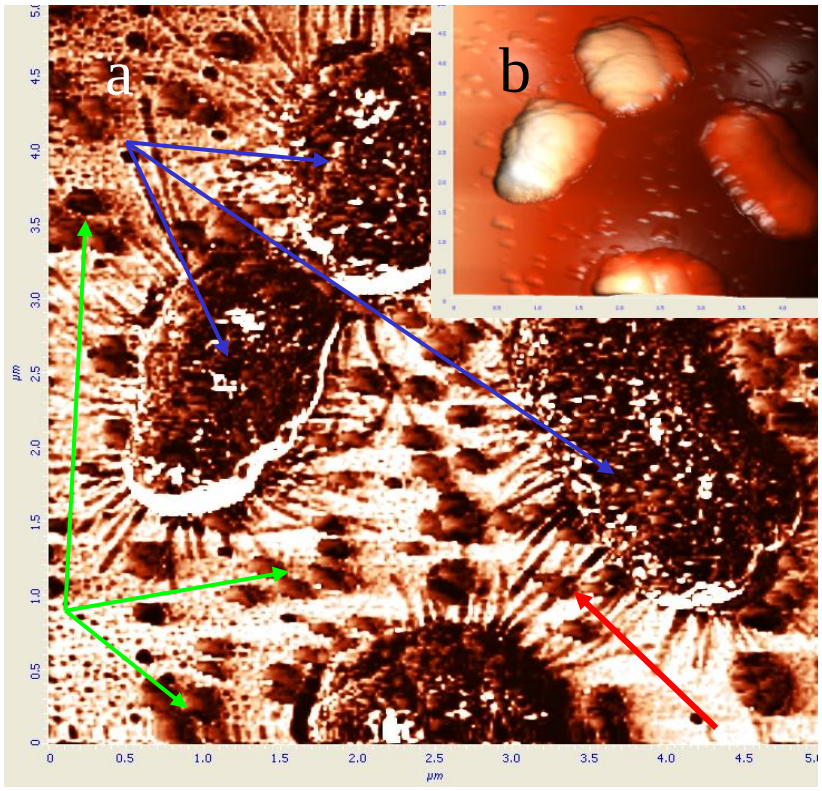

Figure 81: *AFM 5x5µm image of Escherichia coli cells, 10s afterglow treated.* **a.** phase image **b.** height 3D image; Voluminous capsular coat (blue arrows), and capsular material scattered around bacterial cells (green arrows). Pili are visible (red arrow).

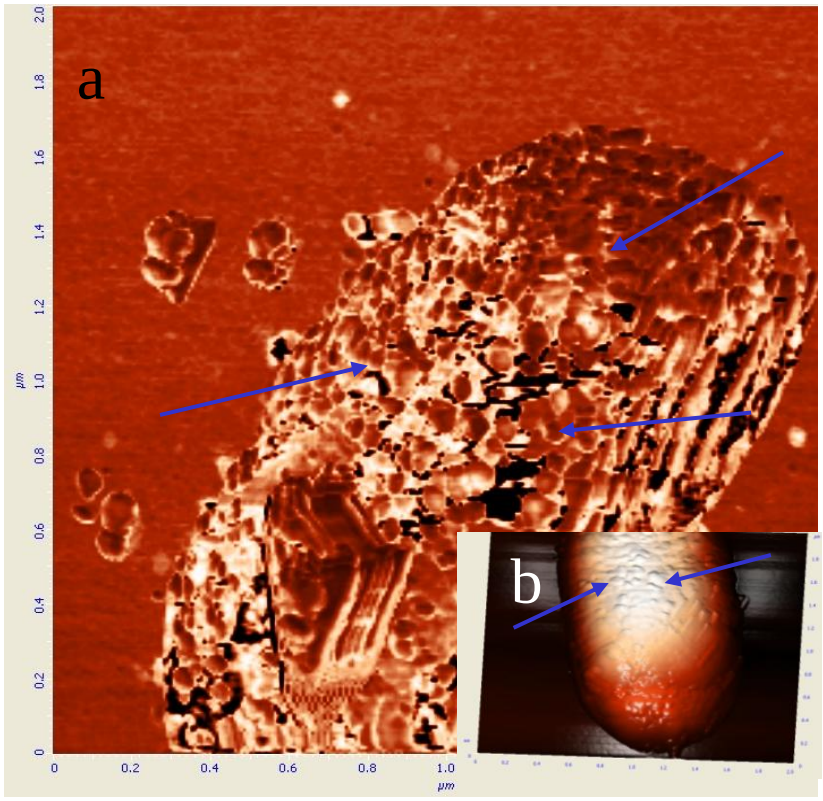

Figure 82: *AFM 2x2µm image of Escherichia coli cell, 15s afterglow treated.* **a.** *phase* image **b.** height 3D image; Modified capsular coat is visible (arrows).

This process of removal continues until approx. 20 seconds when most of capsular material is removed (Figs. 82 - 83), but some amount still can be seen, what is pointed with arrows on Fig. 84.

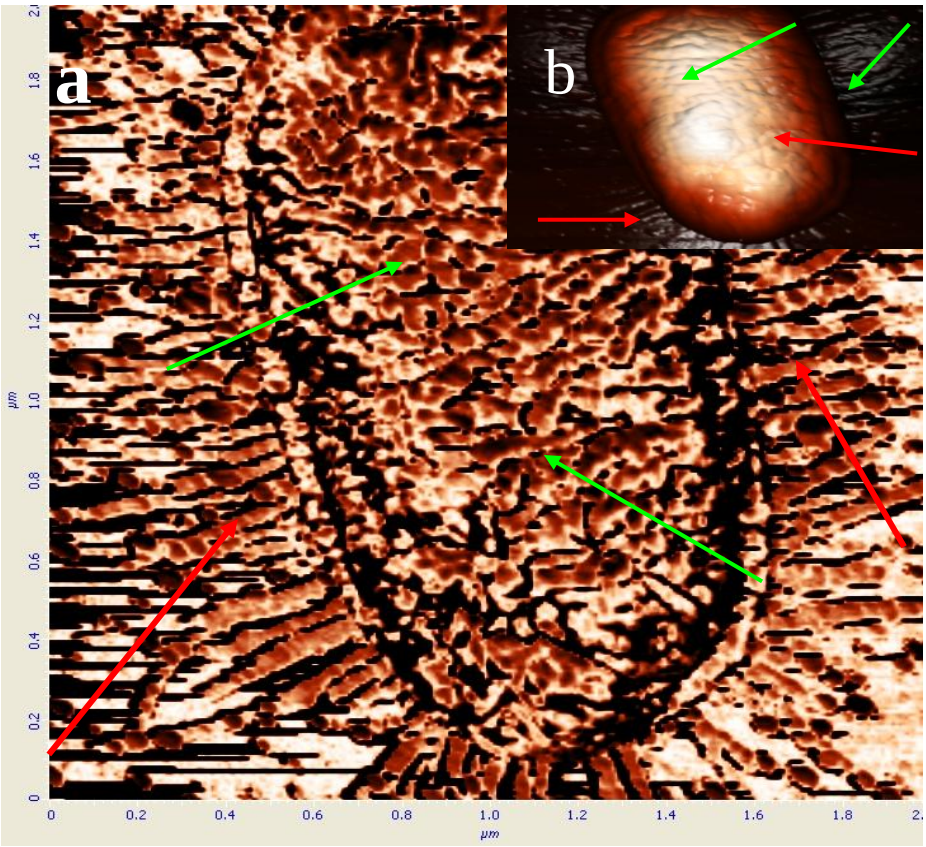

Figure 83: *AFM 2x2µm image of Escherichia coli cell, 20s afterglow treated.* **a.** phase image, **b.** height 3D image; Some amount of capsular material is visible (green arrows). Pili are visible (red arrows).

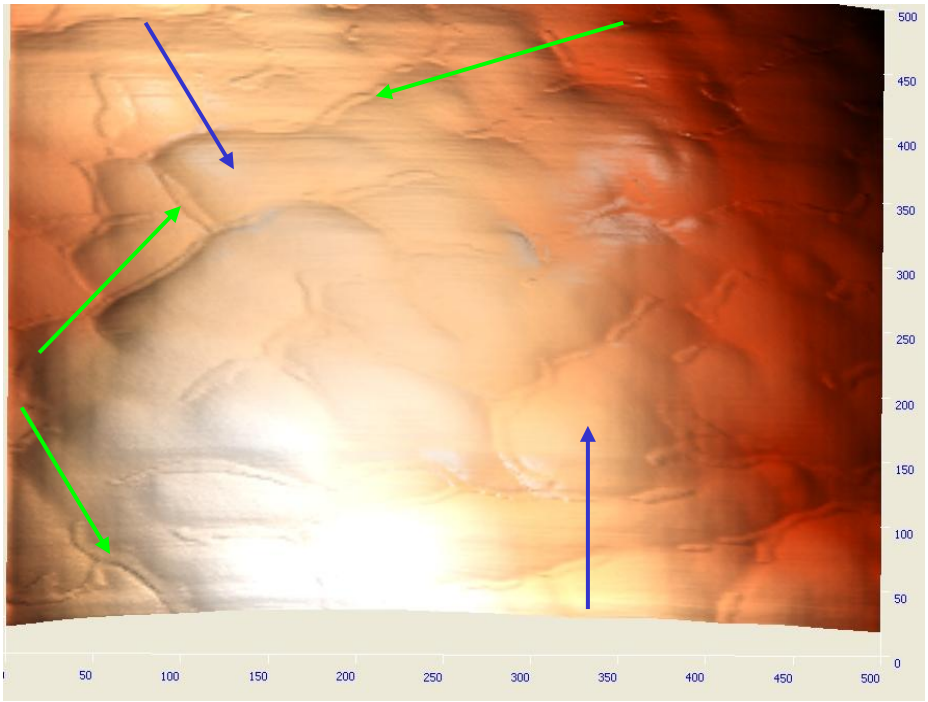

Figure 84: *AFM height 3D 0.5x0.5µm image of Escherichia coli cell, 20s treated.* Voluminous capsular coat disappeared, visible in traces (green arrows). LPS structures become visible (blue arrows).

Lipopolysacharide (LPS) from the bacterial cell wall becomes visible after 20 seconds exposure of bacterial cells (Fig. 84 and 86). In this period, interaction of radicals with this structure starts and structural changes happen. Irregular round shaped particles can be detected, scattered around the cells, about 30 s of exposure to plasma radicals. (Fig. 85) At the same time flagella and pili seen on previos images (Figs. 79, 81 and 83) disappear, what is pointed with red arrows in Figure 85.

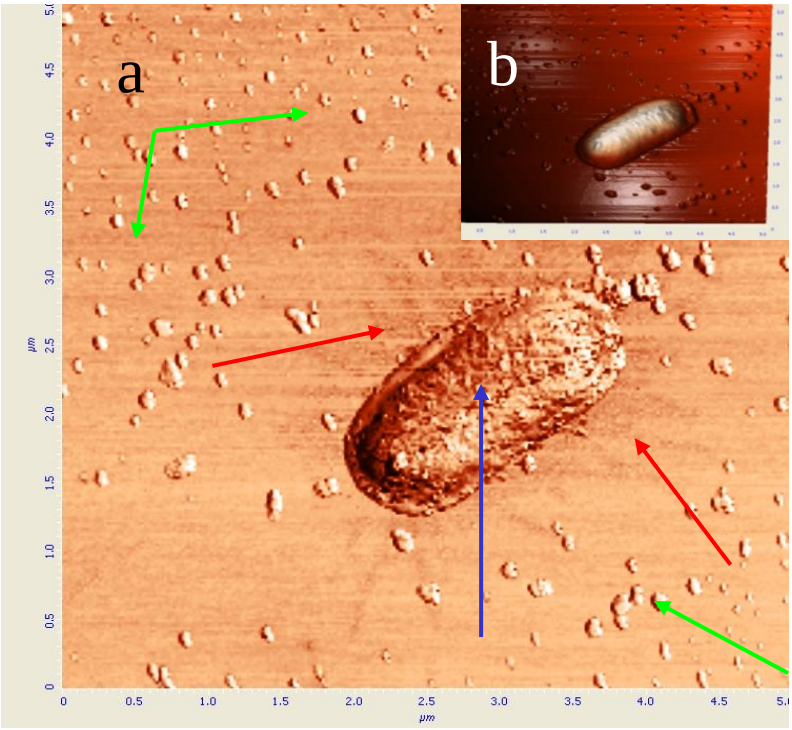

Figure 85: *AFM 5x5µm image of Escherichia coli cell, 30s afterglow treated.* **a.** phase image, **b.** height 3D image; LPS structures on bacterial surface are visible (blue arrow), also scattered around the cell (green arrows). Flagella and pili disappeared (ghosts pointed with red arrows).

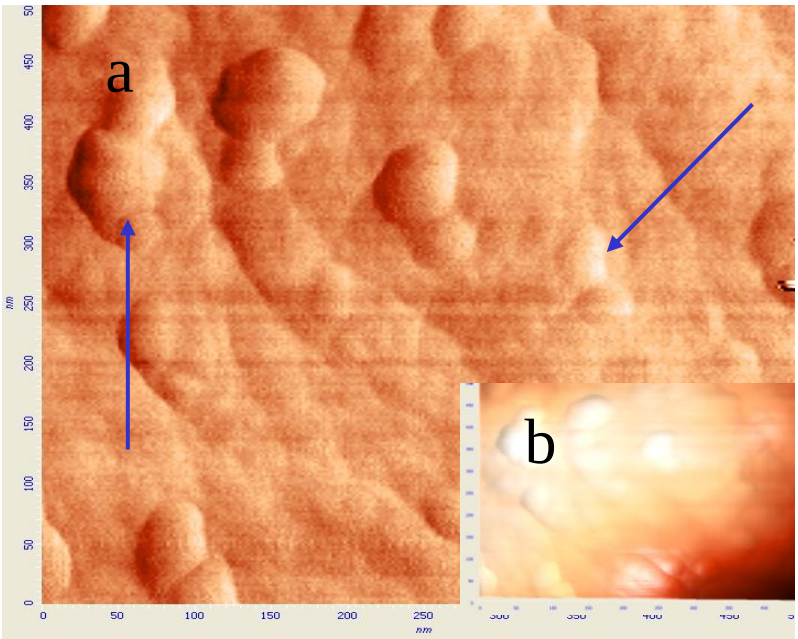

Figure 86: *AFM 0.5x0.5µm image of Escherichia coli cell, 30s afterglow treated.* **a.** phase image, **b.** height 3D image; LPS structures are visible (arrows).

The process of LPS removal continues, so in this period a lot of round shaped pieces are scattered around bacterial cell. (Figs. 87 – 89) Different layers of LPS are exposed to etching during this period (see model of Gram - negative cell wall Fig. 17), so various scattered pieces can be observed.

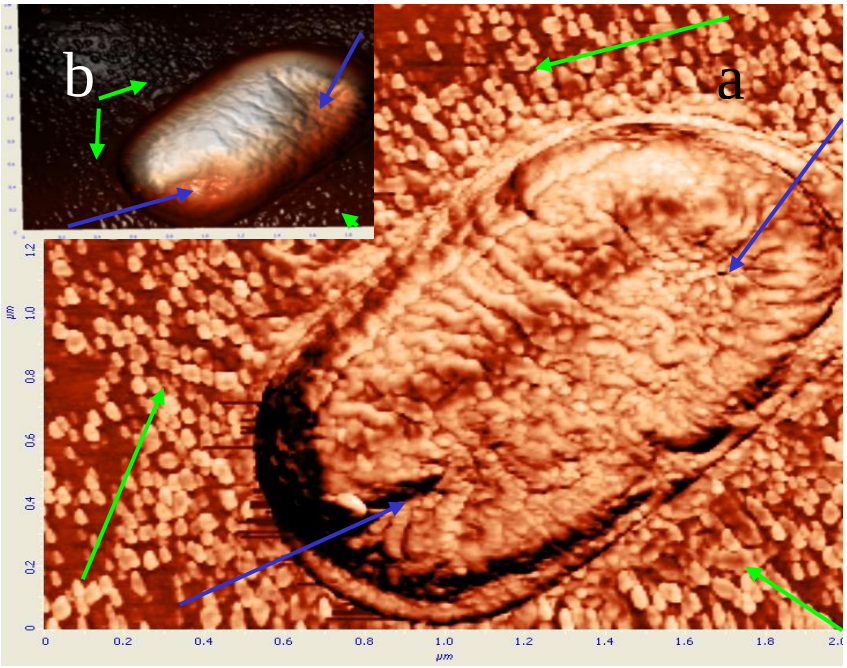

Figure 87: *AFM 2x2µm image of Escherichia coli cell, 45s afterglow treated*. **a.** phase image, **b.** height 3D image; LPS structures, probably O-antigens, massive disruption are visible, (blue arrows), also scattered around the cell (green arrows).

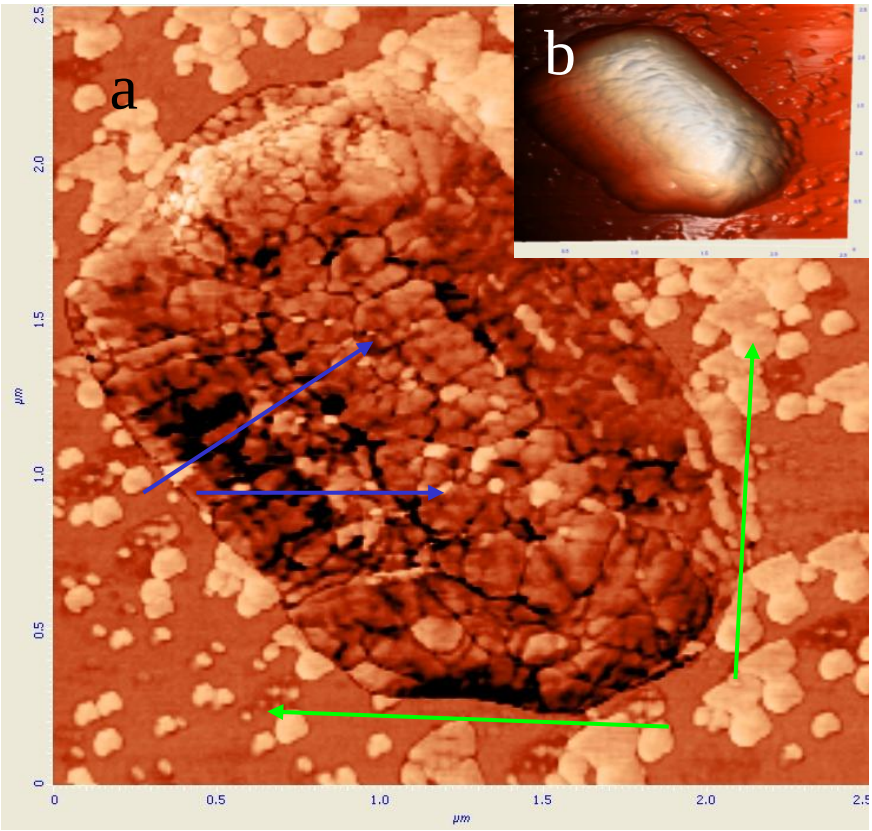

Figure 88: *AFM 2.5x2.5µm images of Escherichia coli cell, 90s afterglow treated.* **a.** phase image, **b.** height 3D image; Structures from outer membrane, probably core, are visible (blue arrows). Pieces of LPS scattered around (green arrows).

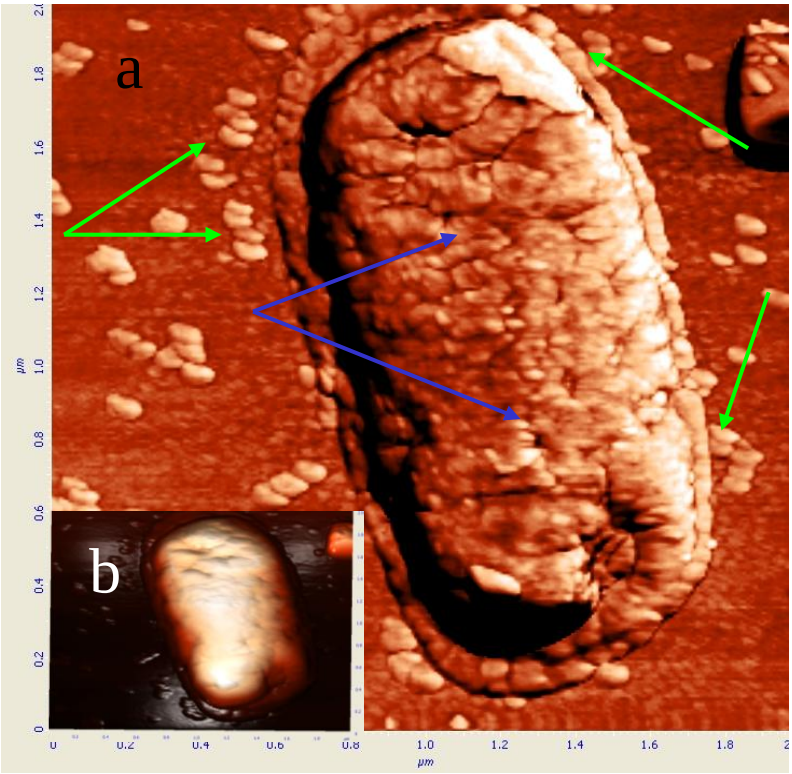

Figure 89: *AFM 2x2µm image of Escherichia coli cell, 120s afterglow treated.* **a.** phase image, **b.** height 3D image. Structures from outer membrane are visible (blue arrows), also scattered around (green arrows).

After approx. 180 seconds all LPS is removed from cell surface. After removal of the LPS layer, etching of peptodoglycan starts. After about 180 seconds exposure to afterglow, massive destruction of thin peptidoglycan layer happens. Surprisingly, pretty organized, flat, round shaped or oval structures has been removed. (Fig. 90). At this period bacterial cell is destructed.

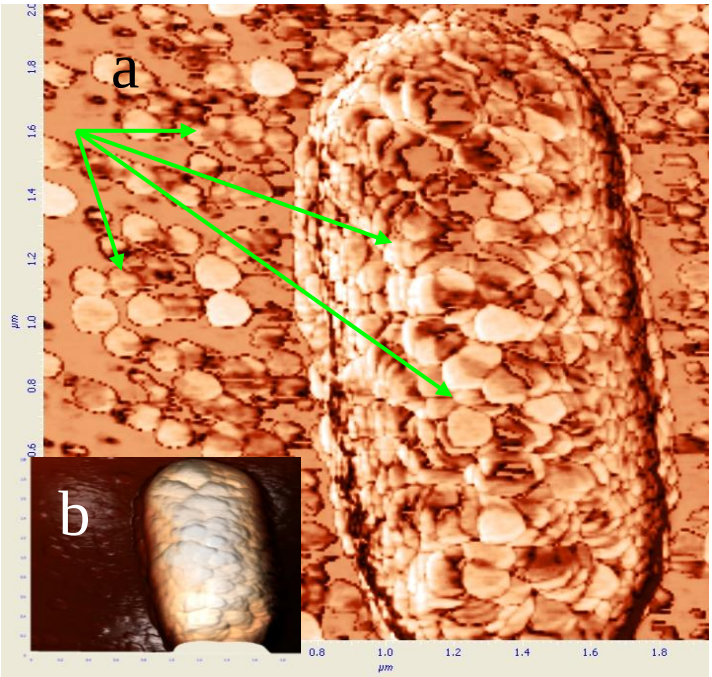

Figure 90: *AFM 2x2µm images of Escherichia coli cell, 180s treated.* **a.** phase image, **b.** height image; Massive destruction of peptidoglycan layer is visible (arrows).

After destruction of bacterial cell wall, thin cytoplasm membrane was disrupted immediately and intracellular material spilled outside. Removal process of intracellular material continues slowly, in period about 500 seconds, until only some ashes left as shown in Figs. 91 and 92.

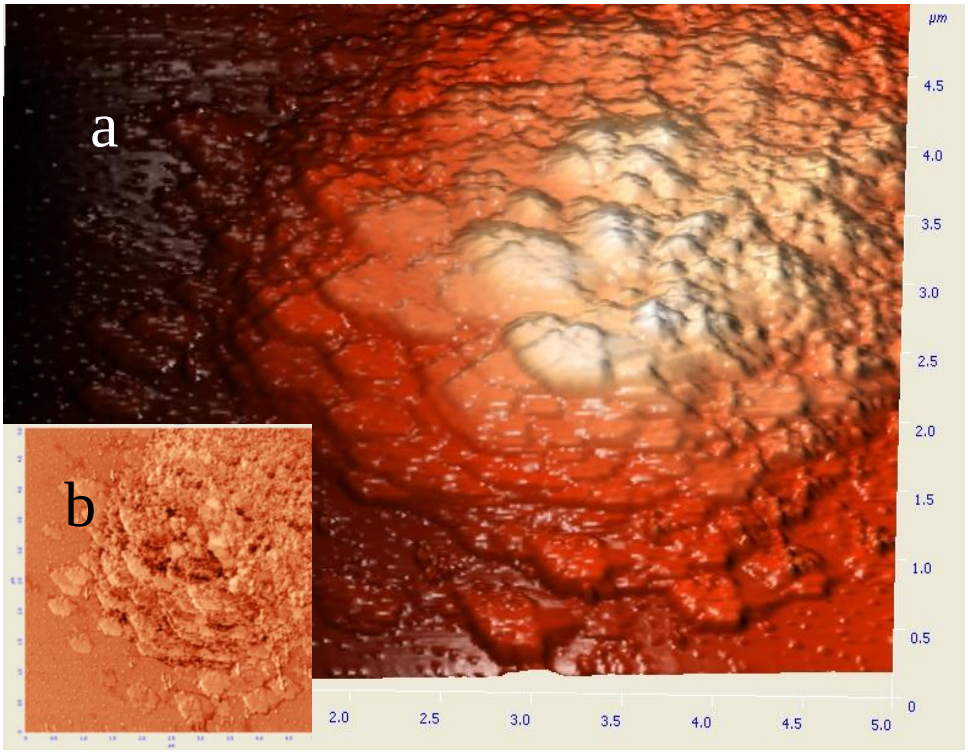

Figure 91: *AFM 5x5µm images of Escherichia coli cell, 360s afterglow treated*. **a.** height 3D image, **b.** phase image; Intracellular structures destroyed and spilled around.

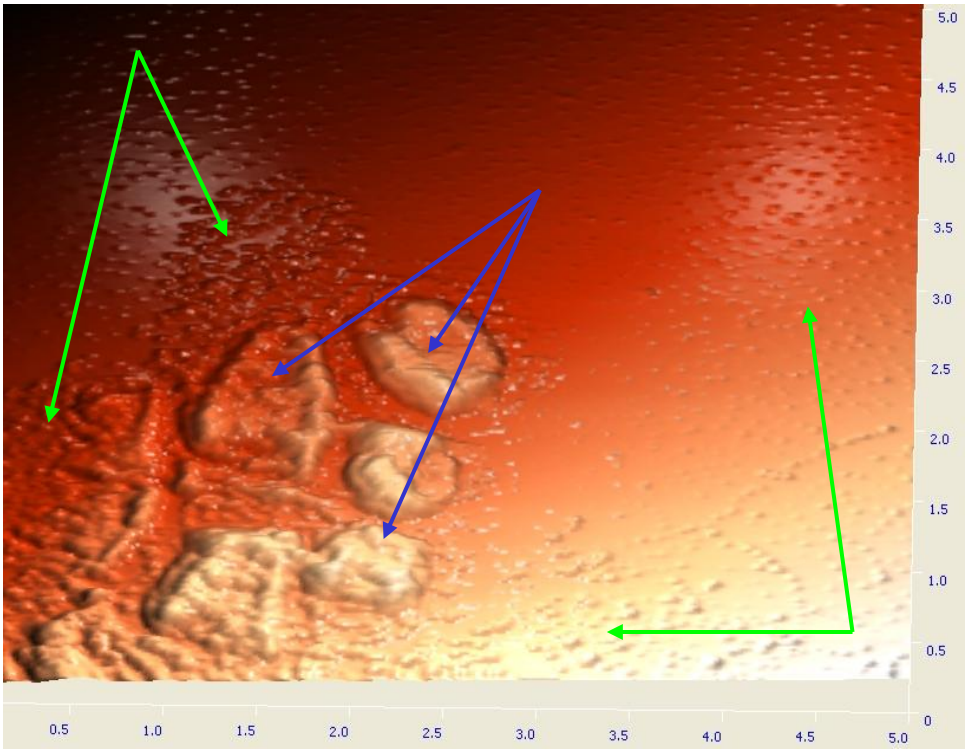

Figure 92: *AFM 5x5µm height 3D image of Escherichia coli cell, 500s afterglow treated.* Intracellular material almost removed (green arrows), some ashes left (blue arrows).

5 Discussion

It has been found recently that gaseous plasma could have some influence on various types of bacteria, mostly negative to their vitality. Different techniques, sources and gases can be used. It has been found that, due to its features, oxygen plasma could act against bacteria, but data sources about basic acting mechanisms, chain of events, acting particles and required doses are limited. The following particles are capable of interacting with bacteria: neutral molecules and atoms (the metastable ones are much denser than others), positively charged molecules and atoms, negatively charged molecules and atoms, and light quanta.

The particular field of our interest is the influence of predominantly neutral radicals that are chemically active to bacteria around us. Typical representatives of two common groups of bacteria, Gram – positive and Gram – negative, were used in our experimental study of the influences of oxygen radical treatment on bacterial structures. For Gram – positive bacteria, *Staphylococcus aureus* was chosen, and for Gram – negative, it was *Escherichia coli*. In both cases, we were acting to the bacterial structures described in Chapter 1.1 especially to outermost layer of bacteria, the capsule, bacterial cell wall and cytoplasmic membrane.

Normal function and integrity of bacterial envelopes prove normal life and vitality of bacteria. Any disturbance or damage of them can lead to the death of bacteria. In our experiment, using plasma radicals, we made efforts to damage and destroy bacterial envelopes, followed by consequent degradation of bacteria and visualized it by Atomic Force Microscopy (AFM) and Scanning Electron Microscopy (SEM).

The experiments were performed using inductively coupled RF oxygen plasma, which is a rich source of neutral oxygen atoms as well as a weak source of ionized oxygen molecules and atoms. Two operation modes have been used, glow and afterglow. In the glow discharge conditions we act with ions and neutral molecules and atoms, while in afterglow there are neutral particles only, and most particles are found in the ground state.

Experimental results reveal some interesting features of destruction of bacteria after receiving a certain dose of neutral oxygen atoms. Both SEM and AFM images show an appearance of small droplets scattered around bacteria (Figs. 41, 42, 43, 55, 63, 64, 65, 66, 67, 68, 80, 81, 82 and 83). Such results are rather unexpected and, to the best of our knowledge, have never been published in relevant literature. Since formation of droplets is unexpected, it deserves a decent discussion.

Here, it is worth mentioning that the formation of the droplets does not appear on substrates without bacteria. Namely, we performed several exposures of plane substrates to plasma or afterglow and never observed formation of any deposits even after prolonged plasma treatment. The formation of droplets is thus a unique feature of plasma treatment of bacteria.

Bacteria that we used in our experiments are originally covered with capsule. The capsule is a jelly material that is rich in water, polysaccharides (mostly acid type). At least some water is chemically bonded, since the sole exposure to vacuum conditions does not seem to dry it significantly (see Figs. 36 and 40). The first effect of exposure of any material to oxygen radicals is formation of a thin surface layer rich in oxygen functional groups. Such formation is usually very rapid and, according to the literature, a dose of about 10^{22} m^{-2} is enough to saturate the surface with such functional groups. The consequence is a dramatic modification of the surface energy of capsule. Since oxygen functional groups are polar, the material exposed to oxygen radicals becomes more hydrophilic – the surface energy increases. The shape of material depends on the properties (especially of the chemical bonds) and the surface energy. A large surface energy would definitely facilitate formation of droplets, while a small surface energy would not be such efficient and would leave the chemical bonds to dictate the shape of the material. In the case of the capsule, which is originally found in the form of a rather uniform film surrounding the bacterium (Figs. 33, 34 and 35 *S.aureus*, 37and 38 *E. coli*), the surface energy is obviously not high enough to facilitate formation of droplets. As soon as our samples are exposed to oxygen radicals, however, the surface energy is increased dramatically and probably becomes high enough to overcome chemical bonds. Here, it should be noted that glycosidic bonds in capsular polysaccharides have in great extent not only β, but and/or α stereochemistry. [26] α stereochemistry is less strong than β stereochemistry (for example α

stereochemistry can be found in starch, which can be hydrolised by water, and β stereochemistry can be found in chitin, which is very strong) [129] and this fact can partly influence transformations of the capsule. The first effect of plasma treatment is thus transformation of the capsule. This transformation, of course, does not appear at once and may not be complete. AFM images reveal that after a brief exposure to plasma the droplets that are scattered all around bacteria are somehow larger than those after prolonged treatment (Figs. 63 vs 68 *S. aureus* and 80 vs 83 *E. coli*). Also, the shape of droplets changes, somehow, with increasing treatment time. At first, they appear pretty spherical, and later, they obtain a rather irregular shape (Fig. 42 vs 65). This effect may be explained with drying up the droplets as well as chemical etching of polysaccharides. Eventually, after around 120 s of treatment in afterglow, the remains of capsule vanish completely. An important conclusion drawn from our research is therefore an almost perfect oxidation of capsule materials. Probably, the destruction is not homogeneous, as the capsule itself is not. However, our experimental techniques are not accurate enough to be able to detect the composition of capsule remains during treatment with oxygen radicals.

Such experiments would require sophisticated equipment, unavailable in our labs. XPS seems a promising technique, but our device has the spot size of about 400 μm, which is orders of magnitude larger than the droplets. As observed from SEM and AFM images, the typical size of the capsule remains is of the order of 10nm. XPS in our laboratory would give results averaged over a large surface consisting predominantly bacteria so the results would not be conclusive. A micro (if not nano) beam of X – rays would be required for decent characterization of the capsule remains. Such a beam is available at 3rd generation synchrotrons, but unfortunately, at this moment we do not have the access to such facilities.

It is also extremely difficult, if not impossible, to separate completely the capsule remains from other materials on our substrates. Namely, due to its features, similar to other sugars, capsular material tends to glue on surfaces. There are techniques for separation of capsule from bacteria, but they are rather aggressive, so the procedure may modify the original structure and perhaps also composition of this delicate jelly material.

From our results we can calculate the dose of atoms required to completely oxidize the capsule. Of course, the result is not extremely accurate due to the fact that some remains of capsule persist when destruction of the cell wall starts. (see Figs. 69a and 70). Nevertheless, the capsule of ***S. aureus*** is almost entirely oxidized in plasma after about 10s. Since the density of atoms in plasma is about $1x10^{22}$, the corresponding dose of O atoms to remove the capsule on *S. aureus* is

$$D_{aP\ cSa} = ¼\ 1x10^{22}\ m^{-3}\ 630\ ms^{-1}\ 10\ s\ = 1.6x10^{25}\ m^{-2}.$$

In the afterglow region the required treatment time is much longer, around 120 s. The density of atoms in the afterglow is lower than in plasma at about $3.5x10^{21}$ m^{-3}. The required dose in the afterglow is thus

$$D_{aA\ cSa} = ¼\ 3.5x10^{21}\ m^{-3}\ 630\ ms^{-1}\ 120\ s\ = 6.6x10^{25}\ m^{-2}.$$

The dose required for total removal of capsule material is about 4 times higher in the afterglow than in plasma. This discrepancy could be attributed to ions that are presented in plasma but not in the afterglow. Let us estimate the influence of positive ions! The ion density in plasma is $1.4x10^{16}$ m^{-3}. The corresponding ion dose received in 10 s is

$$D_{iP\ cSa} = ¼\ 1.4x10^{16}\ m^{-3}\ 630\ ms^{-1}\ 10\ s\ = 2.2x10^{19}\ m^{-2}.$$

If all ions would cause oxidation of the atoms in capsule, they would remove only a few monolayers of atoms from the capsule. Namely, the surface density of atoms is about $1x10^{19}$ m^{-2}. Since the droplets of capsule are much thicker than a few monolayers, we can conclude that the ions cannot be fully responsible for observed rapid oxidation of capsule material in plasma. More probable explanation takes into account thermal effects. Although our plasma is a cold one, the neutral gas temperature does not remain at room temperature but it is elevated. Since it is well known that the oxidation probabilities of organic materials depend largely on the surface temperature, the observed rapid oxidation is rather attributed to somehow increased surface temperature than effects caused by ions. In the afterglow region, however, the neutral gas temperature remained at room temperature throughout our experiments, so influence of the temperature to obtained results can be neglected.

The upper numbers are true for the case of capsule on *S. aureus*. In the case of ***E. coli***, treatment times and required doses of radicals to some events happen, are somehow different. Our experimental data show that the capsule on *E. coli* is well oxidized in, say, 5 s in plasma, and in about 25 s in the afterglow.

The calculated doses are then

$D_{aP\ cEc}$ = ¼ $1x10^{22}$ m^{-3} 630 ms^{-1} 5 s = $0.8x10^{25}$ m^{-2} in plasma and
$D_{aA\ cEc}$ = ¼ $3.5x10^{21}$ m^{-3} 630 ms^{-1} 25 s = $1.4x10^{25}$ m^{-2} in the afterglow.

Again, we can neglect significant contribution of positive ions to oxidation, but the most probable explanation is by taking into account thermal effects.

Here, we have to stress again that the oxidation of capsule is not layer by layer (or atom by atom), but the capsule is first spread to many small droplets and each of these droplets are then slowly oxidized.

Once the capsule is almost entirely destructed, interaction of plasma radicals with cell wall of bacteria starts. The SEM and AFM images show that the destruction is far from being homogeneous.

Let us first consider *S. aureus*. According to the classical literature the original outer surface of bacterial cell wall is not made from pieces, but it is rather compact. This is explained by the classical picture of bacterial wall structure, which predicts continual layered structure of the network (sacculus) made from peptidoglycan. The distance between two subsequent layers was found to be about 4.2 nm. [35] The peptidoglycan forms a kind of a network filled with teichoic acids and some types of proteins. The classical picture is best illustrated in Figure 6. As mentioned earlier, some other authors, however, have recently published a different picture on the structure of the peptidoglycan layer. According to their theory, the peptidoglycan wall is not homogeneous. There are irregularities in peptidoglycan, at least at places where new molecules are inserted during growing of bacterial cell. Namely, the peptidoglycan units are formed within cytoplasm and transferred to the cell wall. There are hydrolytic enzymes that degrade peptidoglycan in the cell wall, with purpose to form binding sites at the places of insertion of new peptidoglycan. [26] This perturbs the original rigid structure of the cell wall.

It is well known that interaction of oxygen radicals with polymer materials cause an increased surface roughness. Even a perfectly flat polymer is etched inhomogeneously, causing formation of textured surface. Typical dimensions of features formed on the surface of polymer materials during treatment with oxygen radicals are of the order of few nm up to few 10 nm. Such inhomogeneous etching is often attributed to small variations in polymer crystallinity as well as in polymer density. Denser parts are etched slowly and the same applies for crystalline parts. In the case of bacteria cell wall, the morphology is found rather rough with typical dimensions of particular segments of several 10 nm. It is difficult to state whether this is the original morphology of the cell wall or a consequence of plasma treatment. If we compare the results with polymers, we would attribute this roughness to small variations of the cell wall structure. As mentioned above, the cell wall of *S. aureus* consists of peptidoglycan and teichoic acids, as well as a certain amount of proteins. It is clear that the oxidation probability for these compounds is not the same. There are several possible explanations for our observations on the initial stage of interaction between oxygen radicals and the cell wall:

- The cell wall is rough originally
- The oxidation of the cell wall forms oxygen rich functional groups that are highly polar and cause a rapid increase of the hydrophillicity
- The capsule itself is not etched homogeneously, consequently the cell wall does not start to etch at the some time at the different places on bacterial cell
- Preferential etching of particular compounds on the surface of the cell wall occurs.

Let us first discuss the first explanation. As mentioned above, the peptidoglycan network is not a perfectly homogeneous grid. The teichoic acids, mostly negative charged, penetrate the structure of peptidoglycan and together with acid polysaccharides, strong negative charge, too, cause local variations in surface energy as well as intermolecular bond strength. This could cause localized perturbances and formation of a hilly surface. Regulatory mechanisms which control production and ratio of peptidoglycan and teichoic acids exist in bacterial cell, but to the best of our knowledge, we did not find exact data on the distribution of teichoic acids on the surface of the cell wall. Probably, it depends on particular conditions such as the environment, nutrients and the growth phase, because it can consist 30 – 50 % of Gram – positive cell wall. The typical distance between such isles of teichoic acid should be not smaller than about 4 nm. Namely, according to the recent model of Dimitriev et al., the typical dimension of unit parts of peptidoglycan oligomers is approximately 4 nm.

The effect of increased surface energy, cased by formation of oxygen rich functional groups on the

surface of cell wall, is probably much less pronounced than in the case of the capsule. Unlike capsule, which is a jelly material, the cell wall of *S. aureus* is well organized and pretty rigid, so the increased surface energy is not enough to overcome the strong bonds between molecules in the cell wall, at least not in the initial stage on plasma interaction with the cell wall.

The effect on inhomogeneous etching of the capsule should cause revealing of certain parts of the cell wall, while other parts are still protected with a thin layer of capsule. As showed above, the remains of capsule on the bacteria are not distributed homogeneously at all (see Fig. 70) Such inhomogenities may cause preferential etching of the cell wall even before capsule is completely removed and would consequently cause the rich morphology observed on the cell wall of *S. aureus*.

Drawing similarities between behavior of polymers and bacterial cell wall during treatment with oxygen radicals would dictate increasing roughness of the cell wall as it is exposed to the radicals. As discussed above, the cell wall may not be that homogeneous as predicted by early authors. Unfortunately, no enough detail picture of the structure of the cell wall is currently available, so no conclusion on the effect of inhomogenicity can be drawn.

As the cell wall is entirely revealed, interaction of oxygen radicals with the peptidoglycane, the teichoic acids and the proteins starts. From both SEM and AFM images we can conclude that etching is pretty intensive. This causes thinning of the cell wall. At a certain dose of the radicals, the cell wall is so badly damaged that disruption occurs. Figures 44, 45, 46, 47 and 72 clearly show segments of the cell wall scattered all around bacteria. These segments are different from those of capsule. While the capsule segments are found in the form of spherical droplets, the segments of the cell wall are found in polygonal form. The typical size of each segment is of the order of 20nm, while clusters may be as big as 100nm. It is interesting that the size of the polygonal segments is the same as the size of hills on the cell wall before etching of the wall started and after removal of the capsule. These segments may well be unit cells of the cell wall network. The length of one disaccharide unit in the peptidoglycan amounts 1.03nm. An average of about 15 disaccharide units in *S. aureus* was found. [26] Different glycan chains do not begin and finish at some places (see Fig. 9), so existing of building block segments of size mentioned above can be possible. Again, our experimental techniques do not allow characterization of the composition of the segments, so we cannot say whether they consist of peptodoglycan only or mixture of peptodoglycan, teichoic acids and some other components.

Once the disruption occurs, the segments are slowly etched (Figs. 44 – 48 and 72 – 76) and after a long treatment time, they practically vanish. Let us estimate total dose of oxygen atoms needed for almost complete oxidation of the *S. aureus* cell wall. The required total treatment time is about 45s in plasma and 350s in the afterglow. The corresponded total doses are then calculated in the same way as in the case of the capsule, and they are

$D_{aP\ cwSa} = ¼\ 1x10^{22}\ m^{-3}\ 630\ ms^{-1}\ 45\ s = 7.1x10^{25}\ m^{-2}$ in plasma and
$D_{aA\ cwSa} = ¼\ 3.5x10^{21}\ m^{-3}\ 630\ ms^{-1}\ 350\ s = 1.9x10^{26}\ m^{-2}$ in the afterglow.

The observation of the disruption is rather surprising and, to the best of our knowledge, has never been reported in literature. As thoroughly written in the Introduction, the current picture of bacteria degradation in gaseous plasma predicts more or less homogeneous etching atom by atom.[91] Our results, however, clearly show that the common picture is wrong, at least for our experimental conditions. As showed with many SEM and AFM images, we always achieve a stage of disruption on *S. aureus*. This disruption is explained by taking into account inhomogenity of cell wall structure, as well as the high pressure in bacterial cell.

Once the majority of the cell wall of *S. aureus* is oxidized, the cytoplasm is exposed to oxygen radicals. Figs.49-53 and 77-78 show the bacteria at this stage. Surprisingly enough, the cytoplasm is not all spread around bacteria, but it remains in the form of a rigid sphere. This result clearly shows that the cytoplasm of *S. aureus* is not made only from a jelly like material, but some rigid structure is observed. This observation is pretty different from the classical picture of bacteria cytoplasm and confirms new models of cytoskeleton existing. In the classical picture, the cytoplasm does not have its own shape but fills the available space within the cytoplasmatic membrane, which itself does not have a rigid structure but it is often described as a semi-liquid mosaic. The thickness of this membrane is of a few nm, so we can conclude that it does not play an important role in description of interaction between oxygen radicals and bacteria. The cytoplasm is, according to relevant literature, rich with DNK molecules, ribosomes, enzymes, and molecules synthesized by alive bacteria, i.e. amino acids, peptides, proteins, fatty acids, lipids, sugars (predominantly monosacharides and olygosaharides) and of course water. As shown in Figs. 49-53 and 77-78 the etching of

this material is also not uniform, which is not surprising due to a large variety of cytoplasm consistuents. What remains after prolonged treatment is just ash. The calculated doses for reaching the stage where the majority of cytoplasm is oxidized after exposure to plasma is

$$D_{aP\ cySa} = ¼\ 1x10^{22}\ m^{-3}\ 630\ ms^{-1}\ 120\ s\ = 1.9x10^{26}\ m^{-2}.$$

The corresponding dose for afterglow treatment cannot be deduced from our experiments. The longest treatment time in the afterglow was 500s and, according to Figure 77 the cytoplasm is still in the form of a sphere. Much longer treatment time is required. Here, we can only conclude that the corresponding value in the afterglow is much more than

$$D_{aA\ cySa} = ¼\ 3.5x10^{21}\ m^{-3}\ 630\ ms^{-1}\ 500\ s\ = 2.7x10^{26}\ m^{-2}.$$

The bacteria are dead well before receiving this dose. We belive that critical dose necessary for definite killing of bacteria is those needed to destroy the peptidoglycan in bacterial cell wall. According to the SEM and AFM images, the average required dose to kill bacteria is

$D_{aP\ killSa} = ¼\ 1x10^{22}\ m^{-3}\ 630\ ms^{-1}\ 35\ s\ = 5.5x10^{25}\ m^{-2}$ in plasma and
$D_{aA\ killSa} = ¼\ 3.5x10^{21}\ m^{-3}\ 630\ ms^{-1}\ 250\ s\ = 1.4x10^{26}\ m^{-2}$ in the afterglow.

These numbers are, of course only approximate and represent order of values. Right values definitely differ from different bacteria of *S. aureus*, depending on the composition and age of each particular bacterial strain.

Let us now discuss the destruction of the *E. coli* cell wall. The picture should be slightly different from *S. aureus*. *E. coli* is a Gram – negative bacteria. The cell wall of *E. coli* is much less rigid than that of *S. aureus*. Outer membrane of *E. coli* cell wall is in form of a paracrystallinic semi – liquid mosaic. The individual components inside are linked to each other by a great diversity of chemical bonds (covalent, H-bridges, chelate like, ionic, hydrophobic). Below there is a thin layer of peptidoglycan, followed by a cytoplasmic membrane.

When the capsule is removed from the surface of *E. coli*, oxidation of the outer membrane mosaic starts. The bacterium quickly loses this mosaic. In the beginning, most prominent O-antigens part of outer membrane is exposed. As described in Chapter 1, O-antigens consist of 20 – 40 repeating building blocks of monosaccharides. These monosaccharides are connected by glycosidic bonds, which some of them have not only β, but α stereochemistry, at least in some *E. coli* strains. [26] As mentioned above, this type of glycosidic bond can be relatively easily broken. Whole structure is stabilized by hydrogen bonds. Hydrogen bond is not true chemical bond and has a low binding energy, up to 40 KJ/mol. [130] Potential energy of oxygen atom is approx. 2.5eV = 240kJ/mol, so oxygen atoms can easily break hydrogen bonds. These facts can explain pretty fast removal of outermost layer of LPS. (Figs. 84 – 87). Nevertheless, some part of O-antigens can be etched during the capsule removal, because capsular polysaccharides (CPS) and O-antigens weave through each other on surface of Gram – negative bacteria.

Once, when O-antigens part of LPS has been removed, core region becomes visible. It is clear why R – forms of Gram – negative bacteria were named, if we see Figs. 88 and 89. Namely, bacteria that do not have O-antigens we call rough forms (R-forms). Core region is distinctly smaller (up to 15 non repeating monosaccharides) than O-antigens region and highly negative charged.

Lipid A consist 6 – 7 fatty acids per molecule, some of them are unsaturated, so they are likely to be attacked by radicals. [62] It is similar in case of phospholipids in outer membrane.

Protein molecules incorporated in the cell wall, which are basically linear chains of aminoacids, are susceptible to oxidation by atomic oxygen. [62] Proteins, especially transmembrane type, play the role of gateways that control the passage of various molecules in and out of cell. Their degradation causes leakage of internal components, which consequently lead to serious damages of bacterial cell. At the same time, connection places between proteins and other components of the cell wall can be weak points, easily attacked by oxygen radicals.

When oxygen radicals destroy the outer membrane, peptidoglycan layer undergo to radical influence. It is found that isolated murein sacculus of *E. coli* can contain one to three peptidoglycan layers. [131] A thickness of a single layer is about 2.5nm. We believe that such a thin peptidoglycan layer is not rigid enough to maintain very well the shape of *E. coli* cell. Because peptidoglycan layer is very thin in Gram – negative bacteria, very soon after destroying outer membrane, this layer has been destroyed and holes are found in the cell wall (Figs 57, 58, 88, 89 and 90). We can clearly claim that at least a part of cytoplasm is

lost into the surroundings and the majority of water is evaporated. This happens only after about 10s in plasma. The dose required to observe such effects is

$D_{aP\ cwEc}$ = ¼ $1x10^{22}$ m^{-3} 630 ms^{-1} 10 s = $1.6x10^{25}$ m^{-2} in plasma and
$D_{aA\ cwEc}$ = ¼ $3.5x10^{21}$ m^{-3} 630 ms^{-1} 180 s = $1x10^{26}$ m^{-2} in the afterglow.

The discrepancy between the corresponding dose in plasma and afterglow is pretty large and it is mostly attributed to increased temperature of the bacteria during plasma treatment. It is known that lipid structures in outer membrane (lipid part of LPS and phospholipids), similar to other types of lipids, appear in two thermal phases, and switch depending on ambiental temperature. At lower temperature the ordered β-phase exists, where fatty acids are mainly in all-*trans* configuration and dense packed, so forming gel-like phase of membranes, while at higher temperatures transition in α-phase become, where percentage of *gauche* conformation increases, and packing density decreases simultaneously, what is a reason for semiliquid state of membranes. [26] In this state, outer membrane is less strong and consequently easily damaged. As already stressed above, the samples mounted inside the afterglow chamber remain at room temperature. Of course, it is well known, too, that all reactions of organic molecules running faster at elevated temperature.

As shown in Figs. 59 and 60, *E. coli* bacteria are almost completely oxidized in total time less than 60 s of plasma treatment.

The calculated doses for reaching the stage where the majority of cytoplasm is oxidized after exposure to plasma is

$D_{aP\ cyEc}$ = ¼ $1x10^{22}$ m^{-3} 630 ms^{-1} 60 s = $9.4x10^{25}$ m^{-2}.

The corresponding dose for afterglow treatment cannot be deduced from our experiments. The longest treatment time in the afterglow was 500s and, according to Fig. 92 the cytoplasm is not removed completely. It is clear that longer treatment time is required. Here, we can only conclude that the corresponding value in the afterglow is much more than

$D_{aA\ cyEc}$ = ¼ $3.5x10^{21}$ m^{-3} 630 ms^{-1} 500 s = $2.7x10^{26}$ m^{-2}.

The bacteria are dead well before receiving this dose. The critical dose required for definite killing of bacteria is those needed to destroy the bacterial cell wall. According to the SEM and AFM images, the required treatment time is

$D_{aP\ killEc}$ = ¼ $1x10^{22}$ m^{-3} 630 ms^{-1} 10 s = $1.6x10^{25}$ m^{-2} in plasma and
$D_{aA\ killEc}$ = ¼ $3.5x10^{21}$ m^{-3} 630 ms^{-1} 180 s = $1x10^{26}$ m^{-2} in the afterglow.

These numbers are only approximate. Exact values definitely differ for different bacteria of this species, depending on the composition and age of each particular bacterial strain.

Summarized events during exposure to oxygen radicals, with exposition times and doses of oxygen radicals necessary to some events happen, for *S. aureus* and *E. coli* are given in Table 6. Comparison of events in glow and afterglow for *S. aureus* and *E. coli* are shown in Table 7.

Table 6: *Exposition times* and necessary doses* of oxygen radicals for some events / effects on bacteria during oxygen radicals treatment.*

event	*S aureus*				*E coli*			
	glow		afterglow		glow		afterglow	
	time(s)	dose	time(s)	dose	time(s)	dose	time(s)	dose
Total removal of the capsule	10	$1.6x10^{25}m^{-2}$	120	$6.6x10^{25}$ m^{-2}	5	$0.8x10^{25}$ m^{-2}	25	$1.4x10^{25}$ m^{-2}

Degradation of the cell wall only	*35*	*5.5 x10^{25} m^{-2}*	*230*	*1.3x10^{26} m^{-2}*	*5*	*0.8x10^{25} m^{-2}*	*155*	*8.5 x10^{25} m^{-2}*
Complete oxidation to the level of the cell wall	45	7.1x10^{25}m^{-2}	350	1.9x10^{26}m^{-2}	10	1.6x10^{25} m^{-2}	180	1x10^{26} m^{-2}
Degradation of the cytoplasm only	*75*	*1.2 x10^{26}m^{-2}*	*>150*	*not available*	*50*	*7.9x10^{25} m^{-2}*	*> 320*	*not available*
Majority of the cytoplasm oxidized	120	1.9x10^{26}m^{-2}	> 500	>2.7x10^{26}m^{-2}	60	9.4x10^{25} m^{-2}	> 500	> 2.7x10^{26}m^{-2}
Definite killing of bacterial cell	35	5.5x10^{25}m^{-2}	250	1.4x10^{26}m^{-2}	10	1.6x10^{25} m^{-2}	180	1x10^{26}m^{-2}

**** average values are given***

Table 7: *Comparisation of events in glow and afterglow for S. aureus and E. coli*

event	*glow*				*afterglow*			
	S. aureus		*E. coli*		*S. aureus*		*E. coli*	
	time(s)	dose	time(s)	dose	time(s)	dose	time(s)	dose
Total removal of the capsule	10	1.5x10^{25}m^{-2}	5	0.8x10^{25}m^{-2}	120	6.6 x10^{25}m^{-2}	25	1.4 x10^{25}m^{-2}
Degradation of the cell wall only	*35*	*5.5 x10^{25}m^{-2}*	*5*	*0.8x10^{25}m^{-2}*	*230*	*1.3 x10^{26} m^{2}*	*155*	*8.5 x10^{25}m^{-2}*
Complete oxidation to the level of the cell wall	45	7.1x10^{25}m^{-2}	10	1.6x10^{25}m^{-2}	350	1.9x10^{26} m^{-2}	180	1x10^{26}m^{-2}
Degradation of the cytoplasm only	*75*	*1.2x10^{26}m^{-2}*	*50*	*7.9x10^{25}m^{-2}*	*>150*	*not available*	*> 320*	*not available*
Majority of the cytoplasm oxidized	120	1.9 x10^{26} m^{-2}	60	9.4x10^{25}m^{-2}	>500	>2.7x10^{26}m^{-2}	> 500	>2.7x10^{26}m^{-2}
Definite killing of bacterial cell	35	5.5 x10^{25}m^{-2}	10	1.6x10^{25}m^{-2}	250	1.4x10^{26}m^{-2}	180	1x10^{26}m^{-2}

When we analyze chain of events during the degradation of bacterial cells, necessary exposure times and required doses of oxygen radicals, it is possible to compare happening in case of *S. aureus* and *E. coli.*

Here, it should be noted, when compare data in Table 6. it is visible increasing time/dose ratio approx. 2.85/1 for treatment in plasma and afterglow, respectively (e.g. twelve times increasing exposure time brings four times larger dose of radicals).

In case of *S. aureus*, twelve times longer treatment time is necessary in afterglow comparing with plasma, for total removal of capsule. More than six times longer treatment in afterglow is necessary for degradation of bacterial cell wall only, and more than four times longer exposure for complete oxidation to the cell wall level. For definite killing of these bacteria more than seven times longer exposure is necessary in afterglow.

In case of *E. coli* five times longer treatment time is necessary in afterglow than in plasma, for total

removal of capsule. More than thirty times longer treatment in afterglow is necessary for degradation of bacterial cell wall only, and more than eighteen times longer exposure for complete oxdation to the cell wall level, as well as for definite killing of these bacteria.

Let us compare some events for *S. aureus* and *E. coli* in glow conditions, as well as in afterglow.

In glow conditions, removal of capsule is two times slower for *S. aureus*. The discrepancy between the results on oxidation of capsule on *S. aureus* and *E. coli* can be attributed to different composition of the capsules. In any case, the necessary dose to this event happen is of the order of 10^{25} m^2. If we compare degradation of the cell wall only, discrepancies are much bigger. Degradation is even seven times longer for *S. aureus*. As mentioned above, probable explanation is high-organized peptidoglycan structure in *S. aureus* cell wall, not easy to etching, as well as much intensive influence of elevated temperature on *E. coli* cell wall, which contains a significant amount of lipid structures in outer membrane. Cytoplasm is etched slightly slower in *S. aureus*, probably due to more organized cytoskeleton. Generally, it is clearly visible that in total time, *S. aureus* is destructed more than three times slower than *E. coli* in glow conditions.

Picture is different in afterglow. As we expected, degradation of bacterial structures is much slower, due to the fact that only oxygen atoms play role in this process. We can neglect influence of any other particle, while temperature in afterglow chamber is room temperature.

In afterglow, capsule of *S. aureus* is etched almost five times slower, if we compare with *E. coli*. Surprisingly, degradation of *S. aureus* cell wall only, is just 1.5 times slower than in case of *E. coli*. Of course, as mentioned earlier, should be keep in mind in case of *E. coli*, that some part of O-antigens can be etched at the same time as capsular polysaccharides. This is a reason why we cannot deduce exact time and required doses of oxygen radicals necessary for oxidizing of these particular parts. However, time necessary for complete oxdation to the level of the cell wall is about two times longer for *S. aureus*. Definite killing of *S. aureus* is 1.4 times longer process than in case of *E.coli*.

Finally, according to our experimental results, let us discuss the organization and three – dimension structure of peptidoglycan, and maybe refine the actual view of the cell wall structure.

In case of *Escherichia coli*, during degradation process, in the phase of peptidoglycan removal, some pretty differentiated structures were observed. (see Fig. 90) According to the present view of bacterial cell wall structure, peptidoglycan is embedded in periplasmic space, forming grid – like structure, as briefly reviewed in Chapter 1. As already mentioned it is organized in one to three layers.

Our experimental results showed a somehow different picture. After removal of outer membrane components, deeper structure becomes visible. As postulated by many authors in the past, this layer contains peptidoglycan only, so we can discuss the spatial organization of peptidoglycan. It is clearly visible, (see Fig. 90 for instance) that many well – defined pieces or, we can say, structural units exist. These structural units are flat, oval or round shaped. Their dimensions were measured, and we always obtained values of 110 – 150 nm in diameter and 20 – 45 Å in thickness as shown in example in Fig. 93)

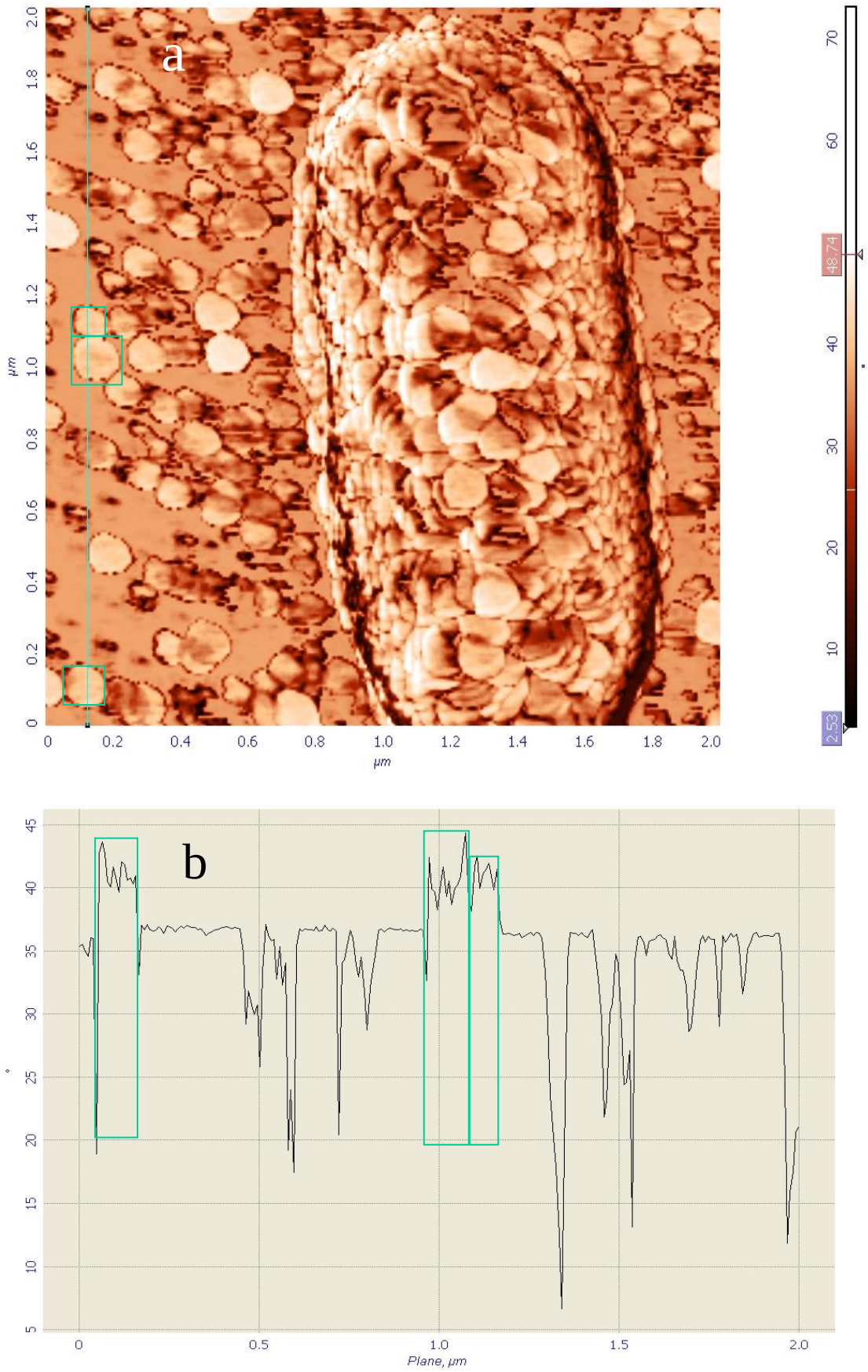

Figure 93. *Example of dimensions measuring of peptidoglycan structural units in E. coli cell wall.*

Measured thickness of some units can be slightly different (false smaller), probably due to etching process. In phase of peptidoglycan removal, many of these pieces are scattered all around bacterium. Pieces on surface of bacterial cell look like fish scales or tiles on a roof. These units are organized in such a manner that overlap each other, as shown schematically in Fig. 94.

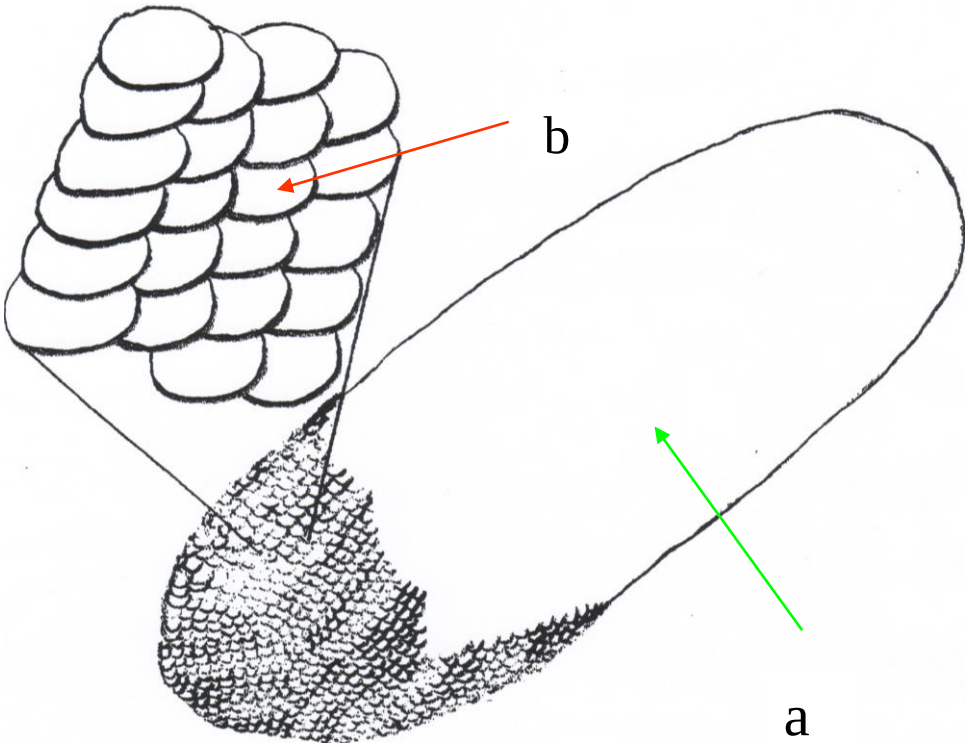

Figure 94. *Schematic model of three – dimensional organization of peptidoglycan in E. coli cell wall.* a. Bacterial cell green arrow pointed; b. Organization of the structural units of peptidoglycan red arrow pointed.

Let's remind some claims of early researchers. A generally accepted theory postulates peptidoglycan chains connected to each other via peptide bridges form flat surface. This flat surface according to Barnickel et al. [131] can be found in murein sacculus of *E. coli* in one to three layers. Thickness of each layer is approx. 2,5 nm. In conceptually new model according to Dimitriev et al. [36] in the case of Gram – negative bacteria theoretical calculated thickness of one turn is 3.92nm. These dimensions are similar to those obtained from our measurements. Koch indicated improbability of parallel glycan strands under the influence of internal cell pressure [33]. According to Koch smallest pores in peptidoglycan called thesserae become hexagonal. Peptidoglycan oriented in such a way can form patches, as shown in Fig 10. [34] This form suggests pretty round or oval shape of structural units, formed from peptidoglycan chains of length mentioned earlier in Introduction. It is shown that some of peptide bounds do not bound chains in the same layer. (see Fig. 9) [132]. So, we can imagine possible way how structural units bond to each other. Of course, we do not forget other possible bonds and forces between various structures on surfaces of the units.

Our model may represent a strong background for solving another important problem of the cell wall structure. It is well known that new peptidoglycan must be synthesized in the internal part of bacterial cell. Until now, some complicated models of incorporating of new peptidoglycan in bacterial cell wall appeared. Our model predicts self – organization of peptidoglycane into unit cells, so, accordingly, new peptidoglycan units can be simply attached to the old ones already existing in the cell wall. Obviously, the new units are attached on the inner side of the cell wall. Any discussion on the regulating mechanisms of elongation (and degradation) process is definitely beyond the scope of this thesis. However, it should be kept in mind that bacteria, due to their mechanisms of reproduction, actually represents continual type of life (in opposite to higher organisms, which we can declare as discontinual). On this way, in growth process, enlargement of peptidoglycan layer can be achieved by continuous adding (gluing) of new patches of structural units.

The experimental results presented in this thesis do not offer enough material for extremely precise and

accurate characterization of Gram – positive cell wall and three dimensional structure of peptidoglycan incorporated inside. As mentioned earlier, we can only conclude that some pieces of peptidoglycan units are removed during treatment with oxygen radicals. Still, our observations on organization of peptidogycan in the cell wall of *E. coli* may indicate that similar structural units (probably more complex) also exist in the cell wall of Gram – positive bacteria. As already stressed this is only our hypothesis and more scientific work supported with top – class characterization is needed to confirm it.

6 Conclusions

Two types of bacteria were exposed to oxygen radicals, i.e. *Escherichia coli* and *Staphylococcus aureus.* The results of systematic experiments confirm some of our hypotesis, and partially confirm some others hypothesis.

The first hypothesis, i.e. that oxygen radicals destroy bacteria by oxidation of organic compounds was confirmed by treatment in atmosphere where only neutral oxygen atoms in the ground state were present – such environment is found in the afterglow of oxygen plasma. The degradation was found to be pretty slow, meaning that the destruction of bacteria was obtained in roughly 200s, enabling ample time to monitor specific features of oxidation.

Since we measured the density of atoms rather precisely, it was possible to calculate the flux of radicals onto the surface and thus the etching probability. The experimental results allowed for calculation of the dose of radicals needed to destroy specific components of bacteria.

An important hypothesis was a non-uniformity of the treatment. Since a bacterium is an inhomogeneous material, certain non-uniformity in etching was expected. Our results not only confirmed this hypothesis, but revealed some rather unexpected features as well. To the best of our knowledge, this thesis represents the first report on spreading of bacterial material into the surroundings during specific phases of the treatment. The first extensive spreading is observed for bacterial capsule. We found that the capsule although "dried" prior to exposure to radicals is spread all around bacteria in few seconds of treatment. This effect was explained by a dramatic increase of the capsule surface energy causing formation of numerous droplets. This spreading of the capsule has an important consequence: The droplets exposed to oxygen radicals are completely destroyed in a much shorter time than it would be the uniform capsule. An important conclusion that can be extracted from these observations is that the removal of bacterial structures i.e. capsule is not etching atom by atom (as suggested by other authors) but destruction into droplets happens firstly and only later by etching atom by atom.

Another non-uniformity in etching was observed for the case of the cell wall. In one of our hypothesis we already stated that the weak point may appear in the cell wall after reciving a certain doses of radicals and that the envelopes may break and parts spread all aroung bacteria. Our experimental results clearly confirmed not only this hypothesis but showed numerous small segments scattered all around bacteria as well. This observation shows that the classical picture of bacterial etching atom by atom is far from being valid, at least for *E. coli* and *S. aureus*. If only atom by atom degradation mechanism acting, it wouldn't be visible particules. Instead, we propose another mechanism: as soon as the cell wall is damaged to a certain degree, segments of peptidoglycan from the cell wall (and other constituents in *E. coli* cell wall) are released and scattered around bacteria. Only after this effect, the etching follows the atom by atom theory.

Our observation of segments with well-defined size and shape may lead to novel or at least improved picture of the bacterial wall structure. Our results clearly show that the segments are similar in shape and size, so any accidental destruction is excluded. Namely, if the destruction was accidental, the size of the segments should be far from equal: some would be very large and others tiny. The segments observed arund bacteria after pretty strong destruction of the cell wall are most probably made from peptidoglicane (which is etched at lower rate than other compounds in the cell wall). Our results suggest that peptoglicane is far from being an uniform layer but it appears in the form of well defined pallets with typical diameter of 30nm and thickness of only few nm.

Our hypothesis that the appearance of craks and holes in the bacterial wall cell would cause leakage of cytoplasm was partly confirmed only for the case of *E. coli*, and not for *S. aureus*. Our results clearly show that the cytoplasm of *S. aureus* is pretty organised so there are structures that cannot leak anywhere. This result represents an excellent confirmation for the novel model of bacterial cytoplasm: it consists a rigid structure called cytoskeleton.

The results of the systematic work show that the segmentation of bacterial structures dramatically increases the destruction rate of the types of bacteria we used. Namely, if the destruction was only by atom by atom etching, the required dose and thus the treatment time would be much longer than determined from our experiments.

According to our experimental results, we proposed a new model of three – dimensional organization of peptidogycan in *E. coli* cell wall. At this model, peptidoglycan is organized in flat, oval or round shaped pieces composed in such a manner, where pieces overlapping each other and looks like fish scales or tiles on a roof.

Our research may have an important influence on further verification of new theories on bacterial structure. As mentioned before, the classical picture of the cell wall structure of Gram – positive bacteria such as *S. aureus* is that peptoglycan forms a uniform (continual) envelope. By our method of slow etching with oxygen atoms, we show a possible way of extremely delicate removal of different consistuents that may allow for detailed study of the envelope construction.

7 Acknowledgements

I would like to express my sincere gratitude to colleagues and institutions for their useful and helpful assistance and support in preparing this work.

Here, I would like to deeply thank the coworkers at Jožef Stefan Institute, Ljubljana, Slovenia: Tatjana Filipič, Ita Junkar and Prof. dr Janez Kovač who helped with AFM analysis and, especially Prof. dr Anton Zalar, the head of research group, for peer review of the manuscript and fruitful suggestions.

I gratefully acknowledge coworkers at National Institute of Chemistry, Ljubljana, Slovenia: Nina Haiptman, dr Marta Klanjšek Gunde and dr Marjan Bele for their help with SEM analysis.

My sincere thanks go to the co-supervisor and supervisor, Prof. dr Uroš Cvelbar and Prof. dr Miran Mozetič from Jožef Stefan Institute and International postgraduate school Jožef Stefan for their contribution in experimental and theoretical work, as well as fruitful discussion.

Many thanks to Sanja Šćepanović from the Institute of Public Health, Podgorica, Montenegro, for proofreading and Dr. Boban Mugoša, director of the Institute, for all kind of support.

Especially, I am grateful to Slovene Human Resources Development and Scholarship Fund-Ad Futura for providing funds to support this research (financial support).

The research was performed within scientific projects funded by Slovenian Research Agency, ZAMTES and the Ministry of Education and Science of Montenegro, the bilateral project “Research of bacteria damages after plasma radical interaction”.

8 References

1. Golding.I.; Cox E.C. Physical nature of bacterial cytoplasm. *Phys Rev Lett.* **96**(9):098102 (2006).
2. Murray P.R. et al. *Medical microbiology 4th ed.* (Mosby, St. Louis, 2002).
3. Karakasevic B. Morfologija i fiziologija bakterija in: Karakasevic B. (ed.) *Mikrobiologija i parazitologija* (Medicinska knjiga, Beograd – Zagreb, 1987).
4. Brooks G.F.; Butel J.S.; Ornston J.N. (eds.) *Jawetz Melnick& Adelberg's Medical microbiology* (Appleton and Lange, Norwalk,1991).
5. URL:http://www.britanica.com/Ebcheked/topics/48203/bacteria/39340The-cytoplasm
6. Jones L.; Carballido-Lopez R.; Errington J. Control of cellshape in bacteria: helical actin-like filaments in *Bacillus subtilis*. *Cell* **104**: 913–922 (2001).
7. Michie K.A.; Löwe J. Dynamic filaments of the bacterial skeleton. *Annu. Rev. Biochem.* **75**: 467–92. (2006).
8. Held W.A.; Nomura M. Structure and function of bacterial ribosomes. XX. Rate-determining step in the reconstitution of Escherichia coli 30S ribosomal subunits *Biochemistry* **12** (17):3273-3281 (1973).
9. URL:http://medgadget.com/archives/2005/11/highres_bacteri.html
10. Thanbichler M.; Wang S.C.; Shapiro L. The Bacterial Nucleoid: A Highly Organized and Dynamic Structure *J Cell Biochem* **96**(3):506–521 (2005).
11. Breier A.M.; Cozzarelli N.R. Linear ordering and dynamic segregation of the bacterial chromosome. *Proc Natl Acad Sci USA* **101**:9175–9176. (2004).
12. Thanbichler M.; Shapiro L. Chromosome organization and segregation in bacteria. *Journal of structural Biology* **156** (2) 292-303 (2006).
13. Woldringh C.L.; Odijk T. Structure of DNA within the Bacterial Cell: Physics and physiology in: Charlebois R. L. (ed.) *Organization of the Prokaryotic Genome.* (ASM Press, Washington, D.C. 1999).
14. URL:http://en.wikipedia.org/wiki/Chromosome
15. Egan E.S.; Fogel M.A.; Waldor M.K. Divided genomes: negotiating the cell cycle in prokaryotes with multiple chromosomes. *Mol. Microbiol.* **56**:1129–1138. (2005).
16. Volff J.N.; Altenbuchner J. A new beginning with new ends: Linearisation of circular chromosomes during bacterial evolution. *FEMS Microbiol. Lett.* **186**:143–150. (2000).
17. Bendich A.J. The form of chromosomal DNA molecules in bacterial cells. *Biochimie* **83**:177–186. (2001).
18. Gitai Z. et al. MreB actin-mediated segregation of specific region of bacterial chromosome. *Cell*. **120**:329-341. (2005).
19. Graumann, P.L. Cytoskeletal elements in bacteria. *Current Opinion in Microbiology* **7** (6): 565–571 (2004).
20. Bartosik A.A. et. al. ParB of Pseudomonas aeruginosa: Interactions with its partner ParA and its target parS and specific effects on bacterial growth. *J Bacteriol* **186**:6983–6998. (2004).
21. Gitai Z. The New Bacterial Cell Biology: Moving Parts and Subcellular Architecture. *Cell*. **120** (5):577-586 (2005).

22. Shih Y.L.; Rothfield L. The Bacterial Cytoskeleton *Microbiol Mol Biol Rev*. **70**(3): 729–754. (2006).
23. Singer S.J. The fluid mosaic model of membrane structure. In: Abrahamson S. Pascher I. (eds.) Structure of biological membranes. *Plenum.* New York , 443-461 (1977)
24. URL:http://en.wikipedia.org./wiki/Image:CellMembraneDrawing.jpg
25. URL:http://www.denniskunkel.com/DK/DK/Medical/1967A.html
26. Seltmann G.; Holst O. *The bacterial cell wall* (Springer-Verlag, Berlin, Heidelberg: 2002).
27. URL:http://www.gsbs.utmb.edu/microbook/ch002.htm
28. Sleytr U.B.; Beveridge T.J. Bacterial S-layers. *Trends Microbiol* **7**: 253-260. (1999).
29. URL:http://web.uct.ac.za/depts/mmi/lsteyn/cellwall.html
30. URL :http://medic.med.uth.tmc.edu/slnk/00001476.gif
31. URL:http://student.ccbcmd.edu/courses/bio141/lecguide/unit1/prostruct/gramstain/gram3.html
32. Labischinski H.; Maidof H. Bacterial peptidoglycan: Overviev and evolving concepts. In: Ghyisen J.M.; Hakenbeck R (eds.) Bacterial cell wall. *New comprehesive biochemistry*. **27** (Elsevier, Amsterdam 23-38 1994).
33. Koch A.L. Orientation of the peptidoglycan chains in the sacculus of Escherichia coli. *Res. Microbiol.* **149**: 689-701 (1998).
34. Koch A.L. How did bacteria come to be? *Adv Microbial Physiol* **40**: 353-399 (1998).
35. Labschinski H. et.al. On the secondary and tertiary structure of murein Low and medium angle x-rey evidence against chitin-based conformation of bacterial peptidoglycan *Eur.J. Biochem.* **95** (1)147-155 (1979).
36. Dimitriev B.A.; Ehlers S.; Retschel E.T. Layered Murein revised: a fundamentaly new concept of bacterial cell wall structure, biogenesis and function. *Med. Microbiol. Immunol*. **187**: 173-181 (1999).
37. URL:http://www.gsbs.utmb.edu/microbook/ch002.htm
38. Ward J.B. Teichoic and teichuronic acids: biosynthesis, assembly and location. *Microbiol. Rev.* **45**: 211-243 (1981).
39. Djikstra A.J.; Keck W. Peptidoglycan as a barrier to transenvelope transport *J.Bacteriol.* **178**: 5555-5562 (1996).
40. Kehoe M.A; Cell wall associated proteins in Gram-positive bacteria In: Ghyisen J.M.; Hakenbeck R. (eds.) Bacterial cell wall. *New comprehesive biochemistry*. **27** (Elsevier, Amsterdam 217-261 1994).
41. Beveridge T. J. Structures of Gram-negative cell walls and their derived membrane vesicles. *J. Bacteriol.* **181**: 4725-4733 (1999).
42. URL:http://student.ccbcmd.edu/courses/bio141/lecguide/unit1/prostruct/gramstain/gram3.html
43. Holst O. Chemical structure of the core region of lipopolysaccharides. In: Brade H. et al.(eds.) *Endotoxin in health and disease.* (Marcel Dekker, New York, 115-154 1999).
44. Jansson P.E. The chemistry of O-polysaccharide chains in bacterial lipopolysaccharides In: Brade H. et al.(eds.) *Endotoxin in health and disease.* (Marcel Dekker, New York, 155-178 1999).
45. Fischetti V.A. Surface proteins of Gram-positive bacteria. In: Fischetti V. A. et al. (eds.) *Gram positive pathogens* (ASM Press, Washington D.C. 11-24 2000).
46. DiRienzo J.M.; Nakamura K.; Inouye M. Outer membrane proteins of Gram-negative bacteria: biosynthesis, assembly and function *Annu. Rev. Biochem*. **47**: 481-532 (1978).
47. Hankock R.E.W.; Karunaratne D.N.; Bernegger-Egli C. Molecular organization and structural role of outer membrane macromolecules In Ghysen J.M.; Hakenbeck R (eds.) Bacterial cell wall. *New comprehesive biochemistry*. **27** (Elsevier, Amsterdam, 263-279 1994).
48. Houvink A.L. A macromolecular monolayer in the cell wall of *Spirillum* spec. *Biochim.Biophys. Acta* **10**:360-378 (1953).
49. Engelhardt H.; Peters J. Structural research on surface layers: a focus on stability, surface layer homology domains and surface layer-cell wall interactions. *J.Structural Biol*.**124**: 276-302 (1998).
50. Sleytr U.B.; Beveridge T.J. Bacterial S-layers. *Trends Microbiol.* **7**: 253-261 (1999).

51. Mahon C.; Manuselis G. (eds.) *Textbook of Diagnostic Microbiology 2nd ed*. (W.B. Saunders, Elsevier Science, Philadelphia, 2000).
52. URL:http://porpax.bio.miami.edu/~cmallery/150/proceuc/c27x7x3flagella.jpg
53. Sneath P.H.A. Endospore forming Gram-positive rods and cocci. In: Sneath P.H.A. et al. (eds.) *Bergey's manual of systematic bacteriology Vol.2*.(Williams&Wilkins,Baltimore,1104-1207 1986).
54. Schmidt C.F. Thermal resistance of microorganisms. In: Redish G.F. (ed.) *Antiseptics, disinfectans, fungicides, and sterilization.* (Lea &Febiger, Philadelphia, 720-759. 1954).
55. Rusell A.D. Principles of antimicrobial activity and resistance. In: Block S.S. (ed.) *Disinfection, sterilisation, and preservation. 5.ed,* (Lippincott, Williams & Wilkins Philadelphia, 31-49 2001).
56. Farkas J. Tolerance of spores to ionizing radiation: mechanisms of inactivation, injury, and repair. *J appl microbiol.* **76**(suppl): 81-90 (1994).
57. Nickoloff J.A.; Hoekstra M.F. (eds.) *DNA damage and repair, vol 1. DNA repair in procaryotes and lower eucaryotes.* (Humana Press, Totowa, 1998).
58. Rusell A.D.; Morris A.; Allwood M.C. Methods of assessing damage to bacteria induced by chemical and physical agents. In: Ribbons D.W.; Norris J.R. (eds.) *Methods in microbiology, vol. 8.* (Academic Press, London, 95-182 1973).
59. Gould G.W.; Rusell A.D.; Stewart-Tull D.E.S. Fundamental and applied aspects of bacterial spores. *The Society for Applied Bacteriology Symposium Series No.23* (Blackwell Scientific Publications, Oxford, 1994).
60. Gould G.W. Modifications of resistance and dormancy. In: Dring G.J.; Ellar D.J.; Gould G.W. (eds.) *Fundamental and applied aspects of bacterial spores.* (Academic Press London,, 371-382. 1985).
61. Bridges B.A. *Survival of bacteria following expousure to ultraviolet and ionizing radiation*. In: Gray T.G.R.; Postgate J.R. (eds.) *The survival of vegetative microbes. Society for General Microbiology Symposium No. 26* (Cambridge university Press, Cambridge, 183-208 1976).
62. Laroussi M. Low temperature plasma-based sterilisation: Overview and state-of-the-art. *Plasma Process. Polym.* **2** (5) 391-400 (2005).
63. Sosnin E.A. et al. The effects of UV irradiation and gas plasma treatment on living mammalian cells and bacteria: a comparative aproach. *IEEE Trans Plasma Sci* **32** (4):1544-1549 (2004).
64. Mosley B.E.B. Ionizing radiation: action and repair. In: Gould G.W. (ed.) *Mechanisms of action of food preservation procedures.* (Elsevier Applied Science, London, 43-70 1989).
65. Fairhead H.; Setlow P. Binding of DNA to α,β-type small, acid solubile proteins from spores of Bacillus or Clostridium species prevents formation of cytosine dimers, cytosine-thymidine dimers and bipyrimidine photoadducts upon ultraviolet irradiation. *J Bacteriol* **174**: 2874-2800 (1992).
66. Pflug I.J.; Holcomb R.G.; Gomez M.M. Principles of the thermal destruction of microorganisms. In: Block S.S. (ed.) *Disinfection, sterilisation, and preservation. 5.th* (Lippincott Williams & Wilkins Philadelphia, 79-124 2001).
67. Gould G.W. Heat-induced injury and inactivation. In: Gould G.W. (ed.) *Mechanisms of action of food preservation procedures.* (Elsevier Applied Science, London, 11-42 1989).
68. Rusell A.D. Sterilisation and disinfection by heat methods. In: Rusell A.D. Hugo W.B. Aylife G.A.J. (eds.) *Principle and practice of disinfection preservation and sterilization. 3rd, ed.* (Blackwell Scientific Publications, Oxford, 629-639 1999).
69. Gould G.W. Heat sterilization : D. application of thermal processing in the food industry. In: Rusell A.D.; Hugo W.B.; Aylife G.A.J. (eds.) *Principle and practice of disinfection preservation and sterilization. 3rd ed.* (Blackwell Scientific Publications, Oxford, 665-674 1999).
70. Pellon J.R.; Sinskey A.J. Heat-induced damage to the bacterial chromosome and repair. In: Andrew M.H.E.; Rusell A.D. (eds.) *The revival of injured microbes. Society for Applied Bacteriology Symposium No. 12.* (Academic Press London,, 105-1251984).
71. Marquis R.E.; Sim J.; Shin S.Y. Molecular mechanisms of resistance to heat and oxidative damage. *J Appl Bacteriol* **76** (suppl.): 40-48 1994.
72. Murell W.G.; Warth A.D. Comparison and heat resistance of bacterial spores. In: Campbell L.L. Halvorson H.O. (eds.) *Spores III.* (American Society for Microbiology Ann Arbor, 1-24 1965).
73. Setlow P. Mechanisms which contribute to long-survival of spores of Bacillus species. *J Apll Bacteriol.* **76** (supll.): 49-60 (1994).
74. Molin G. Inheritant genetic differences in dry heat resistance of some Bacillus spores. In: Baker A.N.; Wolf J.; Ellar D.J.; et al. (eds.) *Spore research 1976.* (Academic Press, New York, 487-500 1977).
75. Northrop J.; Slepecky R.A. Sporulation mutations induced by heat in Bacillus subtilis. *Science*

155: 838-839 (1967).
76. Rowe J.A.; Silverman G.J. The absorption-desorption of water by bacterial spores and its relation to dry heat resistance. *Dev Ind Microbiol* **11**: 311-326 (1970).
77. MacLeod R.A.; Calcott P.H. Cold shock and freesing damage to microbes. In Gray T.G.R.; Postgate J.R. (eds.) The survival of vegetative microbes. *Society for General Microbiology Symposium No. 26* (Cambridge university Press, Cambridge, 81-109 (1976).
78. Kraniak J.M.; Shelef L.A. Effect of ethylenediaminetetraacetic acid (EDTA) and metal ions on growth of Staphylococcus aureus 196E in culture media. *J Food Science* **53**: 910-913 1998.
79. Rusell A.D. Ethylenediaminetetraacetic acid. In: Hugo W.B. (ed.) *Inhibition and destruction of the microbial cell.* (Academic Press, London, 209-225 (1971).
80. Power E.G.M. Aldehydes as biocides. *Prog Med Chem* **34**: 149-201(1997).
81. Gorman S.P.; Scott E.M.; Rusell A.D. Antimicrobial activity, uses and mechanisms of action of glutaraldehyde. *J Appl Bacteriol*. **48**:191-190 (1980).
82. Rutala W.A.; Weber D.J. New disinfection and sterilization methods. *Emerging infectious diseases*. **7** (2):348-352 (2001).
83. Barett B.K.; Newboult L.; Edwards S. The membrane destabilizing action of the antibacterial agent chlorhexidine. *FEMS Microbiol. Lett.* **119**: 249-254 (1994).
84. Hugo W.B. Membrane-active antimicrobial agents: a reappraisal of their mode of action in the light of the chemiosmotic theory. *Int J Pharm*. **1**: 127-131 (1978).
85. Woodcock P.M. Biguanides as industrial biocides. In: Payne K.R. (ed.) *Industrial biocides*. (John Wiley&Sons, Chichester, 19-36 1988).
86. Michael G.T.; Stumbo C.R. Ethylene-oxide sterilization of *Salmonella senftenberg* and *Escherichia coli*: death kinetics and mode of action. *J Food Sci* **35**:631-634 (1970).
87. Young M.; Mandelstam J. Early stages during bacterial endospore formation. *Adv Microbiol Physiol* **20**:103-162 (1979).
88. McDonnell G. Rusell A.D. Antiseptics and disinfectants: activity, action and, resistance. *Clin Microbiol Rev* **12**:147-179 (1999).
89. Rusell A.D.; Chopra I. Understanding antibacterial action and resistance 2^{ed}. (Ellias Horwood, Chichester, 1996).
90. Moisiam M. et al. Low-temperature sterilization using gas plasmas: a review of the experiments and an analysis of the inactivation mechanisms. *Int J Pharmac* **226**:1-21 (2001).
91. Moisiam M. et al. Plasma sterilization. Methods and mechanisms. *Pure Appl Chem* **74** (3):349-358 (2002).
92. Bol'shakov A.A. et al. Radio-frequency oxugen plasma as a sterilization source. *AAIA J* **42** (7):823-830 (2004).
93. Lassen K.S.; Nordby B.; Grün R. The dependence of sporocidal effects on the power and pressure of RF-generated plasma processes. *J Biomed Mater Res Part B: Appl Biomater* **74B**:553-559 (2005).
94. Friedman A.. *Plasma chemistry* (Cambridge University Press, Cambridge, 2008).
95. Vratnica Z. et al. Degradation Degradation of bacteria by weakly ionized highly dissociated radio-frequency oxygen plasma. *IEEE Trans plasma sci* **36** (4) :1300-1301 (2008).
96. Boscariol M.R. et al. Sterilization by pure oxygen plasma and by oxygen-hydrogen peroxide plasma: an efficacy study. *Int J Pharm*. 353(1-2):170-5 (2008).
97. Sharma et al. Analysis of emission data from O_2 plasmas used for microbe sterilization. *J Appl Phys* **95** (7):3324-3333 (2004).
98. Nagatsu M.; Terashita F.; Koide Y. Low-temperature sterilization with surface-wave-excited oxygen plasma. *Jpn J Appl Phys* **42**:856-859 (2003).
99. Vratnica Z et al. Preiskava površine bakterij po obdelavi s plazmo. V: Radić N (ed.) *13. Međunarodni sastanak Vakumska znanost i tehnika Koprivnica 2006, Zbornik sažetaka* (Hrvatsko vakuumsko društvo, Koprivnica, Zagreb, 2006).
100. Vicoveanu D. et al. Pulsed discharge effects on bacteria inactivation in low-pressure radio frequency oxygen plasma . *Jpn J Appl Phys* **47** (2) 1130-1135 (2008).
101. Cvelbar U. Obdelava površine kompozita polimer-grafit s kisikovo plazmo. *Doktorska disertacija*. (Naravoslovnotehniška fakulteta, Univerza u Ljubljani, Ljubljana, 2005).
102. Cvelbar U et al. The influence of substrate material on bacteria sterilization in an oxygen plasma glow discharge. *J.Phys D Appl.phys* **39**: 3487-3493 (2006).
103. Sahoo S.; Rao K.K.; Suraishkumar G.K. Reactive oxygen species induced by shear stress mediate cell death in Bacillus subtilis. *Biotechnol Bioeng* **94**(1) 118-127 (2006)
104. Moreira A..J. et al. Sterilisation by oxygen plasma. *Appl Surf Sci* **235**:151-155 (2004).

105. Ekem N.et al. Sterilization of Staphyloccocus aureus by atmospheric pressure pulsed plasma. *Surf Coating Tech* **201**(3-4) 993-997 (2006).
106. Vujosevic D. et al. Optical emission spectroscopy characterization of oxygen plasma during degradation of *Escherichia coli*. *J Appl Phys* **101**(10) 103305 (2007).
107. Nagatsu M.; Terashita F.; Koide Y. Low-temperature sterilization with surface-wave-excited oxygen plasma.*Jpn J Appl Phys* **42**: 856-859 (2003).
108. Blanchard C.R. Atomic Force Microscopy. The Chemical Educator **1**(5) (Springer-Verlag, New York, 1996).
109. West P. Introduction to Atomic Force Microscopy, Theory, Practice and applications. AFM University.org. http://www.afmuniversity.org/
110. URL:www.weizmann.ac.il/Chemical_Research_Support/surflab/peter/afmworks
111. URL:www.en.wikipedia.org/wiki/Atomic_force_microscope
112. URL:www.bphys.unilinz.ac.at/bioph/download/Principlesof20%Atomic20%Force20%Microscopy
113. Engel A.; Lyubchenko Y.; Muller D. Atomic force microscopy: a powerful tool to observe biomoleculs at work *Trends in Cell Biology* **9** (2): 77-80 (1999).
114. Dufrene Y.F. Atomic force microscopy, a powerful tool in microbiology.**1:** *J. Bacteriol*. **184**(19):5205-13 (2002).
115. Robichon D. et al. Atomic force microscopy imaging of dried or living bacteria *C R Acad Sci III*. **322**(8):687-93 (1999).
116. Touhami et al. Atomic Force Microscopy of Cell Growth and Division in Staphylococcus aureus. *J. Bacteriol.*: **186** (32) 86 (2004).
117. Liu G.Y. Mobashery S. High-Resolution Imaging of Bacteria by Atomic Force Microscopy. *Abstr Intersci Conf Antimicrob Agents Chemother Intersci Conf Antimicrob Agents Chemother*. **39**: 757 (1999).
118. Ahimou, F. et al. Probing microbial cell surface charges by atomic force microscopy. *Langmuir* **18**:9937-9941 (2002).
119. Beech, I. B. et al. The use of atomic force microscopy for studying interactions of bacterial biofilms with surfaces. *Coll. Surf. B Biointerfaces* **23**:231-247 (2002).
120. URL:http://en.wikipedia.org/wiki/Scanning_electron_microscope
121. Egerton, R. F. *Physical principles of electron microscopy : an introduction to TEM, SEM, and AEM*. (Springer Science+Business Media Inc., 2005).
122. URL:http://mse.iastate.edu/microscopy/whatsem.html
123. Kiernan, J. A. "Formaldehyde, formalin, paraformaldehyde and glutaraldehyde: What they are and what they do". *Microscopy Today* **8**(1): 8–12 (2000).
124. URL:http://www.purdue.edu/REM/rs/sem.htm
125. Binnig, G.; Quate, C. F.; Gerber, C. Atomic Force Microscope. *Phys. Rev. Lett.* ***56*** (9): 930 (1986).
126. Cvelbar U. et al. Measurments of atomic oxygen density with fiber optic catalytic probe. Mater. tehnol. **36** (5) 243-245 (2002).
127. Drenik A. et. al. Weakly ionized oxygen plasma. *Inf. MIDEM* **35**: 85-91 (2005).
128. Cvelbar U. et. al. Inductivity coupled RF oxygen plasma characterisation by optical emission spectroscopy. *Vacuum*. **82** (2) 224-227 (2007).
129. Davis B.G.; Fairbanks A.J. *Carbohydrate chemistry*. (Oxford University Press, Oxford, New York, 2002).
130. Filipovic I.; Lipanovic S. *Opca i anorganska kemija*. (Skolska knjiga. Zagreb, 1978).
131. Barnickel G. et al. Conformational energy calculations on the petide part of murein. *Eur Biochem* **95**: 157-165 (1979).
132. Park J.T. The murein sacculus. In: Niedhart et al. (eds.) *Escherichia coli and Salmonella: cellular and molecular biology*. (ASM Press, Washington, 1996).

Index of Figures

Index of Tables

Appendix

List of publications resulted from research performed within this thesis

Papers

CVELBAR, Uroš, VUJOŠEVIĆ, Danijela, VRATNICA, Zoran, MOZETIČ, Miran. The influence of substrate material on bacteria sterilization in an oxygen plasma glow discharge. *J. phys., D, Appl. phys.*, 2006, vol. 39, str. 3487-3493.

VRATNICA, Zoran, VUJOŠEVIĆ, Danijela, CVELBAR, Uroš, MOZETIČ, Miran. Degradation of bacteria by weakly ionized highly dissociated radio-frequency oxygen plasma. *IEEE trans. plasma sci.*, 2008, vol. 36, no. 4, str. 1300-1301.

VUJOŠEVIĆ, Danijela, VRATNICA, Zoran, BUJKO, Marina, CVELBAR, Uroš, MOZETIČ, Miran. Sterilizacija plazmom - tehnologija budućnosti ili alternativa klasičnom postupku. *Med. zap.*, 2004, br. 59, str. 5-10.

VUJOŠEVIĆ, Danijela, VRATNICA, Zoran, VESEL, Alenka, CVELBAR, Uroš, MOZETIČ, Miran, DRENIK, Aleksander, MOZETIČ, Tatjana, KLANJŠEK GUNDE, Marta, HAUPTMAN, Nina. Oxygen plasma sterilization of bacteria. *Mater. tehnol.*, 2006, letn. 40, št. 6, str. 227-232.

DRENIK, Aleksander, CVELBAR, Uroš, VESEL, Alenka, MOZETIČ, Miran, VRATNICA, Zoran, VUJOŠEVIĆ, Danijela. Meritve gostote atomov v šibkoionizirani kisikovi plazmi vzdolž zaprte cevi. *Vakuumist*, 2005, letn. 25, št. 1-2, str. 16-19.

VRATNICA, Zoran, VUJOŠEVIĆ, Danijela, BELE, Marjan, DRENIK, Aleksander, VESEL, Alenka, CVELBAR, Uroš, MOZETIČ, Miran. Preiskave bakterij s sodobnim vrstičnim elektronskim mikroskopom. *Vakuumist*, 2005, letn. 25, št. 1-2, str. 20-23.

Conference contributions

VRATNICA, Zoran, VUJOŠEVIĆ, Danijela, BUJKO, Marina, CVELBAR, Uroš, MOZETIČ, Miran. SEM investigation of bacteria deposited on aluminium foil. V: MOZETIČ, Miran (ur.), ŠETINA, Janez (ur.), KOVAČ, Janez (ur.). 10. združena vakuumska konferenca [tudi] 11. srečanje slovenskih in hrvaških vakuumistov [in] 24. slovenski vakuumski simpozij, 28. september-2. oktober 2004, Portorož, Slovenija = 10th Joint Vacuum Conference [being also] 11th Meeting of Slovenian and Croatian Vacuum Scientists [and] 24th Slovenian Vacuum Symposium, September 28-October 2, 2004, Portorož, Slovenia. *Program in knjiga povzetkov*. Ljubljana: Društvo za vakuumsko tehniko Slovenije, 2004, str. 94.

CVELBAR, Uroš, VUJOŠEVIĆ, Danijela, VRATNICA, Zoran, MOZETIČ, Miran. Treatment of bacteria with inductively coupled oxygen plasma : [invited talk]. V: JVC 11, 11th Joint Vacuum Conference, September 24 - 28, 2006, Prague, Czech Republic. *Programme and book of abstracts*. [S.l.: s.n.], 2006, str. 38.

CVELBAR, Uroš, VUJOŠEVIĆ, Danijela, MOZETIČ, Miran, VRATNICA, Zoran, KRSTULOVIĆ, Nikša, MILOŠEVIĆ, Slobodan, REPNIK, Urška. Monitoring plasma sterilization efficiency. V: 5th Balkan

Congress for Microbiology, 24-27 October 2007, Budva, Montenegro. *[Programme, abstract book]*. Podgorica: Balkan Society for Microbiology: Montenegrian Society for Microbiology, 2007, str. 63.

ELERŠIČ, Kristina, VRATNICA, Zoran, VUJOŠEVIĆ, Danijela, JUNKAR, Ita, KOVAČ, Janez, MOZETIČ, Miran, CVELBAR, Uroš. Surface analysis of demages on Escherichia coli caused by oxygen plasma radicals. V: ICOPS 2008, The 35th IEEE International Conference on Plasma Science, June 15-19, 2008, Karlsruhe, Germany. *IEEE Conference records - abstracts*. Danvers: Institute of Electrical and Electronics Engineers, 2008, str. 293.